Natural Resources Canada
Ressources na Canada

CANADIAN FOREST SERVICE
PACIFIC FORESTRY CENTRE
INFORMATION REPORT
BC-X-423

Quantifying the water resource impacts of mountain pine beetle and associated salvage harvest operations across a range of watershed scales: Hydrologic modelling of the Fraser River Basin

Markus Schnorbus, Katrina Bennett, and Arelia Werner

Canada

The Pacific Forestry Centre, Victoria, British Columbia

The Pacific Forestry Centre of the Canadian Forest Service undertakes research as part of a national network system responding to the needs of various forest resource managers. The results of this research are distributed in the form of scientific and technical reports and other publications.

Additional information on Natural Resources Canada, the Canadian Forest Service, and Pacific Forestry Centre research and publications is also available online at: ***cfs.nrcan.gc.ca/regions/pfc.*** To download or order additional copies of this publication, see our online bookstore at: ***bookstore.cfs.nrcan.gc.ca.***

Quantifying the water resource impacts of mountain pine beetle and associated salvage harvest operations across a range of watershed scales: Hydrologic modelling of the Fraser River Basin

Markus Schnorbus,[1,2] Katrina Bennett,[2] and Arelia Werner[2]

MPB Project 7.29

[1] River Forecast Centre, B.C. Ministry of Environment, 4th Floor, 395 Waterfront Crescent, Victoria, B.C.

[2] Pacific Climate Impacts Consortium, C177, Sedgewick Building, University of Victoria, Victoria, B.C.

Natural Resources Canada
Canadian Forest Service
Pacific Forestry Centre
Information Report BC-X-423

2010

Natural Resources Canada
Canadian Forest Service
Pacific Forest Centre
506 West Burnside Road
Victoria, British Columbia
V8A 1M5

Phone: 250-363-0600

ISBN 978-1-100-13385-0
Cat. no.: Fo143-2/423E

Printed in Canada

Cover photos: (left to right) mountain pine beetle red attack, British Columbia–NRCan, CFS; Selkirk range snow pack–Scott Cramer © 2009; spawning salmon–David Harrison, NRCan, CFS; Fraser River at Rearguard Falls–Bruce Smith (c) 2009; Chilcotin Bridge, British Columbia interior–Wolfgang Zinti © 2008

Library and Archives Canada Cataloguing in Publication

Schnorbus, Markus
Quantifying the water resource impacts of mountain pine beetle and associated salvage harvest operations across a range of watershed scales [electronic resource] : hydrologic modeling of the Fraser River Basin / Markus Schnorbus, Katrina Bennett and Arelia Werner.

(Information report ; BC-X-423)
"MPBI Project # 7.29".
Electronic monograph in PDF format.
Includes abstract in French.
Issued also in printed form.
Includes bibliographical references.
ISBN 978-1-100-13386-7
Cat. no.: Fo143-2/423E-PDF

1. Mountain pine beetle--British Columbia--Fraser River Watershed. 2. Hydrologic forecasting--British Columbia--Fraser River Watershed. 3. Hydrologic models--British Columbia--Fraser River Watershed. 4. Watershed management--British Columbia--Fraser River Watershed. 5. Pine--Harvesting --British Columbia--Fraser River Watershed. 6. Pine--Diseases and pests --British Columbia--Fraser River Watershed. 7. Fraser River Watershed (B.C.). I. Werner, Arelia II. Bennett, Katrina III. Pacific Forestry Centre IV. Title. V. Series: Information report (Pacific Forestry Centre : Online) BC-X-423

SB945 M78 S36 2009 634.9'7516768 C2009-980198-1

Executive Summary

The province of British Columbia, Canada, is currently experiencing the largest mountain pine beetle outbreak ever recorded in North America. Widespread mortality of pine trees has occurred in over 14.5 million hectares of forest (an area roughly twice the size of Ireland) and the outbreak continues to kill mature pine in the province. Although the beetle attacks all pine species native to British Columbia forests, lodgepole pine is the most abundant species by area and the predominant commercial species. Consequently, an aggressive program of salvage harvesting has been initiated and is now superimposed on an already-severe landscape-level disturbance.

The epicentre of the current outbreak is in the Fraser River Basin (230 000 km^2), where roughly 8 million hectares of forest—approximately 35 percent of the drainage area—have been affected. The Fraser River is one of the most productive salmon rivers in the world; its lakes and tributaries provide spawning habitat for all five species of eastern Pacific salmon and more than 100 other species of fish. The basin is also home to 63 percent of British Columbia's population, with many people living close to or within the broad floodplain in the Lower Mainland. Approximately 62 000 hectares of agricultural, residential, and commercial land within this floodplain are protected behind 320 km of dikes built along the river.

In snow-dominated areas, such as British Columbia's interior, the loss of forest cover due to pine death and salvage harvesting results in higher snow accumulation over the winter and higher melt rates during the spring. This effect, combined with a loss of transpiration (i.e., dead trees do not extract moisture from the soil), generally results in more water available for local runoff. This leads to potential increases in magnitude and frequency of peak-discharge events.

Changes in the peak flow can translate directly to increased flood risk and negative impacts on fisheries and aquatic ecosystems. Due to the massive size of the affected area, potential exists for widespread and significant peak-flow changes throughout the basin. The purpose of this project was to assess the potential for impacts and changes to the peak-flow regime throughout various sub-basins of the Fraser River watershed.

The vast size and the physical complexity of the Fraser River Basin make it extremely difficult to directly measure the hydrologic effects of beetle kill and salvage harvesting. As a result, a hydrology model has been used to assess the hydrologic consequences of the current outbreak. The model was used to examine streamflow impacts for 60 sub-basins within the Fraser River Basin. The sub-basins ranged in size from 400 km^2 to 217 000 km^2. Peak-flow impacts were projected as a function of change in forest cover representing mountain pine beetle mortality and various levels of subsequent salvage of pine-forested areas within each of the sub-basins.

The simulation results indicate:

- Forest disturbance tends to increase peak-flow magnitudes, with relative change in magnitude increasing with disturbance severity.
- Peak flow shows more sensitivity (defined as the magnitude of change for a given disturbance) to cumulative effects of beetle-kill and salvage harvesting than to beetle-kill alone.
- Basins with high proportional runoff from pine-forested areas tend to be more sensitive to disturbance than basins with low proportional runoff from pine-forested areas.
- Basins that have a topological connection to the non-forested areas of the sub-alpine and alpine regions of the Coast, Columbia or Rocky mountain ranges tend to have low proportional runoff (and low sensitivity to forest disturbance).

Peak-flow sensitivity to beetle-related disturbance is specific to each region.

The section of the Fraser River main stem from Prince George to Hope and its major tributaries (i.e., North and South Thompson Rivers at Kamloops, Quesnel River at Quesnel, and the Chilcotin River) show little sensitivity to beetle-related disturbance. Streamflow at these locations, which drains from a large area and is predominantly composed of snowmelt runoff from the high snowfields of the Coast, Columbia, and Rocky Mountains, is largely unaffected by forest-cover changes taking place on the pine-dominated Interior Plateau.

The greatest sensitivity to infestation-induced forest disturbance is exhibited by modestly-sized sub-basins located on the Interior Plateau (i.e., Baker Creek, West Road River, Salmon River, Mahood River, and parts of the Nechako and Stuart drainages). These areas are characterized by pine-dominated forest cover (i.e., potentially high-disturbance areas) and low topographic relief (i.e., no significant regions of sub-alpine or alpine runoff). In these areas, where sensitivity is high, peak-flow changes can be substantial and merit further investigation with respect to beetle-infestation impacts on channel morphology, water quality, and aquatic ecosystems. Further studies on potential local changes to flood risk are also merited.

Résumé

La province de la Colombie-Britannique, au Canada, connaît actuellement la plus forte infestation de dendroctones du pin ponderosa jamais enregistrée en Amérique du Nord. La mortalité des pins s'étend sur plus de 14,5 millions d'hectares de forêt (une superficie équivalente à environ deux fois la taille de l'Irlande), et l'épidémie continue de ravager des pins mûrs dans la province. Bien que le dendroctone s'attaque à toutes les espèces de pins indigènes des forêts de la Colombie-Britannique, le pin tordu latifolié, l'espèce la plus abondante par région et la plus exploitée sur le plan commercial, est le plus touché. C'est pourquoi un programme vigoureux de coupes de récupération a été mis en place et est actuellement appliqué à des zones déjà gravement perturbées à l'échelle du paysage.

L'épicentre de l'infestation actuelle se trouve dans le bassin du Fraser (230 000 km^2), où à peu près 8 millions d'hectares de forêt, soit environ 35 % de l'aire de drainage, ont été touchés. Le fleuve Fraser est l'une des rivières à saumons les plus productives de la planète; ses lacs et ses affluents constituent des frayères pour les 5 espèces de saumons du Pacifique de l'est ainsi que pour plus de 100 autres espèces de poissons. Par ailleurs, c'est dans son bassin que réside 63 % de la population de la Colombie-Britannique, dont une grande partie dans la vaste plaine inondable de la vallée du Bas-Fraser ou à proximité de cette dernière. Environ 62 000 ha de surfaces agricoles, résidentielles et commerciales de cette plaine sont protégés par 320 km de digues construites le long du fleuve.

Dans les régions où la neige tombe en abondance, telles celles de l'intérieur de la Colombie-Britannique, la diminution du couvert forestier causée par la dévastation des pins et les coupes de récupération entraîne une augmentation de l'accumulation de neige en hiver et de la fonte au printemps. Ces répercussions, combinées avec une perte de transpiration (c.-à-d. que les arbres morts ne participent pas à l'extraction de l'humidité du sol), se traduisent généralement par une augmentation localisée des eaux de ruissellement. Cela peut entraîner un accroissement éventuel de l'ampleur et de la fréquence des débits de pointe.

Les modifications des débits de pointe peuvent se traduire sans équivoque par un risque accru d'inondation et des répercussions néfastes sur les pêches et sur les écosystèmes aquatiques. Compte tenu de l'énorme superficie de la zone touchée, on peut redouter, à l'échelle du bassin tout entier, d'importants changements des débits de pointe sur une vaste étendue. L'objet de ce projet était d'évaluer les changements potentiels du régime de débits de pointe et les effets de ces changements sur divers sous-bassins versants du Fraser.

L'importance de la taille et la complexité physique du bassin du Fraser rendent extrêmement difficile la mesure directe des effets hydrologiques des pertes de bois causées par le dendroctone et par les coupes de récupération. Un modèle hydrologique a donc été utilisé pour évaluer les conséquences d'ordre hydrologique de l'infestation actuelle. Ce modèle a permis d'étudier les répercussions du débit des cours d'eau pour 60 sous-bassins versants du Fraser. La superficie de ces sous-bassins allait de 330 km^2 à 217 000 km^2. Pour chaque sous-bassin considéré, la projection de l'impact des débits de pointe a été effectuée en fonction de la modification du couvert forestier liée à la mortalité causée par le dendroctone du pin ponderosa et à divers niveaux de coupes de récupération consécutives à cette mortalité dans les zones boisées dominées par les pins.

Résultats de cette simulation :

- Les perturbations forestières tendent à accroître l'ampleur des débits de pointe, la modification relative de l'ampleur augmentant avec la sévérité des perturbations.
- Les débits de pointe s'avèrent plus sensibles aux effets cumulés des pertes de bois dues au dendroctone et des coupes de récupération qu'aux seules pertes de bois dues au dendroctone.
- Les bassins connaissant des taux élevés de ruissellement en provenance de zones boisées dominées par les pins tendent à être plus sensibles aux perturbations que les bassins connaissant de faibles taux de ruissellement en provenance de zones boisées dominées par les pins.
- Les bassins qui ont un lien topologique avec les zones non boisées des régions alpines et subalpines de la chaîne Côtière, de la chaîne Columbia ou des montagnes Rocheuses tendent à afficher des taux de ruissellement peu élevés (ainsi qu'une faible sensibilité aux perturbations forestières).

La sensibilité des débits de pointe aux perturbations liées à la présence du dendroctone est propre à chaque région.

La section de l'axe principal du Fraser allant de Prince George à Hope ainsi que ses principaux affluents (c.-à-d. les rivières Thompson Nord et Sud à Kamloops, la rivière Quesnel à Quesnel ainsi que la rivière Chilcotin) présentent peu de sensibilité aux perturbations liées au dendroctone. À ces endroits, le débit se compose principalement d'eaux de ruissellement provenant de la fonte des neiges des champs de neige en altitude de la chaîne Côtière, de la chaîne Columbia et des Rocheuses, et il est très peu affecté par les changements qui se produisent sur le plateau intérieur, dominé par les pins.

Ce sont les sous-bassins du plateau intérieur (c.-à-d. le ruisseau Baker, la rivière West Road, la rivière Salmon, la rivière Mahood ainsi que certaines parties des bassins hydrographiques des rivières Nechako et Stuart) qui présentent la plus grande sensibilité aux perturbations forestières causées par l'infestation de dendroctones. Ces zones sont caractérisées par un couvert forestier dominé par les pins (c.-à-d. des zones pouvant faire l'objet de fortes perturbations) et un faible relief topographique (c.-à-d. sans zones importantes de ruissellement alpin ou subalpin). Dans ces zones particulièrement sensibles, les changements de débits de pointe peuvent être considérables et demandent un examen plus poussé des répercussions de l'infestation de dendroctones sur la morphologie, la qualité de l'eau et les écosystèmes aquatiques des chenaux. Des études supplémentaires sur les risques d'inondation en raison de modifications possibles au niveau local s'imposent également.

Contents

Tables

Glossary of abbreviations

The VIC vegetation parameter abbreviation key appears in Section 2.4.1, Table 1.

The VIC model's forest cover scenarios abbreviation key appears in Section 2.7.

The sub-basin abbreviation key appears in Appendix Table A2.

AHCCD	Adjusted Historical Canadian Climate Database
BC	British Columbia
BCILMB	British Columbia Integrated Land Management Bureau
BCMoF	British Columbia Ministry of Forests
BCMoFR	British Columbia Ministry of Forests and Range
BEC	Biogeoclimatic Ecosystem Classification
CHRS	Canadian Heritage Rivers System
CC	clearcut
CLASS	Canadian Land Surface Scheme
ECA	equivalent clearcut area
est	estimate
GSDT	Global Soil Data Task
IRF	instantaneous response function
LAI	leaf area index
LNSE	Nash–Sutcliffe Efficiency of a log-transformed discharge; see NSE
LRDW	Land and Resource Data Warehouse
MOCOM	Multi-Objective Complex Evolution
MPB	mountain pine beetle
NSE	Nash–Sutcliffe Efficiency
NOP	non-vegetated opening
NTS	National Topographic Series
PCS	Projected Coordinate System
PRISM	Precipitation-elevation Regressions on Independent Slopes Model
RESULTS	Reporting Silviculture Updates and Land status Tracking System
SPOT-4	Satellite Pour l'Observation de la Terre (satellite with vegetation imaging capabilities)
SRTM	Shuttle Radar Topography Mission
SYMAP	Synagraphic Mapping Program
TFL	tree farm licence
VGT	vegetation
VIC	variable infiltration capacity
VOP	vegetated opening
VRI	Vegetation Resources Inventory
WSC	Water Survey of Canada

1. Introduction

1.1 Background

The mountain pine beetle has been a natural component of British Columbia's forests for millennia. Although the beetle's population normally exists at endemic levels, outbreaks do occur, and populations have reached epidemic levels several times during the past decades (Taylor and Carroll 2004). The abundance of mature pine and a series of warmer than normal winters have made the present outbreak, which started in the early 1990s, grow to the most extensive ever recorded in the province (Wilson 2004). The British Columbia Ministry of Forests and Range estimates that, as of 2008, the cumulative area of provincial Crown forest affected to some degree (by either red attack or grey attack) was about 14.5 million ha (BCMoFR 2009).

The infestation is expected to continue for at least another 10 years and kill at least 80% of the merchantable pine volume in the province (Westfall 2005). Although the beetle attacks all pine species native to British Columbia, lodgepole pine is both the most abundant species by area and the predominant commercial species. Consequently, an aggressive salvage-harvesting program is underway to recover as much economic potential as possible from the dead timber (BCMoF 2004) and to mitigate the spread of the beetle infestation to high-risk areas (BCMoFR 2005).

Extending from the Rocky Mountains to the Coast Mountains and draining the province's extensive Interior Plateau, the Fraser River lies squarely within the epicentre of the current beetle outbreak. Of the 14.5 million ha infested, more than 8.0 million ha (or 55%) lie within the Fraser River drainage. The scale of the infestation and its associated salvage-harvest operations may affect local and regional hydrology and runoff-generation processes throughout the Fraser River Basin.

The integrated effect of these factors may be significant and detectable changes to the streamflow regime within the main stem (that is, the principal river channel that collects all the tributaries) of the Fraser River. To the best of the authors' knowledge, such large-scale land-cover change in such a short time has never been recorded in any continental-scale river basin in North America.

This project determined potential impacts of the infestation and associated harvest activities on water resources within the Fraser River Basin. We aimed to gain knowledge relating to the hydrologic effects for the basin as a whole, as well as for its main tributaries, whose drainages range in scale from 400 km^2 to 217 000 km^2.

We specifically assessed the potential for impacts and changes to the peak-flow regime. Changes in peak-flow regime can translate directly to increased flood risk due to increased frequency and duration of threshold events. Geomorphically significant discharge is also associated with events that recur every 1 to >100 years (Beschta et al. 2000, and references therein), such that alteration of peak-flow regime can alter channel evolution and affect channel morphology (Ziemer and Lisle 1998). Consequently, such changes can jeopardize availability of stream-associated resources and disturb fisheries and aquatic ecosystems.

1.2 The Fraser River

The Fraser River is the largest drainage basin in British Columbia. It drains 230 000 km^2 (one-third of the province's area), and its main stem runs roughly 1400 km from its headwaters in the Rocky Mountains (near Jasper, Alberta) to the Pacific Ocean at Vancouver (Figure 1). Stretching as it does across the southern breadth of the province from the Rockies to the Coast Mountains and north to Takla Lake, the basin is climatically and geographically diverse; it contains 12 ecoregions and 9 biogeoclimatic zones. Mean annual precipitation ranges from 230 mm in the lower Thompson valley-bottom to more than 5000 mm in the Cascade Mountains near the Lower Mainland. Temperature is similarly variable, with mean annual daily maximum temperature ranging from 2° C–15° C and an annual daily minimum temperature ranging from 6° C to –8° C (derived from Precipitation-elevation Regressions on Independent Slopes Model [(PRISM) 1961–1990 climate normals]. Approximately 177 000 km^2 of the basin, or 76% of total drainage area, is forested (BCILMB 1995). Roughly 33% of the basin (40% of the forested area) is affected by the current mountain pine beetle infestation, as it lies mostly within the province's Interior Plateau. The study area of this project includes the entire Fraser River drainage upstream of Hope (217 000 km^2; Figure 1); this is the entire drainage with the exception of the Lillooet-Harrison, Chilliwack, and Lower Mainland watersheds.

Discharge in the Fraser River is snowmelt driven. Monthly average discharge at Hope (drainage area of 217 000 km^2) ranges from 7000 m^3/s in June to only 900 m^3/s throughout

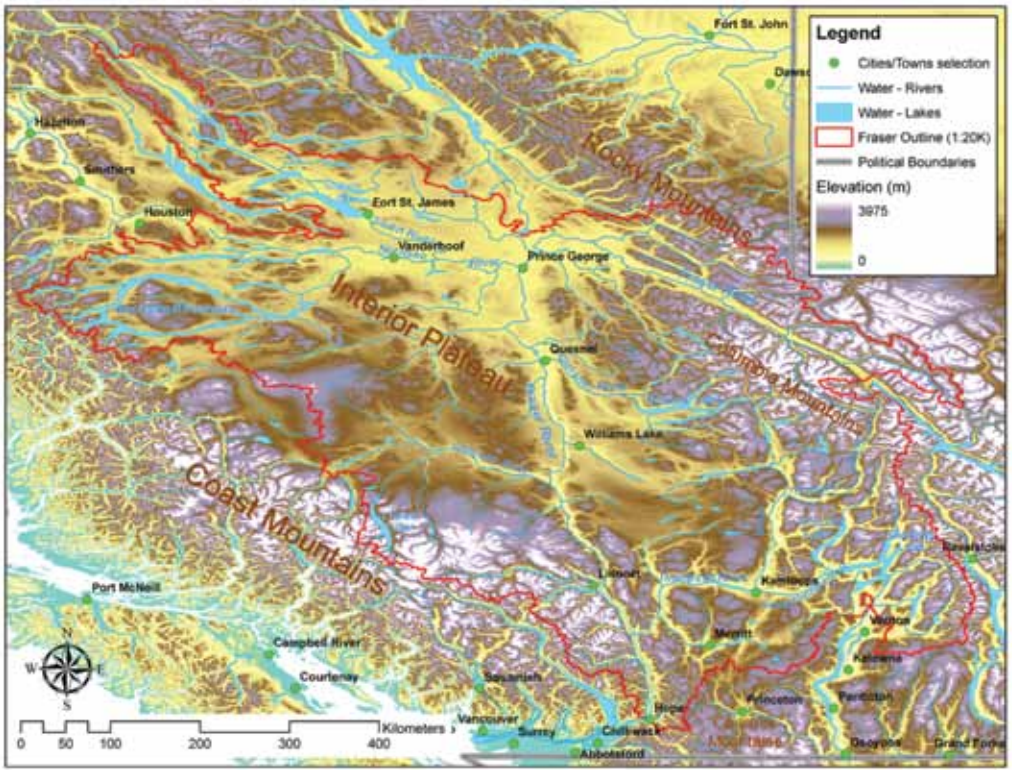

Figure 1. Fraser River Basin study area showing outline of drainage basin above Hope, BC (WSC gauge 08MF005, Fraser River at Hope)

January, February, and March. Drainage production is distributed unevenly throughout the basin: high-elevation snow in the Rocky, northern Columbia, and southern Coast Mountains creates the most runoff. The Upper Fraser River Basin (drainage area upstream of Prince George) and the Thompson River Basin, which combine to encompass 38% of the drainage area above Hope, contribute 54% of annual runoff. The lower Fraser tributaries produce roughly 13% of total Fraser River discharge from only 3% of the total drainage area above Hope. By contrast, runoff from the Interior Plateau is quite low, where roughly 33% of annual runoff is generated from nearly 59% of the total drainage area.

Although the Fraser River main stem has no lakes, several major tributaries are affected by large lakes or lake systems. The largest of these include Shuswap and Adams lakes in the South Thompson River Basin, Quesnel Lake in the Quesnel River Basin, Chilko Lake in the Chilcotin, and Takla and Stuart Lakes in the Stuart River Basin (Figure 1). In addition, discharge in the Nechako River is affected by regulation of the Nechako reservoir (Figure 1). The reservoir is formed by the diversion of the Nechako River (via the Kenney Dam, located in the Nechako Canyon) through the Coast Mountains to sea level at the community of Kemano. The creation of the reservoir flooded a series of lakes, including Ootsa Lake, Whitesail Lake, and Tahtsa Reach in the north arm, and Eutsuk Lake, Natalkuz Lake, Knewstubb Lake, Tetachuck Lake, and others in the south arm. Roughly 62% of the Nechako reservoir inflow is diverted from the Fraser River to the Kemano powerhouse (based on 1999 to 2008 data; BC Ministry of Environment, unpublished info).

The Fraser River is arguably the economic, social, and cultural heartland of British Columbia. It is one of the most productive salmon rivers in the world; its lakes and tributaries provide spawning habitat for all five species of eastern Pacific salmon. The river and its estuary also provide habitat for more than 100 other species of fish (CHRS 2009).

The basin is also home to 63% of British Columbia's population, with many people living close to or within the broad floodplain in the Lower Mainland (CHRS 2009). Several of the largest communities in British Columbia are located along the Fraser and its tributaries. Approximately 62 000 ha of agricultural, residential, and commercial land within this floodplain are protected behind 320 km of dikes built along the Fraser River main stem (BC Water Resources Atlas, available at http://www.env.gov.bc.ca/wsd/data_searches/wrbc/index.html). The Fraser River and its major tributaries also serve as major rail- and highway-transportation corridors. Economic activity within the basin accounts for 80% of provincial and 10% of federal gross domestic product (CHRS 2009).

1.3 The mountain pine beetle and forest hydrology

The mountain pine beetle (*Dendroctonus ponderosae*, Hopkins) is a bark beetle that kills pine by burrowing galleries beneath the bark of mature pine trees. The galleries disrupt the tree's vascular systems, which kills the tree.

Death of the trees stops transpiration. Consequent defoliation reduces interception loss and alters the below-canopy energy budget. A predominant effect of forest removal in snow-dominated watersheds is increased snow accumulation, the extent of which partly depends on the relative change in canopy density (Winkler et al. 2005). Consequently, watershed studies in snow-dominated basins consistently report the greatest increase in water yield to occur in spring during the rising limb of the hydrograph (Cheng 1989; MacDonald and Stednick 2003). The effect of forest removal during the falling limb and during periods of low flow is less consistent. Studies in Colorado suggest that annual yield increases come strictly from increased spring runoff and that runoff during the remainder of the year is unaffected (MacDonald and Stednick 2003). Based on a paired-basin study in British Columbia, Cheng (1989) observed that flow increases following forest harvesting also occur during the August to November low-flow period, although increases were statistically significant in all months and years. Simulations conducted for small watersheds in British Columbia led Schnorbus and Alila (2005) to conclude that runoff increases throughout the spring, summer, and fall, with the largest relative increase occurring during the summer/fall low-flow period. However, the largest absolute flow increase occurs on the rising limb.

Forest removal in snowmelt-dominated areas is generally expected to increase the magnitude and frequency of peak-discharge events (Schnorbus and Alila 2004; MacDonald and Stednick 2003). This is due to several factors: forest removal increases melt rates via increased solar radiation and higher turbulent and latent heat transfers (Adams et al. 1998), which often occur in combination with a more persistent snowpack (due to increased peak snow water equivalent, see above) and larger snow-covered area (Kattelmann 1991). The magnitude of observed changes in peak flow following forest disturbance and harvesting varies, as reported by several paired-basin studies in snow-dominated regimes (Potts 1984; Troendle and King 1985, 1987; Cheng 1989; Megahan et al. 1995; Burton 1997). It likely depends on climate, basin topography (slope, aspect, and elevation), amount of forest cover removed, disturbance type and pre-disturbance forest cover, and other factors. Regardless, conclusions derived from paired-basin studies are often limited to the mean peak-flow response, because studies typically lack observations of sufficient duration to quantify pre- and post-disturbance peak-flow regimes. Again, most literature regarding peak-flow changes is based on forest harvesting; what little information that addresses the effect of defoliation due to insect outbreak is, on its own, inconclusive.

A largely unaddressed issue is the degree to which hydrologic impacts vary between forests affected solely by beetle-kill and those subjected to salvage harvesting, typically occurring in the form of clearcuts. A beetle infestation in mixed stands and in stands with a functional understorey would likely leave vegetation capable of interception and transpiration (Schmid et al. 1991). As such, forest areas that retain residual vegetation after infestation would be less affected by changes in annual and seasonal water balance than completely beetle-killed or harvested stands would be. The impact on peak flow by forest disturbance also would vary between natural beetle-kill and salvage-harvest disturbances. Changes in the snow surface energy balance are expected to vary, based on the degree of residual stand density and forest cover remaining following the disturbance (Teti 2009). Conversion of forest cover via clearcut salvage harvesting would likely increase melt and runoff rates more than beetle-kill by itself would. Any retained vegetation and dead standing timber following a less severe disturbance would likely reduce potential melt-rate increases by maintaining some degree of energy attenuation due to continued solar-radiation shielding and dampening of dynamic and convective turbulence (Boon 2009). Scherer 2001, Hélie et al. 2005, Uunila et al. 2006, Winkler et al. 2008, and Redding et al. 2008 provide more comprehensive reviews of current understanding of the hydrologic impact of both mountain pine beetle infestation and forest management in general.

This project is part of a larger effort in quantifying the water resource impacts of the pine beetle and salvage harvesting across a range of watershed scales. A complementary project is the development of peak- and low-flow hazard models for a risk-based assessment of beetle-related disturbance effects on third-order catchments in the Fraser River Basin (Carver et al. 2010a, b).

2. Methods

2.1 The Variable Infiltration Capacity (VIC) model

Much of what we know about how forest removal influences streamflow comes from observing watersheds up to 1000 km^2. However, most published work is based on stand-level studies and watersheds of the order of 10 km^2. At that scale, climatic and physiographic factors and runoff generation are fairly uniform.

A major challenge is to determine how these results scale to 10^4–10^5 km^2, where the spatial complexity makes extrapolating small-scale relationships non-trivial. The scale and physiographic, climatic, and topographic heterogeneity of the Fraser River Basin preclude both direct observation and extrapolation of hydrologic impacts observed on these few stand-level and small-basin experiments. Instead, we used the Variable Infiltration Capacity (VIC) hydrology model (Liang et al. 1994) to quantify these hydrologic impacts to the Fraser River Basin.

The VIC model is a spatially distributed macro-scale hydrology model originally developed as a soil-vegetation-atmosphere transfer scheme for general circulation models (Liang et al. 1994). Some distinguishing features of the VIC model include (Figure 2):

- multiple-layer characterization of the soil column (three in the Fraser River application);
- subgrid variability in soil infiltration, represented by a spatial probability distribution;
- drainage from the lower soil layer (baseflow) as a nonlinear recession;
- subgrid variability in land surface vegetation classes;
- subgrid variability in topography represented using elevation bands;
- multiple soil rooting zones and variable root distribution;
- multi-layer energy balance snow model incorporating canopy effects (e.g., attenuation of wind and solar radiation, canopy interception, and sublimation) (as per Storck and Lettenmaier 1999);
- wet canopy evaporation, dry canopy transpiration, and bare soil evaporation represented using the Penman–Monteith approach and including canopy effects to wind profile and surface radiation (as per Wigmosta et al. 1994).

Using the supplied driving data and specified initial states, the VIC model solves the one-dimensional water and energy balance for each grid cell. The VIC model is run at a daily timestep (one-hour timestep for the snow model), generating daily baseflow and "fast" runoff fluxes from each grid cell. These fluxes are then collected and routed downstream using an offline routing model (see Lohmann et al. 1996 for details). The VIC model was applied to the Fraser River Basin at 1/16° resolution (approximately 27–32 km^2, depending upon latitude) and used to quantify streamflow impacts for 60 sub-basins of the Fraser ranging from 330–217 000 km^2. Setting up and preparing the VIC model boundary conditions requires constructing the driving data (Section 2.2); specifying soil properties (Section 2.3), vegetation classes (Section 2.4), and the drainage network (Section 2.5); and calibrating and validating the model (Section 2.6). Analyzing the impacts of mountain pine beetle infestation and harvest disturbance requires constructing several forest-cover scenarios (Section 2.7). A summary table of all data and parameter sets specifying boundary conditions for the Fraser River application of the VIC model is provided in Appendix Table A1.

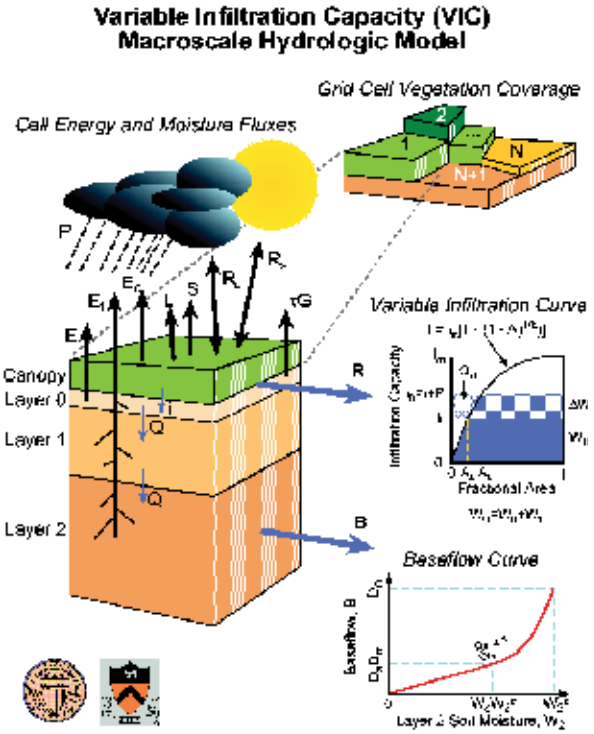

Figure 2. Schematic representation of the Variable Infiltration Capacity (VIC) model with three soil layers (diagram courtesy of the Dept. of Civil and Env. Eng., University of Washington; http://www.hydro.washington.edu/Lettenmaier/Models/VIC/)

2.2 Driving data

The VIC model is forced with daily surfaces of maximum and minimum temperature, precipitation, and daily average wind speed at 1/16° resolution. The generation of the daily surfaces followed the technique described by Maurer et al. (2002) and Hamlet and Lettenmaier (1995). The temperature and precipitation surfaces were gridded from daily station observations collected by Environment Canada during the period 1915 through 2006 using the SYMAP algorithm (Shepard 1984). Topography effects are addressed by adjusting the raw interpolated fields of temperature and precipitation using the 1961 to 1990 PRISM climatology of western Canada (Daly et al. 1994; available from The Climate Source, http://www.climatesource.com/). Using the Adjusted Historical Canadian Climate Data (AHCCD) (Mekis and Hogg 1999; Vincent and Gullett 1999; available from http://www.cccma.ec.gc.ca/hccd/), the interpolated data were temporally homogenized to reduce spurious trends or artifacts introduced by changes in collection techniques, station relocations, or inclusions of stations with different record lengths. This interpolation and gridding technique maintains as much spatial information as possible from the relatively high-density Environment Canada station observations. It also adjusts the time-series characteristics of the gridded data to be consistent with those of the fewer, highly quality-controlled and homogenized AHCCD stations. Daily wind speed surfaces were generated by re-gridding estimates of 10-m wind speed from the National Centers for Environmental Prediction–National Center for Atmospheric Research historical re-analysis (Kalnay et al., 1996). Temperature, precipitation, and wind surfaces were produced for all of British Columbia (Figure 3; Appendix Table A1). Daily maximum and minimum temperature and precipitation fields for the Fraser River Basin for 1961–1990 are shown in Figure 4, Figure 5, and Figure 6, respectively.

Additional meteorological "drivers," which include daily solar (direct and diffuse) and longwave radiation and dewpoint temperature, were derived from the daily temperature and precipitation observations using techniques described in Maurer et al. (2002). Generally, dewpoint is derived from relationships between daily minimum temperature and precipitation; downward shortwave radiation is estimated from the diurnal temperature range, dewpoint temperature, and precipitation; and downward longwave radiation is estimated from daily air temperature and dewpoint temperature.

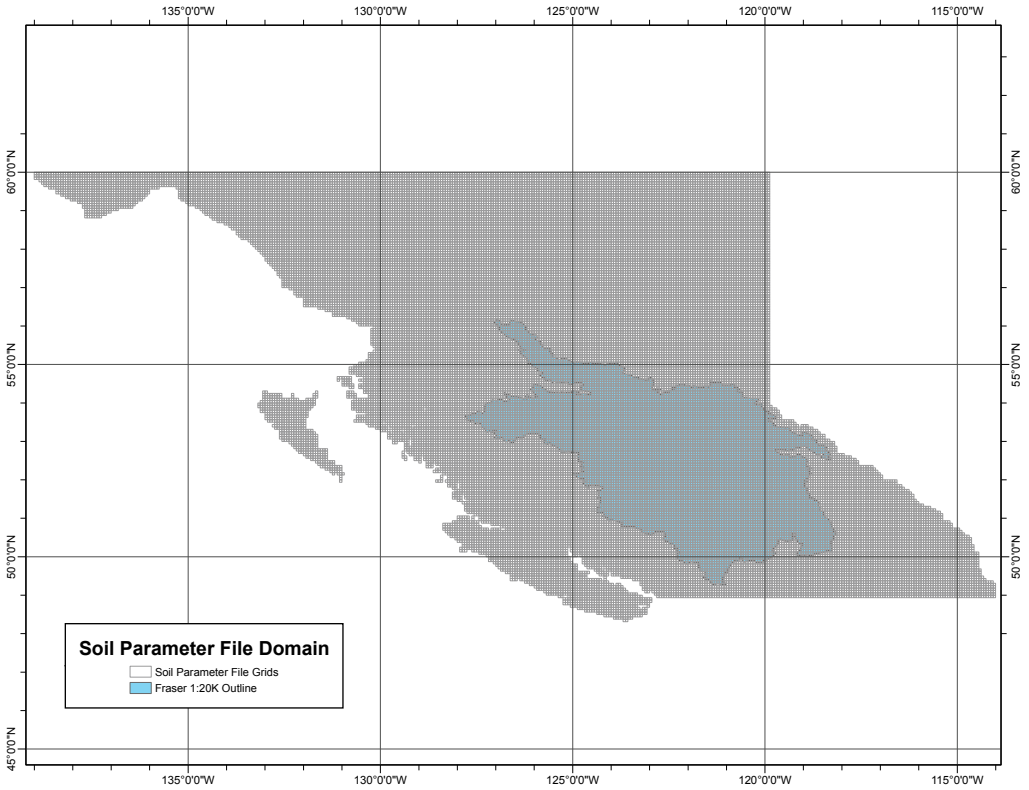

Figure 3. Spatial extent of VIC model domain (based on soil parameter file) for British Columbia showing model grid at 1/16° resolution. Also shown is the mask for the Fraser River application (using Fraser outline upstream of Hope at 1:20 000 scale).

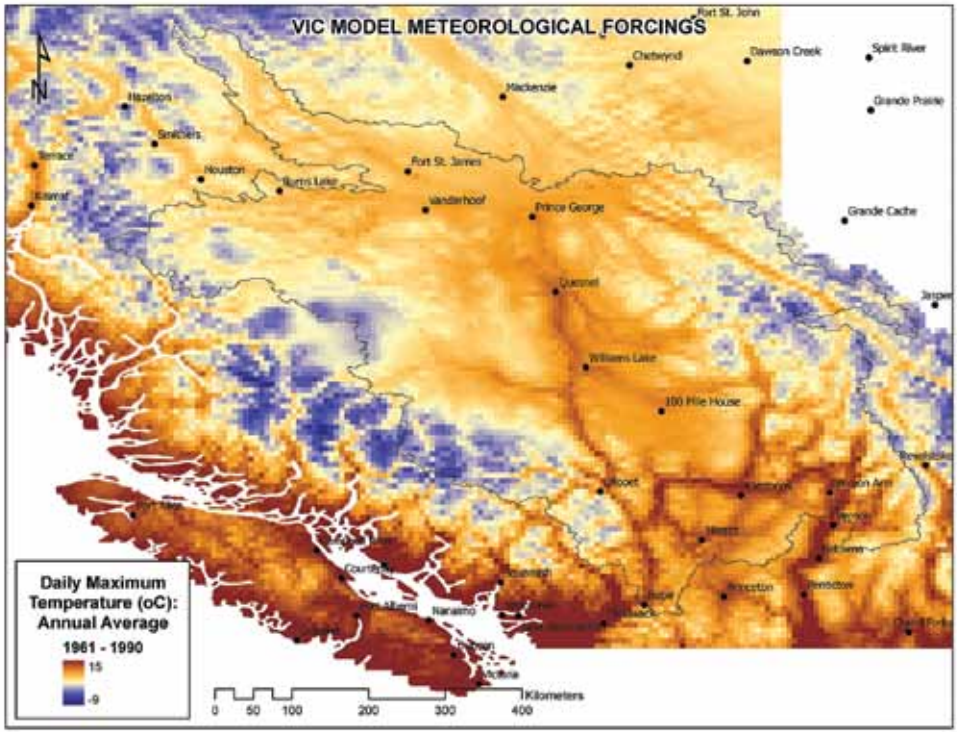

Figure 4. Average daily maximum temperature field at 1/16° resolution for 1961 to 1990

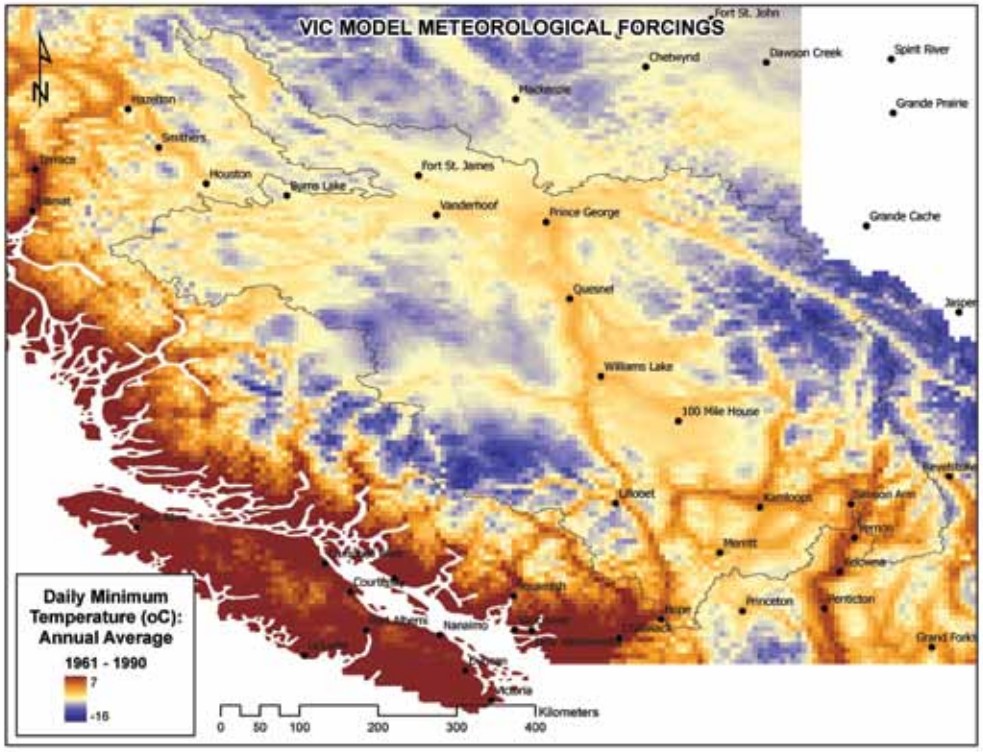

Figure 5. Average daily minimum temperature field at 1/16° resolution for 1961 to 1990

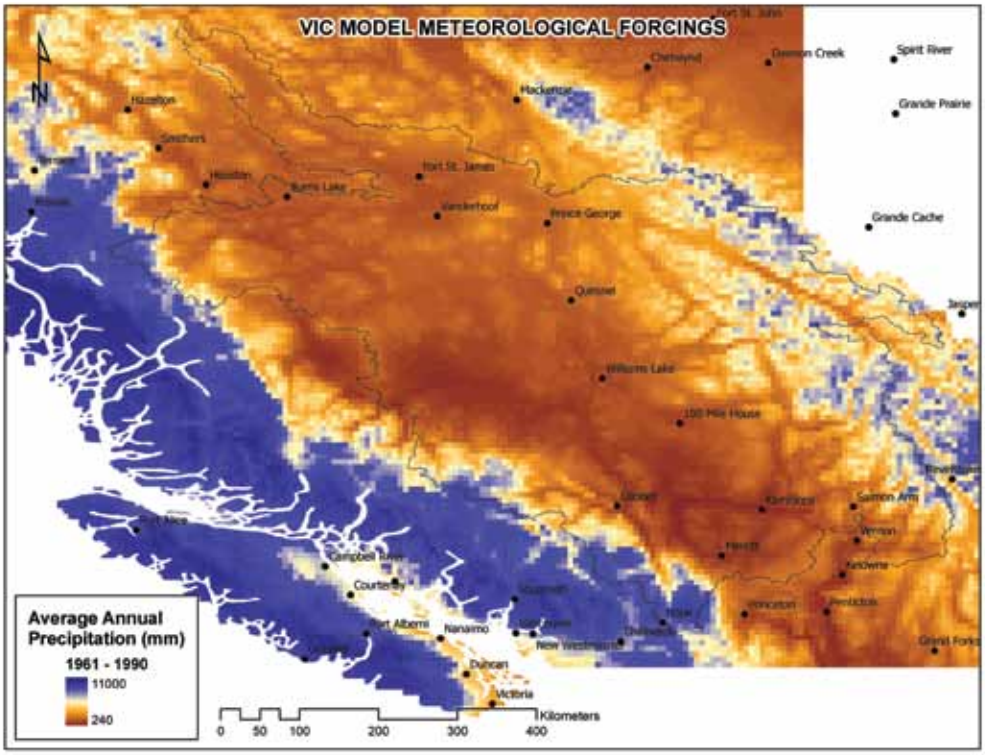

Figure 6. Average daily precipitation field at 1/16° resolution for 1961 to 1990

2.3 Soils data

Soil classification and the estimation of associated hydrologic and hydraulic parameters have been completed, and a VIC model soil parameter file has been produced for the entire province (Figure 3; Appendix Table A1). There are 54 classes of soils information in the soils parameter file. Classification and parameterization were based primarily on physical soil data from the Soils Program in the Global Soil Data Products CD-ROM (GSDT 2000). The data were extracted from the Soils Program, interpolated to the 1/16° grid scale, and used to generate the remaining values required to run the VIC model. Hydraulic conductivity, bulk density, porosity, wilting point, texture, and other parameters are extracted directly from the Soils Program. Field capacity is estimated from the Cosby et al. (1984) look-up table, based on the USDS soil texture triangle.

These parameters are then used to calculate other hydraulic properties of soil, including soil density, initial soil moisture, residual soil moisture, and bubbling pressure of the soil. Average grid-cell elevations are specified in the soil file and are derived from a post-processed version (Version 3) of the Shuttle Radar Topography Mission (SRTM)–based 90-m digital elevation model downloaded from the Consultative Group on International Agricultural Research's Consortium for Spatial Information website (http://srtm.csi.cgiar.org/). Soil depth values for the province at 1/16° resolution were estimated by relating soil depth to elevation and slope and using arbitrary minimum and maximum depth limits of 0.1 m and 3.5 m, respectively (soil depth for the Fraser is shown in Figure 7).

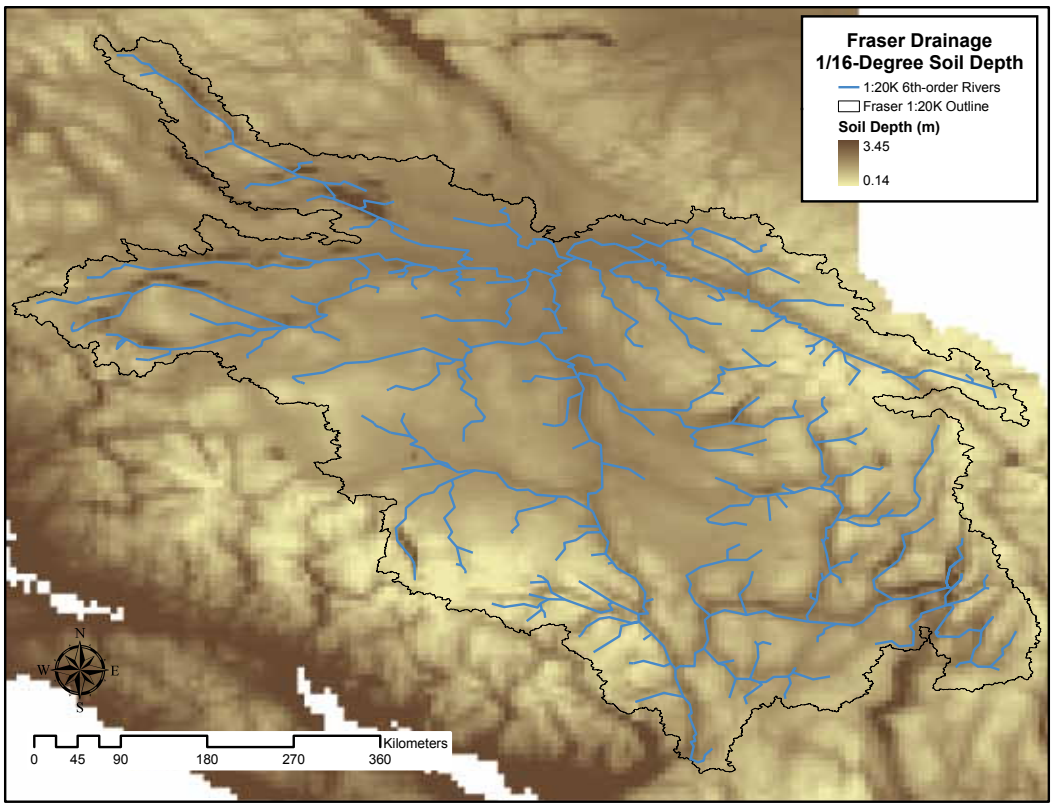

Figure 7. Estimated soil depth at 1/16° resolution for the Fraser River Basin

2.4 Vegetation cover

2.4.1 Vegetation classification

Land cover within the VIC model is described by assigning vegetation classes to each model grid cell. A cell can have more than one vegetation class; in such cases, vegetation classes are assigned a fraction of the grid cell. In addition to vegetation classes, the VIC model has an internal default bare soil class, which is applied to portions of a grid cell without vegetation (Liang et al. 1994). A vegetation classification scheme has been created based predominantly upon attribute information found in the British Columbia Ministry of Forest and Range's (BCMoFR) Vegetation Resources Inventory (VRI) database (VRI is described at http://www.for.gov.bc.ca/hts/vri/; spatial data available from the Land and Resource Data Warehouse (LRDW) at http://www.lrdw.ca/ under the title "VRI – Forest Vegetation Composite Polygons and Rank 1 Layer"). This classification scheme is used to specify both 1995 and 2007 forest cover conditions within the Fraser River Basin. The 1995 forest cover also forms the basis for five hypothetical forest disturbance scenarios (see Section 2.7). The classification scheme is designed to discriminate various (relatively) homogeneous vegetation types for incorporation into the VIC model, based on the parameters given in Table 1. Each vegetation class will (in theory) have a unique set of values for the model's vegetation parameters, which are supplied as a vegetation library.

Table 1. VIC vegetation parameters

Variable Name	Description
overstorey	Overstorey flag
rarc	Architectural resistance
rmin	Minimum stomatal resistance
LAI	Monthly leaf area index
albedo	Monthly shortwave albedo
rough	Monthly roughness length (function of vegetation height)
displacement	Monthly displacement height (function of vegetation height)
RGL	Minimum incoming shortwave radiation at which transpiration occurs
rad_atten	Radiation attenuation factor
wind_atten	Wind speed attenuation through the overstorey
trunk_ratio	Ratio of total tree height that is trunk

Vegetation classification for the VIC model is based on two themes: 1) cover type and 2) age class. Cover type captures biophysical properties that vary between species, particularly leaf area index and growth rate. Age classification captures within-species variation, by age, of certain vegetation properties such as vegetation height, as well as changes in pine susceptibility to beetle infestation. Cover types are classified by grouping species by *inventory type* group (identified in the VRI) and *growth type* (see Table 8.20 of BCMoF 1981). There are 42 inventory type groups (or tree species associations) and 17 growth types. Cover type is determined by grouping inventory type groups within growth types, with some groups joined and/or split based on similarity in growth rates taken from current inventory data for the Fraser River Basin. Non-treed vegetation is identified and classified using the British Columbia land cover classification scheme recorded in the VRI data. Additional cover types have been added to address infested pine stands (as compared to undisturbed or healthy pine stands) and forest harvesting. Eighteen cover types have been identified: 11 describe coniferous forest types, two describe deciduous forest types, three describe beetle-killed pine stands, one describes vegetated openings (natural and anthropogenic), and one describes non-vegetated openings (i.e., rock, ice/snow, and water bodies).

Existing treed vegetation classes are sub-classified to capture stand-age variation in the biophysical parameters height and LAI. Age is closely correlated to tree height (which is used to directly estimate *rough* and *displacement*), and both stand age and height are available directly from the VRI. However, the age and height values from the VRI are projected from the date of interpretation, often by several years or decades. These projections are based on growth and yield models in which age and height (among other variables) are interrelated. Therefore, the degree of correlation between age and height is to some degree an artifact in the database. Also, age and height refer to the leading species in a stand polygon. Age is assumed to be a suitable proxy for describing the variation of additional vegetation parameters (particularly LAI, e.g., Ryan et al. 1997).

Six age classes are used, based on all the cover types' growth rates. Two age classes, 1–10 years (class 2) and 11–20 years (class 3), are introduced to capture the rapid growth of recently harvested and regenerating stands. An age class of 21–60 years (class 4) is intended to capture the immature growth cohort and represents the period of peak stand

growth (Ryan et al. 1997). An age class of 61–120 years (class 5) represents mature vegetation, and an age class of >120 years (class 6) represents old-growth forest, where growth is essentially static. These age classes are applied to all treed coniferous vegetation types. The deciduous treed vegetation classes OP and OPQ do not live as long as conifer species and do not use age class 6; instead, age class 5 represents > 60 years. Recent forest disturbance is represented using age classes 1 and 2 for the treed vegetation classes. Age class 1 (stand age of 0 years) represents clearcuts (i.e., just harvested) and is set common to all treed vegetation classes. Class 2 cover types are re-assigned as vegetated openings for all treed vegetation classes, representing open forest stands regenerating from a recent disturbance. Therefore, each treed vegetation class will have four specific growth rate classes (3, 4, 5, and 6), with growth rate class 1 and 2 set common to all.

For pine stands, the growth rate categories must also identify stands at risk for mountain pine beetle infestation. Although such risk depends on many factors related to both stand susceptibility (such as abundance of susceptible pine, age of live pine, density of the stand, and location of stand) and beetle pressure (such as size and proximity of mountain pine beetle populations) (Shore et al. 2006), we use only stand age here as a simple indicator of stand risk. Shore and Safranyik (1992) state that a pine tree's risk of succumbing to a beetle infestation is low for stands < 60 years, intermediate for stands 60–80 years, and high for stands > 80 years. Therefore, the identified age classes also conveniently distinguish between low-risk (age classes 2–4) and high-risk (age classes 5 and 6) pine stands with respect to beetle infestation. The final vegetation classification scheme incorporates both cover and age classes for a total of 59 vegetation classes (Table 2).

All anthropogenic forest openings are identified using either the clearcut or the vegetated opening (CC and VOP, respectively, in Table 2) classes. The clearcut class represents clearcut harvest in the current year (i.e., age is 0) and describes a forest opening completely devoid of vegetation (i.e., no over- or understorey). The VOP class represents either a natural vegetated opening (such as grassland) or an area clearcut within the previous decade (i.e., age is 1 to 10 years). It is assumed to have an understorey but no overstorey.

Large spatial gaps exist in the VRI where inventory data have not been recorded; these correspond to deliberate omissions (mainly provincial parks and tree farm licenses), which are classified as "Unreported"(Figure 8). Records in which the inventory, species, and British Columbia land cover classification scheme attributes have null values are treated as "Unknown" records. In "Unreported" areas, vegetation classes have been inferred by cross-referencing known vegetation classes with the intersecting Biogeoclimatic Ecosystem Classification (BEC) subzones variants (Meidinger and Pojar 1991) that have been mapped in areas unreported in the VRI database. The process involves: a) determining the majority cover type in each BEC subzone variant where VRI and BEC mapping overlap, and b) assigning that cover type to the same BEC subzone variant in the unreported area. This majority assignment process was subdivided and conducted separately for each ecosection (as per Demarchi 1996) within the Fraser drainage. Approximately 99% of unreported area was reassigned in this fashion. The remaining 1% of the unreported area was located in BEC subzones that did not overlap with reported cover types. These areas were assigned cover types based on the species composition of the zonal site series identified in the relevant field guides. Parkland and woodland variants are relatively new and were not included in many of the field guides; woodland was assigned a vegetative cover (inferred from the VRI or field guide) and parkland was assigned vegetated opening (VOP). Those VRI entries having "Unknown" forest cover were assigned the non-vegetated opening category (NOP) as they represent a tiny area of the Fraser River drainage. The age class of each reassigned cover type was based on the mean age for each majority cover type in the BEC subzone–cover type intersection. In most cases vegetation was reassigned to age class 6 (>120 years). Where age couldn't be estimated from the VRI data, age class 6 was assigned.

2.4.2 Forest cover, 2007

Forest disturbance and harvest history for the 2007 forest cover classification was estimated from two data sources: the Reporting Silviculture Updates and Land status Tracking System (RESULTS; http://www.for.gov.bc.ca/his/results/) database and Landsat data (unpublished BCMoFR data). Polygons identified as an opening in the RESULTS data with a timestamp between 1/1/1997 and 1/1/2007 were classified as VOP. Polygons overlapping the Landsat 1999–2006 cutblock locations were also classified as VOP. Polygons identified in the RESULTS data with opening ID timestamps between 1/1/2007 and 31/12/2007 were classified as clearcut. Cutblock locations for the 2007 forest cover are shown in Figure 9. Management activities as captured in the RESULTS and VRI databases are not up to date (T. Salkeld, BC MoFR, Forest Analysis and Inventory Branch, personal communication) and may consequently underestimate or misrepresent forest management and harvesting activities.

Non-harvested pine stands were reclassified into beetle-kill using the 1999–2006 cumulative pine kill data from the British Columbia Ministry of Forests and Range's BCMPB.v4 infestation projection (Walton et al. 2007; the 1999–2007 cumulative kill data was unavailable when this work was conducted). The cumulative pine kill data (original

Table 2. Vegetation classifications, shown as the intersection of 18 cover types and 6 age classes

	Age Classes						Cover Class Description‡
Cover Type	1 (0 yrs)	2 (1–10 yrs)	3 (11–20 yrs)	4 (21–60 yrs)	5 (61–120 yrs)	6 (> 120 yrs)	
AC			AC3	AC4	AC5	AC6	Fd (>80%) or mixed, Py
BC			BC3	BC4	BC5	BC6	Mixed, Fd leading
D			D3	D4	D5	D6	Mixed, L, Fd or Pw/Pa
E			E3	E4	E5	E6	Mixed, C or Cy leading
FGH			FGH3	FGH4	FGH5	FGH6	H (>80%) or mixed, H leading B
H		Recent	H3	H4	H5	H6	B (>80%) or mixed, B leading S
I	Clearcut	Opening	I3	I4	I5	I6	S (>80%)
JK		(VOP)	JK3	JK4	JK5	JK6	Mixed, S leading
L			L3	L4	L5	L6	Pl (>80%)
MN			MN3	MN4	MN5	MN6	Mixed, Pl leading (>40% and < 80%)
AK			AK3	AK4	AK5	AK6	Mixed, Pl second (<40%)
OP			OP3	OP4	OP5		Mixed, Bi and A
OPQ			OPQ3	OPQ4	OPQ5		Mixed, Act, D and Mb
Lx					Lx5	Lx6	Pl (>80%), Infested
MNx					MNx5	MNx6	Mixed, Pl leading (>40%) and <80%), infested
AKx					AKx5	AKx6	Mixed, Pl second (<40%), infested
VOP	VOP						Non-treed vegetation (natural)
NOP	NOP§						Unvegetade, glacier/snow field, water body

‡ By typical association of the following species: A = aspen/cottonwood/poplar; Act = cottonwood; B = fir; Bi = birch; C = cedar; Cy = yellow cedar; D = alder; Fd = Douglas-fir; H = hemlock; L = larch; Mb = bigleaf maple; Pa = whitebark pine; Pl = lodgepole pine; Py = ponderosa pine; Pw = western white pine; S = Spruce

§ This class is included for information purposes only,. In cases where NOP exists in a cell, VIC's default "bare soi" class is used

400-m resolution grid in a PCS projection converted to a geographic 3-arc seconds grid) was overlain on the VRI polygon records to derive zonal average cumulative kill values. Polygons identified as unharvested pine with a zonal average pine volume kill ≥ 20% were classified as beetle-killed (vegetation classes Lx5, CC6, MNx5, MNx6, AKx5, and AKx6 in Table 2).

The final forest cover classification representing estimated forest cover conditions in the Fraser River drainage for 2007 is shown in Figure 10. The fractional area of each forest cover type within the Fraser River Basin is given in Table 3 and Figures 8, 9, and 10. Approximately 13% of the basin by area is classified as healthy pine classes, 20% as beetle-killed pine, 14% as vegetated openings, 37% as various forest cover types (mostly conifer), and 16% of the basin is classified as non-vegetated openings (which includes bare ground, rock, lakes, reservoirs, permanent snow, and ice).

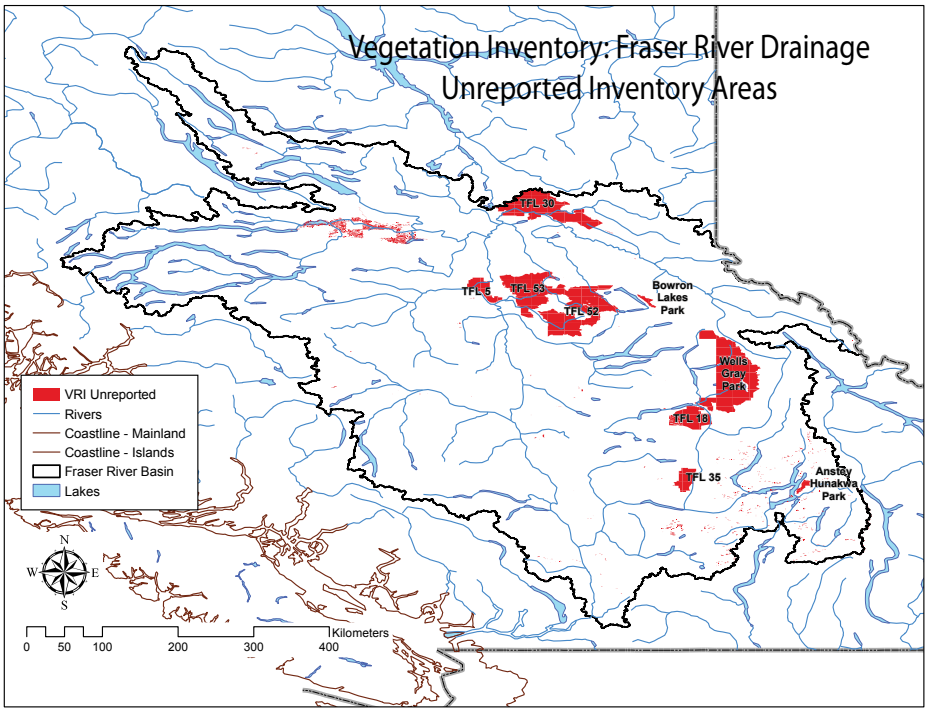

Figure 8. Distribution of VRI "unreported" areas within the Fraser River study area. Unreported areas located within the basin are labelled by park name or Tree Farm License (TFL) number.

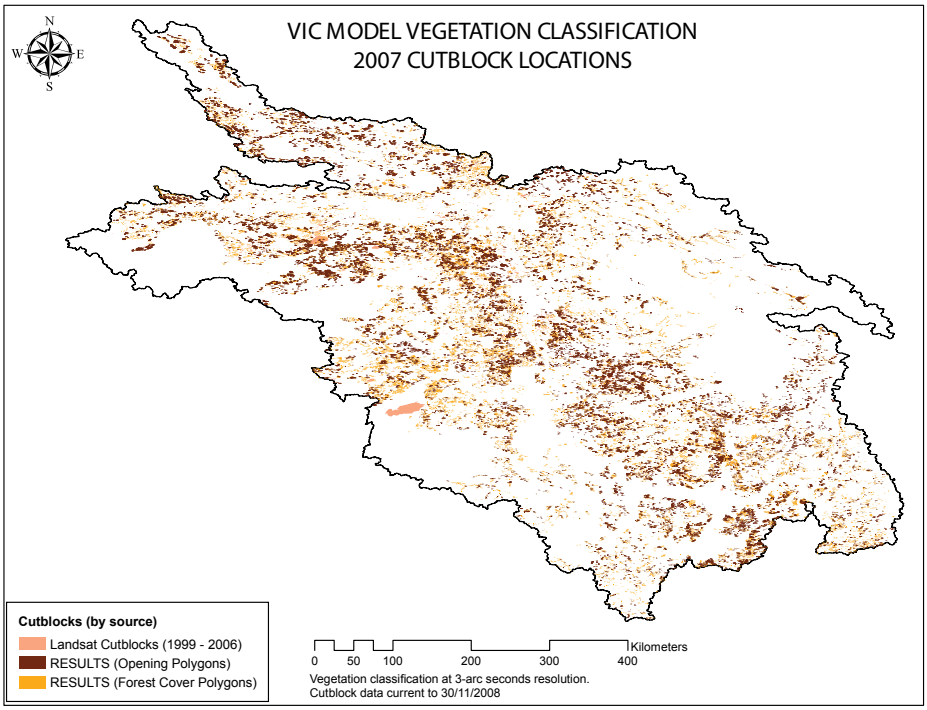

Figure 9. Estimated cutblock locations for 2007 forest cover. These locations are represented using the VOP vegetation class

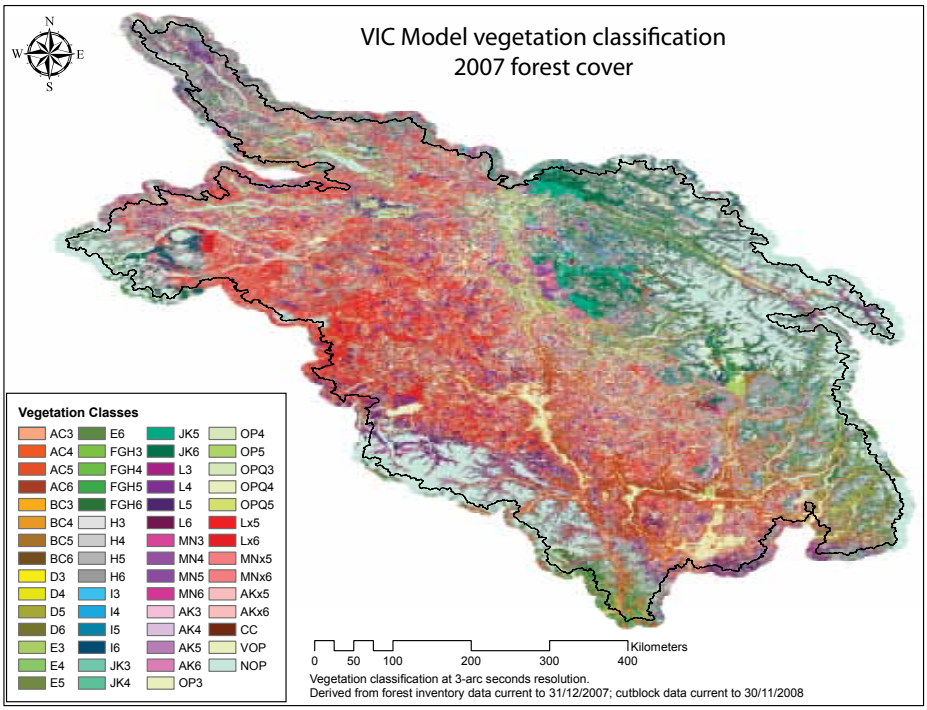

Figure 10. Distribution of vegetation classes for the 2007 forest cover

Table 3. Forest cover type area fractions, by classification year and disturbance scenario

COVER TYPE	Fraser River Basin area fraction by year		2007/1995 area ratio	Fraser River Basin area fraction by disturbance scenario				
	1995	2007		*95_100K*	*95_25HF*	*95_50HF*	*95_75HF*	*95_100HF*
AC	0.056	0.056	100	No change from 1995				
BC	0.026	0.026	1.00					
D	0.005	0.004	0.80					
E	0.011	0.011	1.00					
FGH	0.019	0.019	1.00					
H	0.098	0.098	1.00					
I	0.026	0.028	1.08					
JK	0.085	0.085	1.00					
L	0.167	0.059	0.35	0.030				
MN	0.109	0.046	0.42	0.016	No change from 95_100K			
AK	0.050	0.021	0.42	0.009				
OP	0.037	0.039	1.05	No change from 1995				
OPQ	0.003	0.003	1.00					
Lx	0.016	0.114	7.13	0.153	0.088	0.039	0.011	0.000
MNx	0.003	0.063	21.00	0.095	0.088	0.065	0.028	0.000
Akx	0.002	0.030	15.00	0.043	0.043	0.041	0.034	0.000
CC	0.003	0.003	1.00	No change from 1995				
VOP	0.118	0.135	1.14	0.118	0.190	0.263	0.336	0.409
NOP	0.166	0.160	0.96	No change from 1995				

2.4.3 Forest cover, 1995

The VRI database, which acts as the basis for this classification scheme, is a rolling database. Its data records are continuously updated, usually based on recent management activity or ongoing local inventory surveys. The VRI is thus assumed to represent "current" forest cover conditions, although there is considerable uncertainty as data can span several years, and even decades in some portions of the province (although stand age and height are projected to the current inventory year). Despite the temporal range, data in the VRI cannot be used to provide a snapshot of past forest inventory; such information must be inferred by other means. Inferring or "rolling-back" the 2007 forest cover to 1995 relied on a few simple assumptions. First, vegetation cover types (other than clearcuts and anthropogenic VOP) are assumed to be the same in 1995 and 2007. Second, age classification for 1995 was derived by subtracting 12 years from the 2007 projected stand age and re-assigning age classes based on the 1995 stand age. Third, stands classified as clearcuts were reclassified to the cover type assigned in the original base VRI record, assuming age class 6 (> 120 years). Fourth, all 2007 VOP classes were re-assigned based on the original cover type identified in the VRI (either remaining VOP in the case of natural openings or reverting to a treed vegetation cover at age class 6 in the case of anthropogenic openings).

Following the initial roll-back from 2007 to 1995, forest disturbance and harvest history for the 1995 forest cover classification was estimated from the British Columbia Ministry of Forests and Range's vegetation resource history data (from Forest Inventory Planning files). A VOP was assigned to polygons with a history ID indicating a logging disturbance and an activity start date between 1/1/1985 and 1/1/1995. Polygons with a history ID with logging as the disturbance and a start date between 1/1/1995 and 31/12/1995 were assigned as clearcuts.

Beetle-killed stands for the 1995 forest cover were identified using the aerial detection survey mapping (spatial data available from the LRDW under the title Forest Health Survey Data). Infested pine stands were assessed as those areas recording a mountain pine beetle infestation (either light' moderate, or severe) between 1982 (the earliest records) and 1995.

The final forest cover classification representing forest cover conditions in the Fraser River drainage for 1995 is shown in Figure 11. The fraction of each forest cover type within the Fraser River Basin is given in Table 3. In 1995 the basin, by area, was composed of approximately 33% healthy pine classes, only 2.5% beetle-killed pine, and 12% vegetated openings; 17% was non-vegetated, and the remaining 35.5% was composed of various non-pine forest cover types. Between 1995 and 2007, continued beetle attack reduced healthy pure, leading, and second pine stands by 65%, 58%, and 58%, respectively and increased beetle-killed pure, leading, and second pine stands roughly 7-, 21-15-fold, respectively. The incidence of vegetated openings increased 1.14 times between 2007 and 1995, whereas clearcut area remained the same. Given these vegetation class differences between 2007 and 1995 and the past decade's accelerated salvage harvesting, the 2007 forest cover may underestimate the actual extent of the VOP and CC classes.

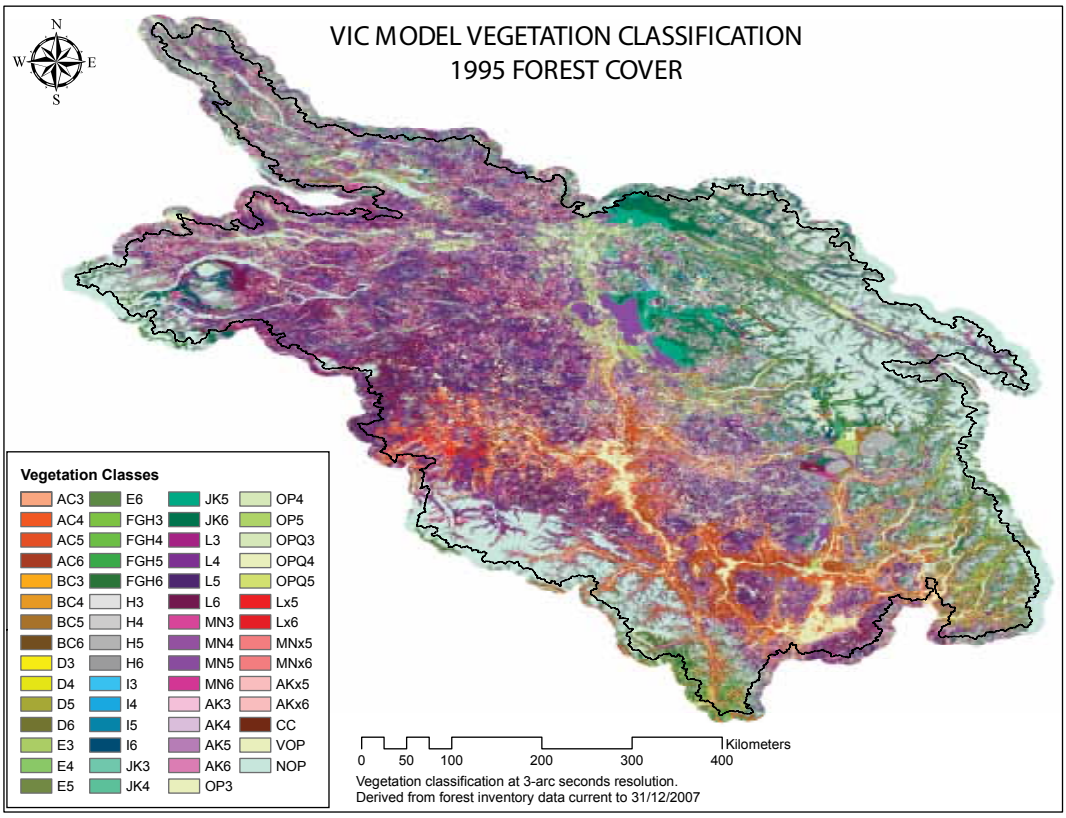

Figure 11. Distribution of vegetation classes for the 1995 forest cover

2.4.4 Vegetation parameters

The VIC model requires monthly leaf area index (LAI; one-sided projected leaf area per unit ground area) values for each treed vegetation class and age subclass. These LAI values were derived from the Canada-wide 1-km, 10-day LAI time series produced by Natural Resources Canada. This product is a SPOT-4 VEGETATION (VGT) satellite-derived 10-day composite LAI coverage of Canada at a 1-km resolution, shot in April through October 1998 through 2004. A more complete description is provided by Fernandes et al. (2003) and Abuelgasim et al. (2006). LAI values were estimated for all non-pine vegetation classes using the most current 2004 SPOT-4 VGT-based LAI product, as this was the closest capture date to the 2007 inventory data. Parameterization of LAI for beetle-killed pine stands was also based on the 2007 forest cover, but parameters were derived using only unharvested pine stands with more than 20% of its volume killed based on the 1999–2004 cumulative pine volume kill estimates (Eng et al. 2005). The AK, L, and MN vegetation cover types are meant to capture parameterizations for healthy pine (i.e., not beetle-attacked). However, as most pine stands within the Fraser River Basin were affected to some extent by beetle infestation in 2004, parameterization used the earliest LAI data from 1998 in conjunction with the 1995 forest cover. Still, even in 1998, the latest mountain pine beetle infestation was so extensive that only select regions of the Fraser were considered suitable for estimating LAI for healthy pine stands. Therefore, to avoid stands infested with the latest mountain pine beetle outbreak (commencing ca. 1995) or the previous outbreak in the Chilcotin (ca. 1985) (Wood and Unger 1996), estimation of LAI values for healthy pine-class stands was constrained to a small sub-region of the Fraser corresponding to the NTS 1:250 000 map sheets 092I, 092P, and 093J (not shown). An example of the spatial distribution of final grid cell-averaged LAI values within the Fraser River Basin is shown in Figure 12 for the June (i.e., summer) 1995 forest cover.

Following beetle attack, pine stands lose canopy coverage as dead pine trees lose all their needles within 3–5 years and most branches by 10–15 years, and their fall rate gradually increases over time, peaking at about 10–12 years (Huggard and Lewis 2008). Secondary structure—collectively, seedlings, saplings, sub-canopy, and canopy trees that will survive a beetle attack—even in pine leading stands, and natural regeneration over time keep canopy coverage from disappearing entirely following attack (Coates et al. 2006; FPB 2007b). Huggard and Lewis (2008; Effects of salvage options for beetle-kill stands on ECA: February 2008 Update, BC Ministry of Environment, unpublished report) modelled equivalent clearcut area (ECA) in pine stands in several biogeoclimatic units. They determined that unsalvaged stands have a low initial ECA (due to contributions from dead pine and non-pine over- and understorey), which peaks after about 10 years, then declines following natural regeneration and release; peak ECA values ranged from 40% to 90%. These trends are qualitatively reflected in the June LAI values for healthy and beetle-killed pine (Table 4). The beetle-kill LAI values are the median value for each vegetation class taken over a wide range of stand types in which beetle attack/kill is assumed to have occurred within the previous decade (i.e., sometime between 1995 and 2004). Beetle-kill reduces LAI by roughly 20% in 61–120-year-old stands and by 30% for stands older than 120 years.

Given the purpose of the VIC application to the Fraser River—namely, to model the effect of forest cover loss on streamflow generation—accurate parameterization of the effect of a vegetation canopy on radiation transmittance is crucial. The VIC model estimates the fraction of shortwave radiation transmitted by the overstorey using the Beer-Lambert model (Liang et al. 1994):

$$\tau_o = exp\ (-rad\_atten \quad LAI) \tag{1}$$

Table 4. June leaf area index (LAI) for healthy and beetle-killed pine classes

Age Class	LAI (m^2/m^2) for healthy pine cover types			LAI (m^2/m^2) for beetle-killed cover rypes		
	L	MN	AK	Lx	MNx	AKx
11–20	2.2	2.6	2.6	N/A	N/A	N/A
21–60	2.7	3.0	3.0	N/A	N/A	N/A
61–120	2.5	3.0	3.1	2.0	2.3	2.4
> 120	2.4	2.7	2.8	1.6	1.9	2.1

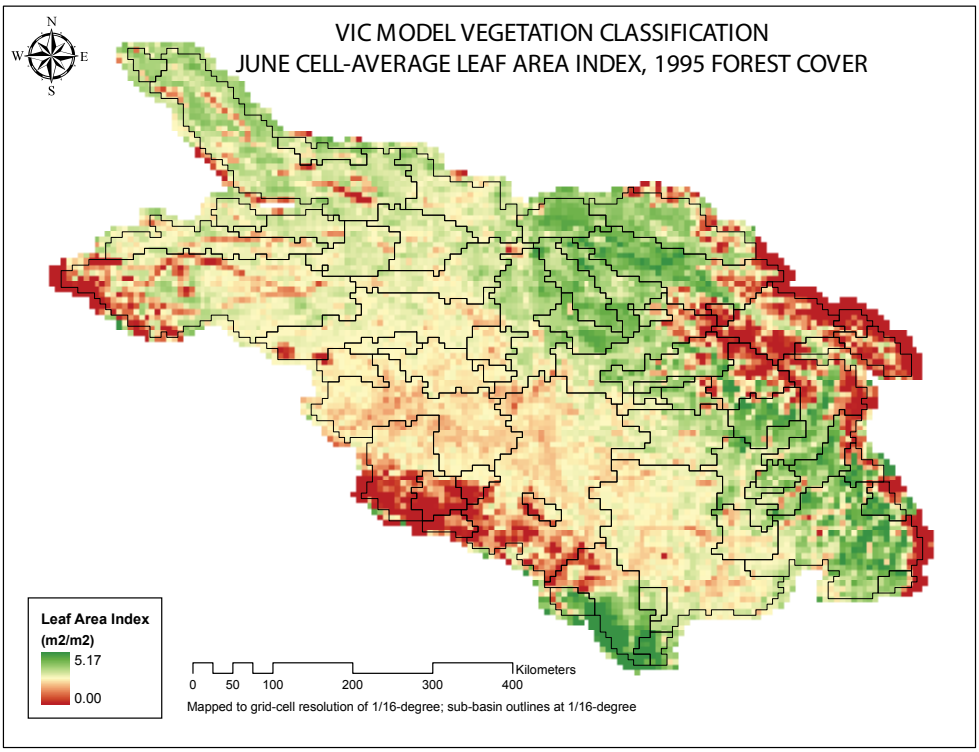

Figure 12. Distribution of VIC grid-cell average leaf area index for June 1995

where rad_atten is the canopy attenuation coefficient (Table 1). Using measurements of canopy transmittance (S_i / S_t; where S_i is below-canopy shortwave radiation and S_t is total incoming shortwave radiation) and LAI, Pierce and Running (1988) determined that 0.52 is an appropriate average extinction coefficient for conifer canopies. However, Duursam et al. (2003) concluded that rad_atten varies inversely with LAI, a relationship they describe with a non-linear regression model giving a range of rad_atten from 0.7 and 0.4; observed mean estimate rad_atten was 0.47. Canopy transmittance has also been measured in 36 lodgepole pine plots in the British Columbia Interior Plateau region (Teti 2009; R. Winkler, unpublished data). Using these measured values, along with several assumed values for rad_atten, Equation 1 was inverted to estimate leaf area index (LAI_{est}). The relationship between LAI_{est} and stand age was compared to the relationship between observed leaf area index (LAI_{VGT}) and stand age to qualitatively infer the most appropriate value for rad_atten (Figures 13 and 14 show results for healthy and infested lodgepole pine stands, respectively). These qualitative comparisons indicate that a canopy attenuation coefficient of 0.5 is a suitable value for lodgepole pine stands, which is close to mean observed values reported in the literature for conifers. A constant value of rad_atten = 0.5 was thus used for all vegetation classes.

Although not used directly in the VIC model, vegetation height, h, is used to estimate the roughness length ($rough$) and displacement height ($displacement$). As discussed earlier, vegetation height is taken directly from the VRI and is based on the projected height of the leading species in a given stand. Stand height for age classes 3–6 was set to its age range's median value for each vegetation type. Stand height for age class 2 was set to the median value across all vegetated cover types (0.5 m). Stand height was set to zero (0) for age class 1 (i.e., recent clearcut, stand age = 0 years). The parameters $rough$ and $displacement$ were set as functions of vegetation height (h), where $rough = 0.123h$ and $displacement = 0.67h$ (Campbell and Norman 1998).

Due to a lack of species- and age-specific information, the remaining parameters ($rarc$, $rmin$, $albedo$, RGL, $wind\_atten$, and $trunk\_ratio$) for the vegetation library were predominantly set to uniform values. Parameters $rarc$ and $rmin$ were set to 2.0 s/m and 100 s/m, respectively, for all vegetation types (except the NOP, where such parameters

do not apply) (Ducoudré et al. 1993; Shuttleworth 1993). Vegetation albedo varies with height and roughness of the vegetation: deep forest canopies' efficiency in trapping solar radiation makes their albedo much lower than that of short vegetation (Roberts 2000). Bare soil and rock also tend to have higher albedo than vegetation. Consequently, albedo was set to 0.12, 0.18, 0.13, 0.20, and 0.22 for coniferous, deciduous, clearcut, VOP, and NOP vegetation classes, respectively (Bras 1990; Campbell and Norman 1998); values were assumed uniform throughout the year. RGL was set to 30 W/m^2 for all vegetation classes, which is the approximate radiation threshold above which transpiration occurs (Dickinson et al. 1991; Roberts 2000). The $wind\_atten$ was set to 0.5 and $trunk\_ratio$ to 0.2 for all vegetation classes (VIC default value). Rooting depths were specified for each vegetation class such that short vegetation draws moisture mainly from the upper soil layer while trees draw moisture from deeper soil layers (Jackson et al. 1996). The final effective root distribution within the three model soil layers was determined during model calibration by allowing the depth of the second (middle) soil layer to vary.

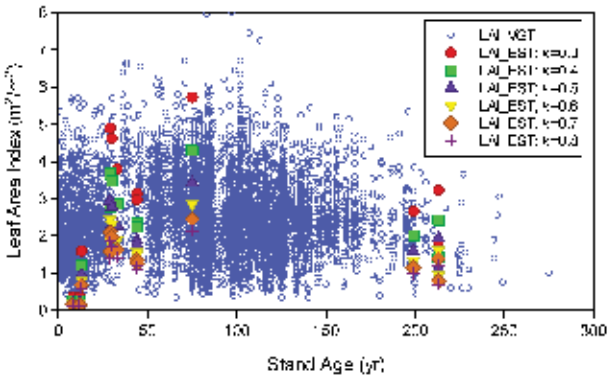

Figure 13. Observed leaf area index (LAI_{VGT}) versus estimated leaf area index (LAI_{est}) by inversion of Equation 1 using various values of the attenuation coefficient (rad_atten) and radiation transmittance observed in healthy pine stands (classes L3 through L6)

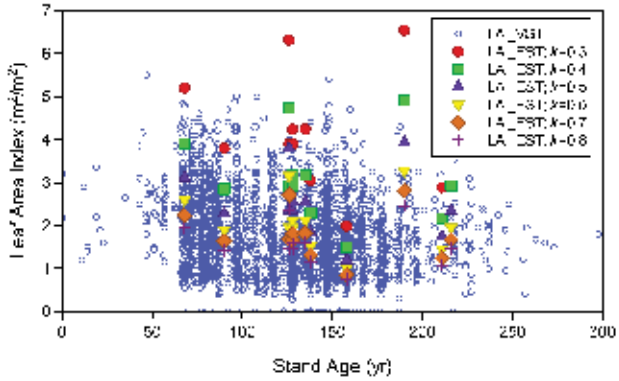

Figure 14. Observed leaf area index (LAI_{VGT}) versus estimated leaf area index (LAI_{est}) by inversion of Equation 1 using various values of the attenuation coefficient (rad_atten) and radiation transmittance observed in infested pine stands (classes L5x and L6x)

2.5 Surface routing and the drainage network

The VIC model simulates water flow by modelling surface runoff and baseflow for each grid cell to its outlet then into the river system (see Lohmann et al. 1996, 1998a, b, for a full description of the routing model methodology). The model assumes that river flow is the only way water leaves a grid cell. The in-grid dynamics of surface routing are described with a grid cell instantaneous response function (or IRF, i.e., unit hydrograph), and is intended to capture the flow of water through the sub-grid surface runoff network to the grid cell"outlet." Rivers are routed (i.e., surfaces between grid cells are routed) using the linearized Saint-Venant equations based on the model river network shown in Figure 15.

The model domain was divided into sub-basins of varying scale along the Fraser River main stem and most tributaries. Sub-basins were delineated based on the locations of Water Survey of Canada (WSC) hydrometric gauges whose streamflow data was suitable for calibration (see Section 2.6). Stations were considered suitable if data were available for the entire calibration/validation period and drainage area exceeded 400 km^2. Based on initial screening, 60 sub-basins qualified (Figure 15; see Appendix Table A2 for relevant metadata).

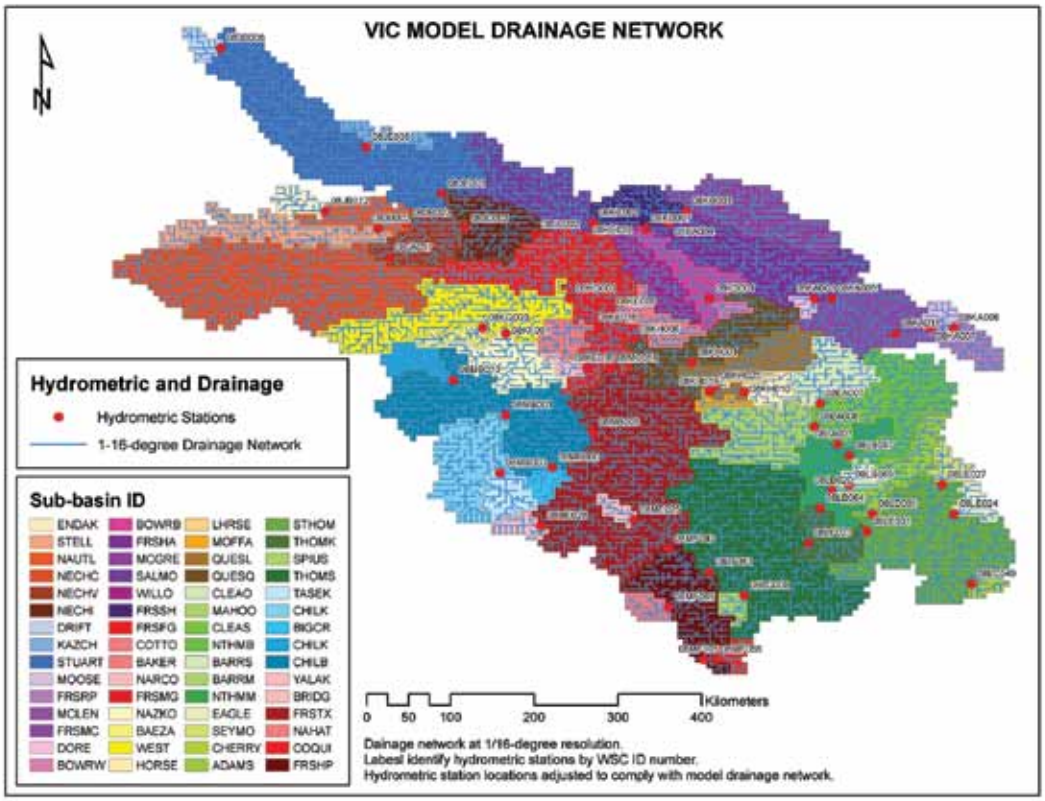

Figure 15. VIC model drainage schematic of the Fraser River Basin upstream of Hope showing the 1/16° model drainage network, WSC hydrometric sites, and sub-basin delineation.
Sub-basin IDs and WSC numbers are cross-referenced in Appendix Table A2.

2.6 Calibration and validation

2.6.1 Routing model

The grid cell IRF was not calibrated per se, but specified *a priori* based on certain assumptions. The VIC model and subsequent routing model are applied at 1/16° resolution, or approximately 27–32 km^2 per grid cell. At this scale, surface routing to the grid cell "outlet" takes several hours. At a daily time step, a grid cell with a runoff pulse will emit a discharge pulse at its outlet well within the step. Consequently, the IRF specifies that a runoff pulse generated in time step *t* routes 90% of its runoff to the grid cell outlet within the time step, and 100% of it within *t*+2. The delay in routing the final 10% accounts for sub-grid surface storage, such as in small lakes or wetlands. Calibration of the inter-cell surface routing network was simplified by classifying the drainage network into channels or lakes (not shown), with parameters estimated using streamflow observations at select nested gauging sites throughout the Fraser River Basin.

2.6.2 VIC model

Preliminary VIC model runs for the entire model domain revealed significant errors in estimating snow accumulation and ablation. Comparing simulated snow water to observations collected at snow pillows throughout the Fraser indicated the VIC model tends to underestimate peak snow accumulation and overestimate melt rate. Although it is acknowledged that inherent bias exists when comparing (simulated) area-average to (observed) point snow water, it was felt that, generally, too little snow was accumulating and snow was melting too fast and too soon in the simulations. Although the source of this error is not yet known (and may be related to errors in estimating solar radiation from temperature or to the need to account for slope and aspect at 1/16° resolution), the problem was corrected by adjusting the snow albedo curve parameters. Specifically, initial snow albedo was increased, and the rate of albedo decay was decreased during snow melt (see Figure 16). Additionally, the temperature thresholds governing precipitation type (rain or snow) were expanded from limits of –0.5° C–0.5° C to 0° C–6° C (i.e., no rain below 0° C; no snow above 6° C; see Figure 17). This relationship resembles the one used in the Canadian Land Surface Scheme (CLASS) model, version 3.1 (Bartlett et al. 2006), which was based on precipitation state observations at 39 stations across Canada. A similar relationship, albeit with bounds of 0° C and 4° C, is given by Gray and Prowse (1993).

VIC model grid cell fluxes were calibrated by using the Multi-Objective Complex Evolution (MOCOM) method (Yapo et al. 1998). MOCOM is an automated calibration technique that solves the multiple objective global optimization problems. As multi-objective problems rarely have unique solutions, MOCOM converges to and provides the Pareto set, which is the set of all parameter vectors that produce non-dominated values of the objective function vector. Automatic calibration was based on comparisons of observed and simulated daily discharge at the hydrometric locations identified in Section 2.5. Applying MOCOM required selecting multiple objective functions, which were chosen to constrain different aspects of the streamflow regime. For the Fraser River application of the VIC model, three objective functions were used. The first is the Nash-Sutcliffe Efficiency (NSE):

$$NSE = 1 - \frac{\sum_{t=1}^{T}(Q_o^t - Q_m^t)^2}{\sum_{t=1}^{T}(Q_o^t - \bar{Q}_o)^2} \quad (2)$$

where Q_o^t and Q_m^t are observed and modelled discharge, respectively, at time t, and $\bar{Q}_O$ is average observed discharge over time $t = 1$ to T. Nash-Sutcliffe efficiencies can range from $-\infty$ to 1. An efficiency of 1 ($NSE = 1$) indicates that the modelled discharge matches the observed data perfectly. An efficiency of zero ($NSE = 0$) indicates that the model predictions are no better than using the mean of the observed data, whereas an efficiency less than zero ($-\infty < NSE < 0$) indicates that the observed mean is a better predictor than the model. The second objective function is the NSE of the log-transformed discharge ($LNSE$). This is equivalent to Equation 2 except that the discharge values are substituted with the natural log-transformed values. The third objective function is the relative bias error which is

$$RB = 100 \cdot \frac{(\bar{Q}_m - \bar{Q}_o)}{\bar{Q}_o} \quad (3)$$

where $\bar{Q}_m$ is the average modelled discharge. All objective functions were calculated based on daily discharge. These three objective functions tend to produce parameter sets that create different simulated hydrographs. The NSE function tends to emphasize high/peak-flow periods and therefore produces parameters that optimize hydrograph performance during the freshet period. The $LNSE$ objective tends to place more uniform emphasis through the entire flow range, which generates parameter sets that have better hydrograph performance during the recession

and low-flow periods. The RB objective strictly emphasizes volume conservation over the calibration period and is robust to errors in streamflow timing or seasonality.

Calibrating the VIC model centers on adjusting empirical soil parameters that regulate soil infiltration, baseflow, and transpiration, as these are the least well-defined parameters within the VIC model (i.e., not directly observed and mostly conceptual). Specifically, runoff fluxes were calibrated by adjusting five soil parameters: $B\_infilt, Ds, Ws, Dsmax$ and $D2$. B_infilt divides net precipitation and snowmelt into surface (or quick) runoff and infiltration (and ultimately baseflow), affecting the flashiness of the hydrograph. Ds, Ws, and $Dsmax$ control baseflow discharge (Figure 2) and influence the overall magnitude and timing of the hydrograph. The baseflow curve influences the rate of change of soil moisture storage, which affects the volume of moisture available for transpiration. $D2$ specifies the depth of the second of three soil layers, which indirectly affects root partitioning between the second (unsaturated zone) and third (saturated zone) soil layers. Root partitioning in turn directly affects transpiration.

Automatic calibration by strictly adjusting the soil parameters assumes that precipitation, P, in the driving data is without error and that adjusting evaporation and soil storage produces the correct runoff for any given grid cell. This assumption is valid for the majority of sub-basins and achieves a reasonable calibration. However, in the handful of sub-basins where very large RB prevents the simulated and observed streamflow hydrographs from converging, precipitation is unconstrained and allowed to vary by introducing the $Padj$ parameter into the automatic calibration process. The $Padj$ parameter is a precipitation multiplicative factor that is applied uniformly to grid-cell precipitation within a sub-basin, i.e., adjusted precipitation $P' = Padj \quad P$. Applying all six parameters to the relevant cases produced vastly superior calibration results than were achieved using only the five original soil parameters. Final $Padj$ values for those basins requiring such adjustment are shown in Figure 18. The distribution of $Padj$ parameters reveals a bias in the driving precipitation data, with precipitation overestimated along the leeward side of the Coast Mountains ($Padj < 1.0$) and underestimated along the windward side of the Columbia and Rocky Mountains ($Padj > 1.0$). Such biases are expected, considering grid-cell precipitation values are interpolated from limited information in a sparse climate network weighted towards lower elevations (Stahl et al. 2006).

Calibration and model validation are based on streamflow observations between January 1, 1985, and December 31, 1995. This period was chosen for its relatively stable forest cover (it was during a respite from major mountain pine beetle outbreaks in the Fraser). In addition, the pre-disturbance 1995 forest cover, which is already extrapolated (or "rolled-back") from the 2007 VRI snapshot, can be used as a reasonably accurate representation of forest cover during this period. An earlier calibration period would require extrapolating the forest cover data further into the past. VIC parameters were calibrated for each sub-basin. Downstream sub-basins (i.e., not headwaters) were calibrated to local inflow only, where discharge from upstream sub-basins was supplied as a boundary condition in the form of observed streamflow. The sub-basin containing the Nechako Reservoir (sub-basin NECHC; see Figure 15 and Appendix Table A2) was calibrated using a naturalized discharge time series, where effects of regulation and diversion were removed (A. Chapman, River Forecast Centre, BCMoE, unpublished data). Six years (1985–1990) were used directly for model calibration, four years (1991–1995) were held back for validation, and the year 1984 was used for model spin-up.

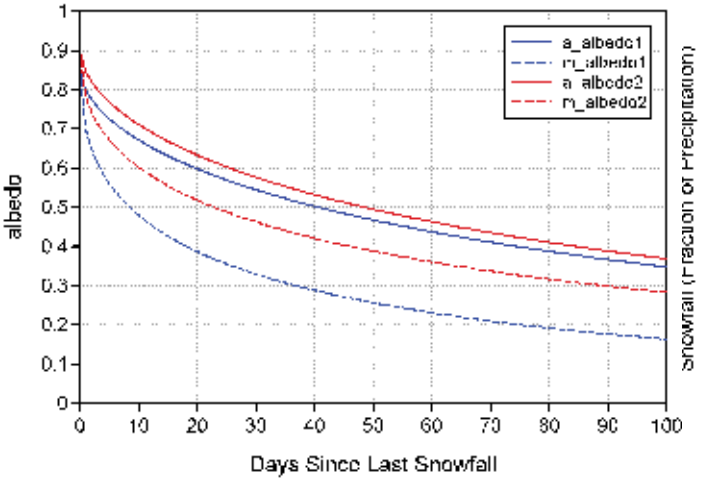

Figure 16. Various parameterizations of the accumulation and melt snow albedo curves. The final calibrated model utilizes the *a_albedo2* decay rate for snow accumulation and the *m_albedo2* decay rate for melt conditions.

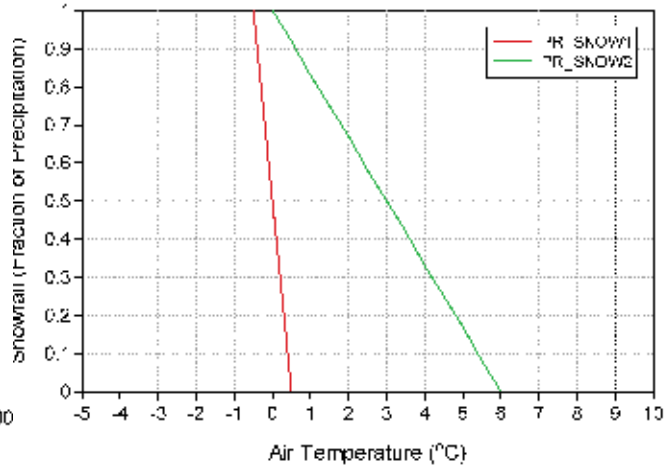

Figure 17. VIC model relationship between proportion of precipitation falling as snow and air temperature. *PR_SNOW1* is the original relationship; *PR_SNOW2* relationship is used in the calibrated model.

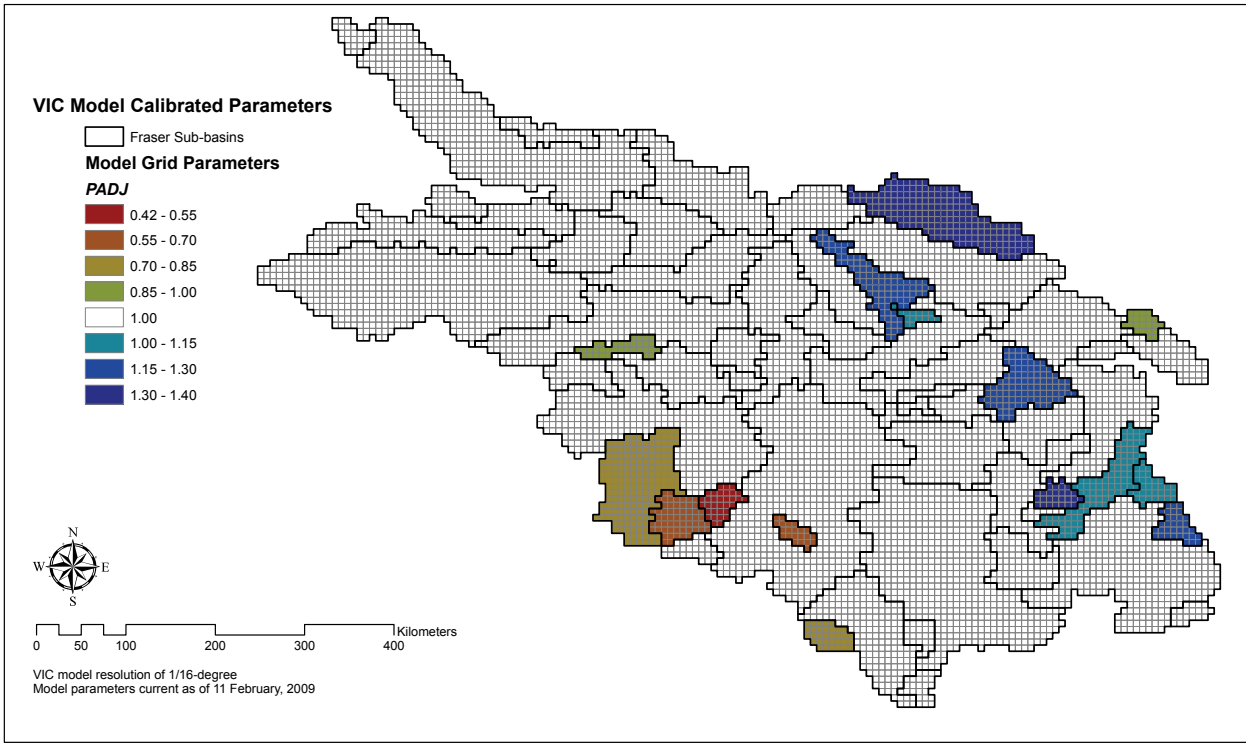

Figure 18. Final *Padj* parameters for the VIC Fraser River application

2.6.3 Calibration results

Results of the combined routing and VIC model calibration are summarized in Table 5. Final screening revealed some data limitations, which prevented calibration of some sub-basins; results are included for only 48 sub-basins. The final parameter vector for each sub-basin was chosen from the respective Pareto set to maximize NSE performance while still, where possible, keeping RB within ± 10%. Such parameter selection was often at the expense of $LNSE$ performance. Consequently, the model performed better during calibrating and validating for NSE than for $LNSE$, indicating that the model is tuned to represent the high-flow, or freshet, periods better than the low-flow periods. Most sub-basins have a negative RB (for both calibration and validation periods)—that is, they fail to simulate sufficient runoff, indicating a bias in either the precipitation forcing (too low) or the representation of evaporation (too high). Nevertheless, RB tends to be within ± 0.20 during the calibration period [with some notable exceptions, specifically SALMO (0.45), NAZKO (0.47), SPIUS (0.53) and COQUI (0.34)]. For most sub-basins NSE and $LNSE$ values are > 0.60 during the calibration period. Sub-basins SPIUS and COQUI performed poorly, attaining negative NSE values. Both are small headwaters in the wet/dry transition of the Cascades in the southern-most part of the Fraser basin. As expected, performance tends to degrade during the validation period. RB values generally increase during the validation period, however, the RB performance is substantially poorer for many basins in the relatively arid Fraser Plateau and Chilcotin basin (i.e., BAEZA, BAKER, BIGCR, CHILB, CHILK, TASEK, and WEST). The NSE and $LNSE$ values also indicate poorer performance during the validation period, though to a lesser extent than RB; most sub-basins still have NSE and $LNSE$ values > 0.60. A comparison of modelled and observed discharge is shown for some select sub-basins in Figure 19. Figure 19a plots discharge for the calibration and validation period for Fraser River at Hope, which is the entire study basin (217 000 km^2). Figure 19b shows the South Thompson River at Chase (16 200 km^2), which simulates discharge from the Shuswap Lake basin, with headwaters in the Columbia Mountains. Figure 19c shows the Chilko River (6 940 km^2) located in the headwaters of the Chilcotin River, a high elevation, high relief sub-basin draining the leeward side of the Coast Mountains. Figure 19e shows Baker Creek (1 570 km^2), a small, relatively low-relief basin located in the semi-arid Fraser Plateau.

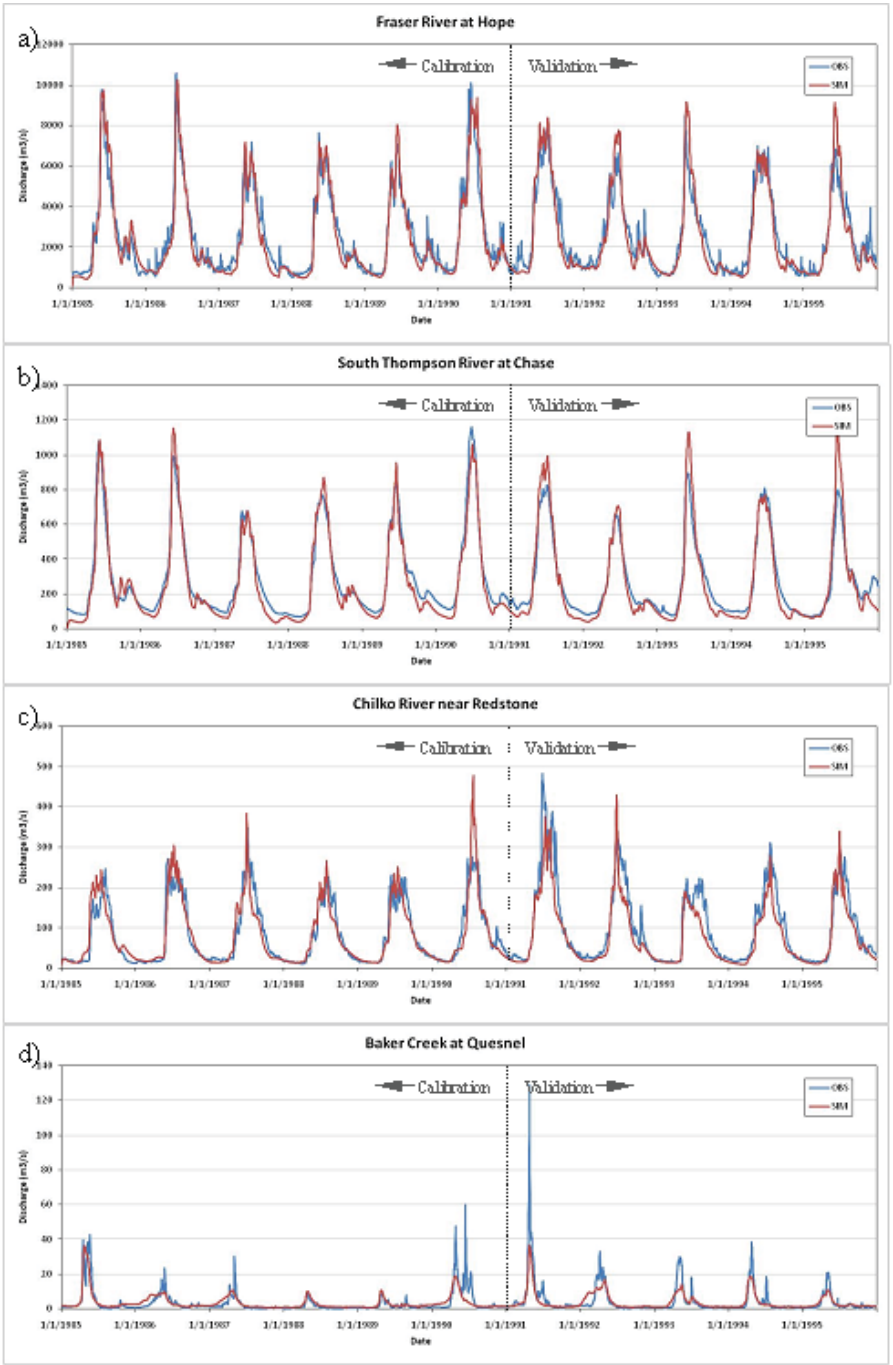

Area = 216 627 km^2

Calibration:	*Validation*:
NSE = 0.93	NSE = 0.87
$LNSE$ = 0.88	$LNSE$ = 0.87
RB = –0.04	RB = –0.05

Area = 15 656 km^2

Calibration:	*Validation*:
NSE = 0.94	NSE = 0.88
$LNSE$ = 0.73	$LNSE$ = 0.76
RB = –0.10	RB = –0.05

Area = 6 604 km^2

Calibration:	*Validation*:
NSE = .84	NSE = 0.81
$LNSE$ = 0.92	$LNSE$ = 0.89
RB = –0.02	RB = –0.21

Area = 1 552 km^2

Calibration:	*Validation*:
NSE = 0.61	NSE = 0.66
$LNSE$ = 0.72	$LNSE$ = 0.82
RB = 0.01	RB = –0.18

Figure 19. Observed and simulated discharge for a) the Fraser River at Hope (FRSHP), b) the South Thompson River at Chase (STHOM), c) the Chilko River near Redstone (CHILK), and d) Baker Creek at Quesnel (BAKER). Basin area and calibration / validation statistics are shown to the right of each respective panel.

Table 5. VIC model discharge performance statistics, by sub-basin

Sub-basin	Calibration Statistics				Validation Statistics			
	N	*RBIAS*	*NSE*	*LNSE*	*N*	*RBIAS*	*NSE*	*LNSE*
STELL	2191	0.01	0.79	0.70	1826	-0.10	0.64	0.77
NAUTL	2191	0.02	0.77	0.76	1826	-0.04	0.65	0.71
NECHV	2191	0.01	0.96	0.94	1826	0.01	0.92	0.90
NECHI	2191	0.05	0.87	0.76	1826	0.08	0.86	0.76
DRIFT	2191	-0.16	0.81	0.75	1598	-0.04	0.86	0.78
STUAR	2191	-0.07	0.79	0.52	1826	-0.02	0.82	0.68
DORE	2191	-0.01	0.73	0.86	1826	-0.03	0.69	0.83
FRSHA	2191	-0.04	0.86	0.81	1826	0.02	0.73	0.69
FRSMC	2191	-0.05	0.80	0.84	1826	-0.04	0.73	0.83
FRSRP	2191	0.02	0.82	0.91	1826	0.07	0.85	0.92
MOOSE	2191	-0.01	0.73	0.89	1826	0.01	0.78	0.90
FRSSH	2191	-0.10	0.88	0.77	1826	-0.03	0.77	0.67
MCGRE	2191	-0.04	0.78	0.34	1826	0.12	0.54	0.32
SALMO	2191	0.48	0.69	0.58	1662	0.47	0.66	0.61
BOWRW	2132	-0.06	0.83	0.43	1826	-0.02	0.56	0.07
WILLO	2191	-0.09	0.71	0.54	1826	0.04	0.54	0.48
BOWRB	2191	-0.02	0.86	0.60	1826	0.02	0.74	0.45
COTTO	2191	-0.09	0.61	0.66	1826	-0.13	0.59	0.63
BAKER	2191	0.01	0.61	0.72	1826	-0.18	0.66	0.82
NAZKO	608	0.47	0.54	0.41		No Data		
WEST	2191	0.00	0.78	0.84	1826	-0.22	0.63	0.83
BAEZA	2191	0.01	0.55	0.48	1826	-0.22	0.39	0.64
QUESL	2191	-0.21	0.86	0.57	1826	-0.22	0.78	0.42
QUESQ	2191	-0.20	0.85	0.49	1826	-0.20	0.77	0.47
HORSE	2191	0.13	0.61	0.83	1826	0.05	0.51	0.71
MOFFA	1954	0.08	0.64	0.85		No Data		
CLEAS	2191	-0.10	0.89	0.81	1826	-0.17	0.85	0.67
CLEAO	2191	-0.16	0.78	0.35	1579	-0.19	0.79	0.22
BARRM	2191	-0.05	0.88	0.90	1826	-0.11	0.90	0.93
NTHMB	2191	-0.06	0.76	0.68	1826	-0.11	0.79	0.69
NTHMM	2191	-0.10	0.90	0.80	1826	-0.15	0.87	0.72
BARRS	2191	-0.03	0.88	0.92	1826	-0.10	0.88	0.92
ADAMS	2191	-0.07	0.85	0.69	1826	-0.05	0.82	0.72
EAGLE	2191	-0.03	0.79	0.39	1826	-0.05	0.78	0.44
SEYMO	2191	-0.05	0.79	0.17	1826	-0.06	0.75	0.21
STHOM	2191	-0.10	0.94	0.73	1826	-0.05	0.88	0.76
THOMS	2191	-0.07	0.94	0.81	1826	-0.12	0.90	0.73
SPIUS	2191	0.53	-0.84	0.74	1826	0.26	-0.25	0.61
CHILK	2191	-0.02	0.84	0.92	1826	-0.21	0.81	0.89
TASEK	2191	-0.03	0.76	0.90	1826	-0.20	0.74	0.87
CHILB	2191	0.06	0.82	0.90	1826	-0.18	0.79	0.89
BIGCR	2191	-0.03	0.60	0.88	1826	-0.32	0.45	0.82
FRSMG	2191	-0.04	0.92	0.88	1826	-0.01	0.85	0.86
YALAK	2191	0.02	0.76	0.86	1826	-0.12	0.67	0.86
FRSHP	2191	-0.04	0.93	0.88	1826	-0.05	0.87	0.87
FRSTX	2191	-0.04	0.90	0.88	1826	-0.04	0.84	0.85
NAHAT	1824	-0.07	0.56	0.49	1825	-0.21	0.35	0.33
COQUI	1092	0.34	-0.36	0.40	1826	0.22	-0.47	0.16

2.7 Forest cover scenarios

The sensitivity of the Fraser River and its sub-basins to beetle and anthropogenic forest disturbance (based on sub-basins shown in Figure 15) was assessed using several hypothetical forest cover scenarios. Due to uncertainties in the VRI and RESULTS databases, forest cover conditions for 1995 and 2007 should only be considered estimates, particularly regarding harvesting during that time. Further, converting projections of actual planned harvest operations and subsequent silvicultural treatments into VIC model scenarios was not feasible. Consequently, the scenarios are considered hypothetical, and they investigate the local and regional sensitivity of the Fraser River study area by subjecting the model domain to increasingly severe snapshots of forest disturbance. They are not intended to portray an actual timeline of forest disturbance.

Scenario construction was based on the following assumptions:

a) when the current outbreak ends, most, if not all, the mature pine in the Fraser River Basin will have been killed by the beetle;

b) harvesting will occur only in dead pine stands; and

c) any imposed disturbance will be spatially uniform (e.g., if all pine-leading stands in the Fraser River are assumed dead with a 50% salvage harvest, the salvage harvest will be imposed as 50% salvage of all pine-leading stands in each respective model grid cell).

Seven forest cover scenarios were developed:

1) *95_BASE:* Baseline based on the 1995 forest cover (Section 2.4.3);

2) *07_CURR:* Current conditions based on the estimated 2007 forest cover (Section 2.4.2);

3) *95_100K:* Infestation terminates with 100% kill of all mature lodgepole pine from *95_BASE;*

4) *95_25HF:* Scenario *95_100K* plus 25% harvest by area of beetle-killed pine;

5) *95_50HF:* Scenario *95_100K* plus 50% harvest by area of beetle-killed pine;

6) *95_75HF:* Scenario *95_100K* plus 75% harvest by area of beetle-killed pine; and

7) *95_100HF:* Scenario *95_100K* plus 100% harvest by area of beetle-killed pine.

The hypothetical disturbance scenarios *95_100K* through *95_100HF* were constructed by manipulating the pine (L5, L6, MN5, MN6, AK5, and AK6), dead pine (Lx5, Lx6, MNx5, MNx6, AKx5, and AKx6), and VOP cover types (Table 2). For example, Scenario *95_100K* converts all vegetation classes L5, L6, MN6, MN6, AK5, and AK6 to classes Lx5, Lx6, MNx5, MNx6, AKx5, and AKx6, respectively; Scenario *95_25HF* converts 25% by area of classes Lx5, Lx6, MNx5, MNx6, AKx5, and AKx6 to class VOP. Given the nature of the VIC model, one cannot explicitly resolve or address harvest-related issues at the sub-grid scale of the model resolution (< 27–32 km^2), such as the effects of road density or layout on runoff and infiltration or the spatial distribution of cut blocks/buffers. A summary of forest cover types by scenario is provided in Table 3. Disturbance scenarios employ the VOP vegetation class to represent forest harvesting, not the CC (i.e., clearcut) class. This assumes that scenarios *95_25HF* through *95_100HF* portray a snapshot disturbance landscape that has been salvage harvested within the prior decade. For these scenarios the CC class is retained mainly to capture 1995 and 2007 forest cover conditions. Several hypothetical disturbance scenarios depict an extreme (i.e., *95_75K* and *95_100K*) extent of forest harvesting; nevertheless, they are included to show the upper limit in terms of potential hydrologic impacts. The spatial distribution of beetle-killed pine and vegetated openings (VOP) for the various scenarios is shown in Figures 20 to 27. Each scenario is forced with the 1915–2006 driving data; however, the year 1915 is used for model spin-up (to remove any memory of the initial model state) and subsequently discarded from further analysis.

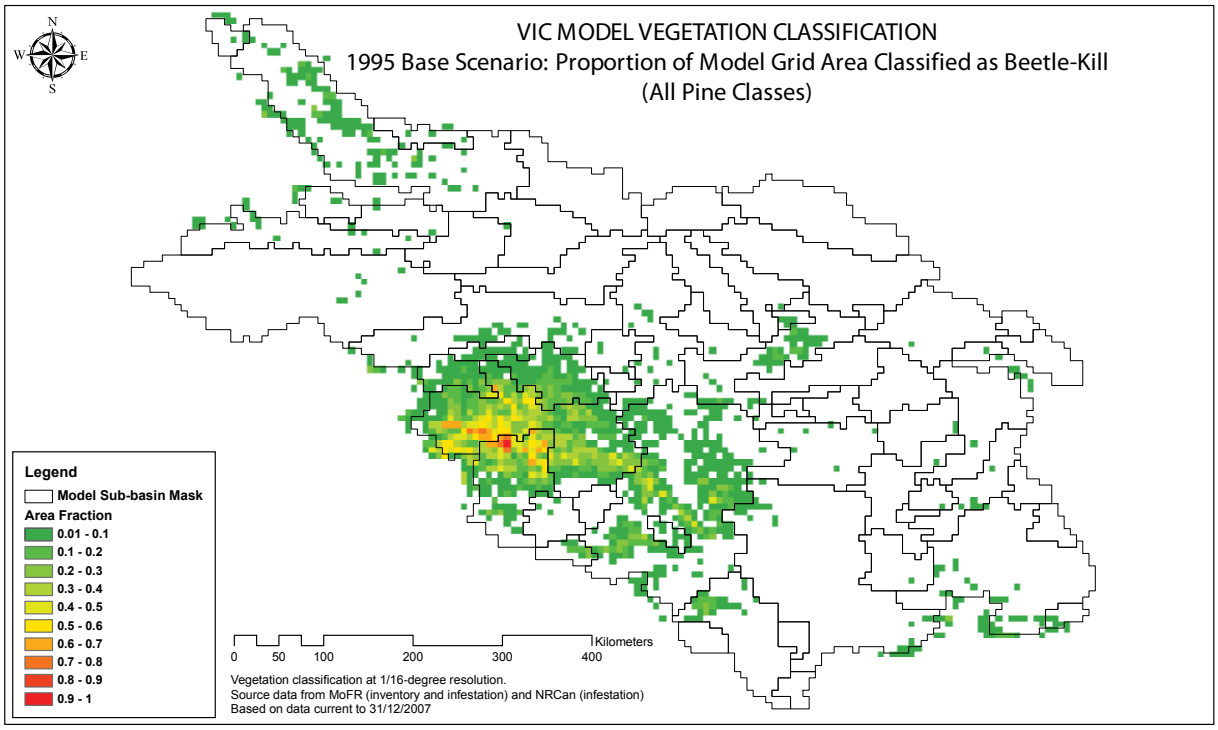

Figure 20. Area fraction of beetle-killed pine (all pine classes: Lx5, Lx6, MNx5, MNx6, AKx5, and AKx6) within each VIC model grid for 1995 forest cover

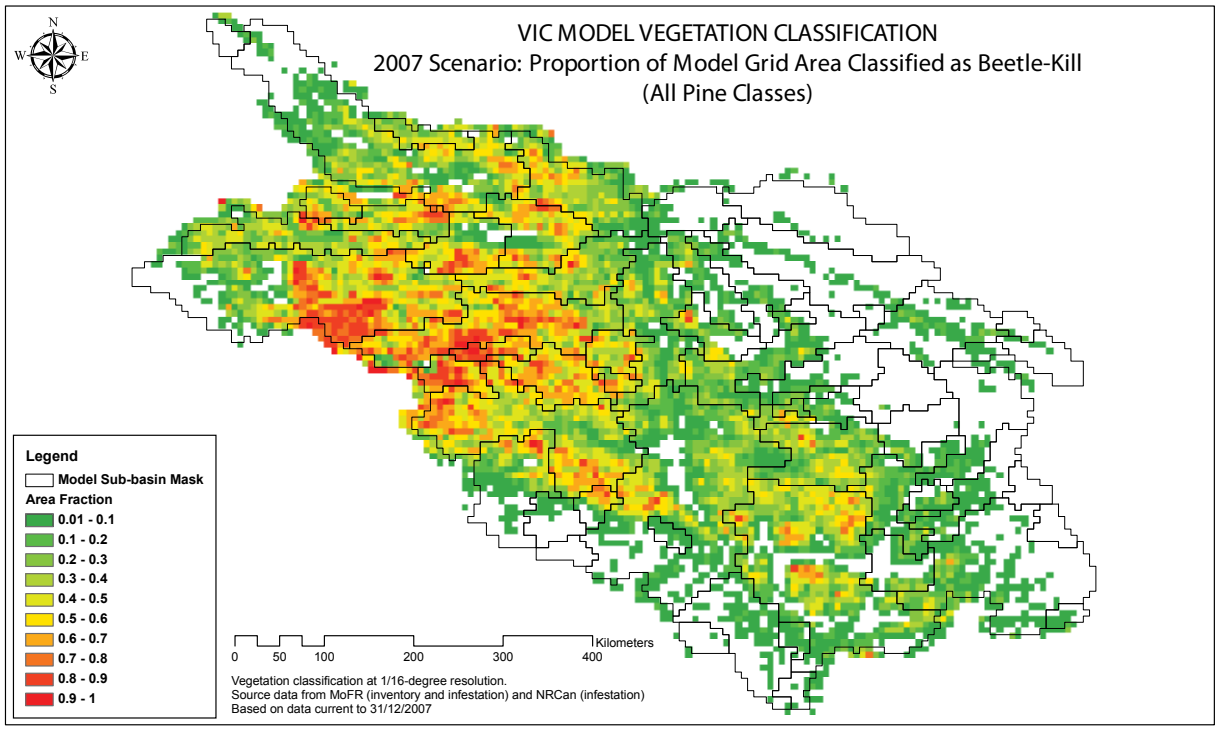

Figure 21. Same as Figure 20, but for 2007 forest cover

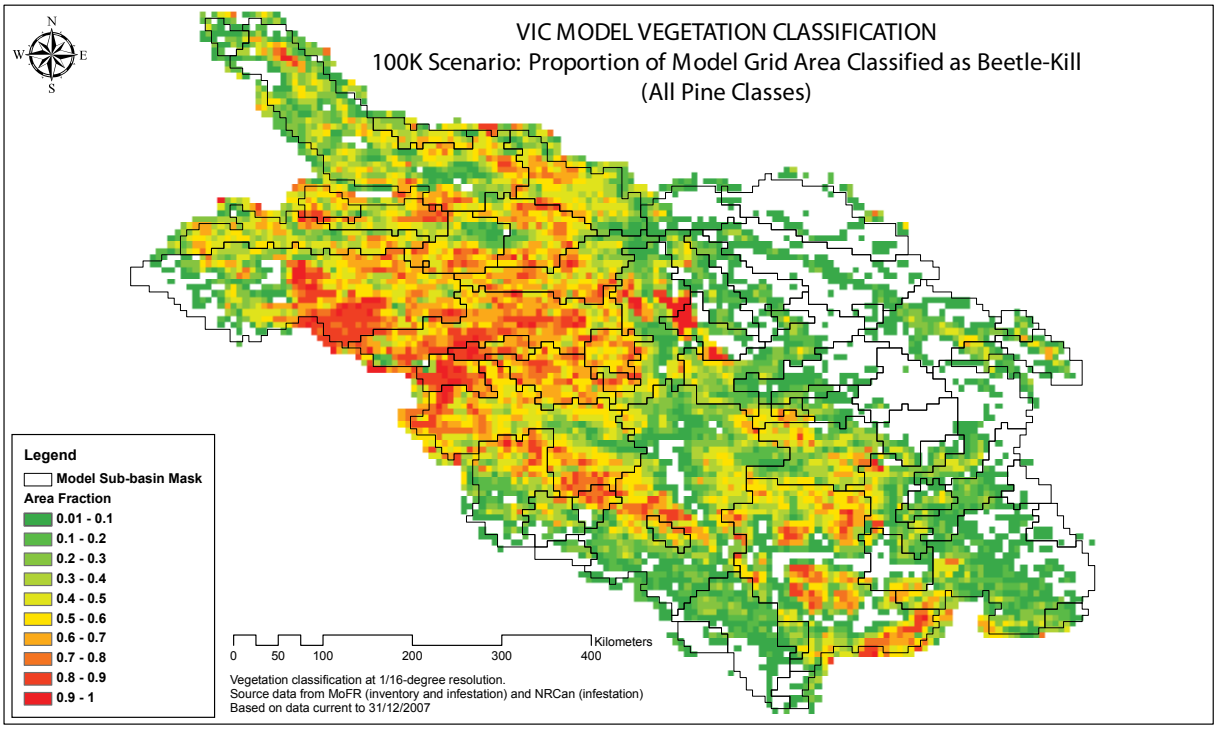

Figure 22. Same as Figure 20, but for scenario *95_100K*

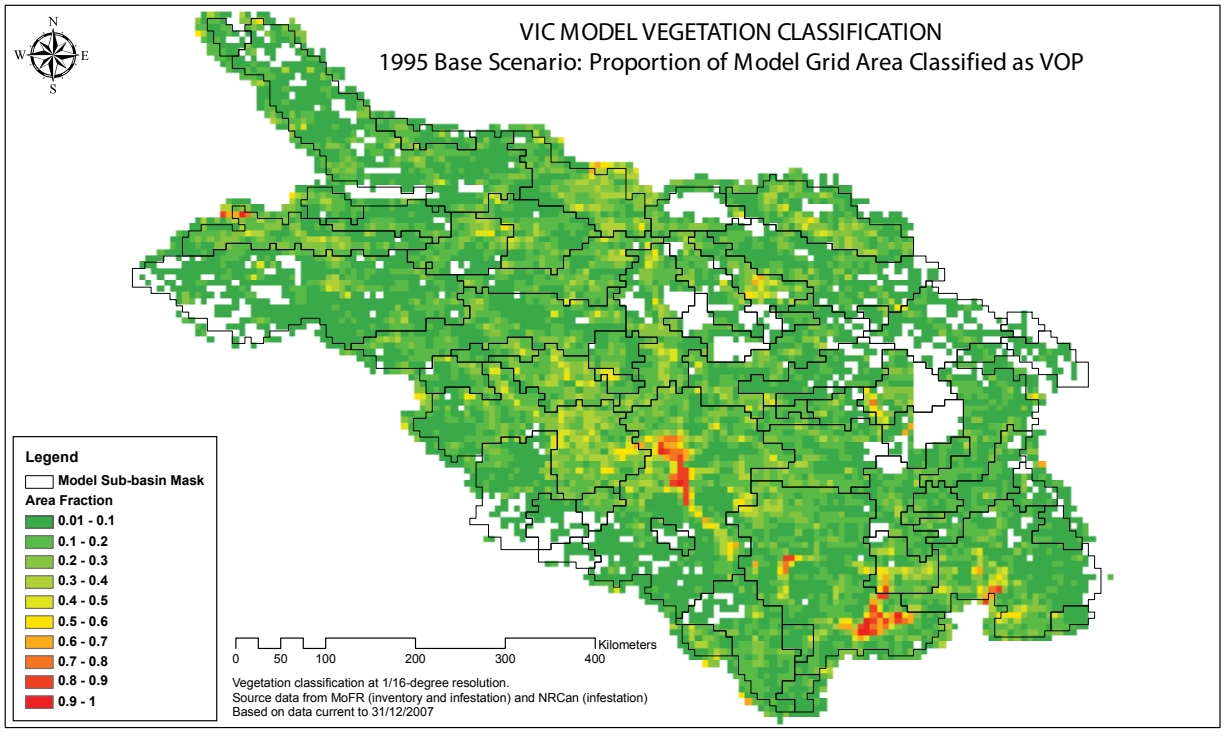

Figure 23. Area fraction of *VOP* (natural and anthropogenic openings) class within each VIC model grid for 1995 forest cover

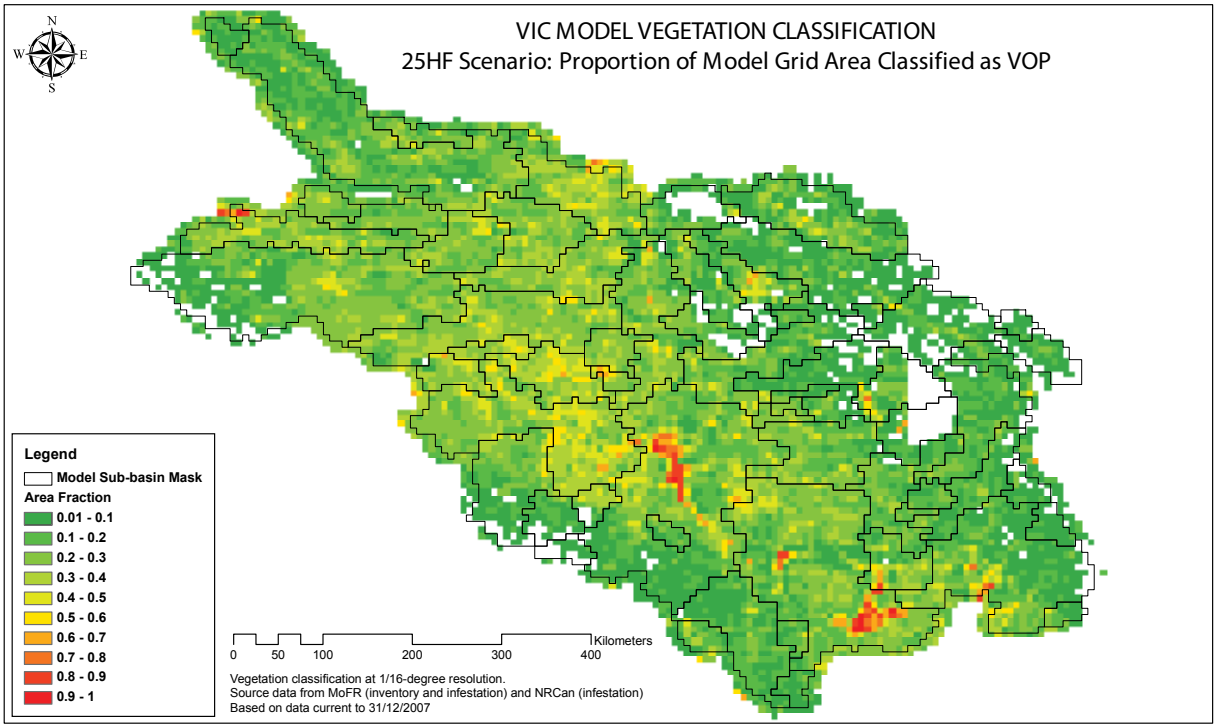

Figure 24. Same as Figure 23, but for scenario *95_25HF*

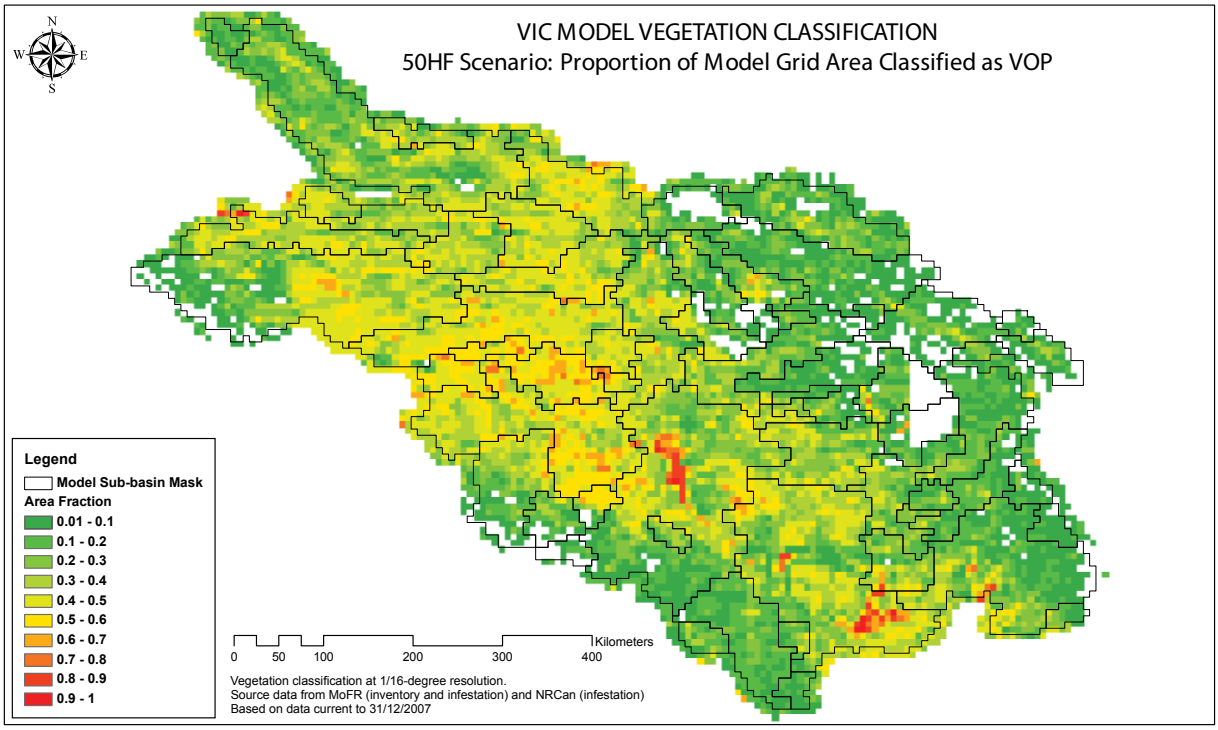

Figure 25. Same as Figure 23, but for scenario *95_50HF*

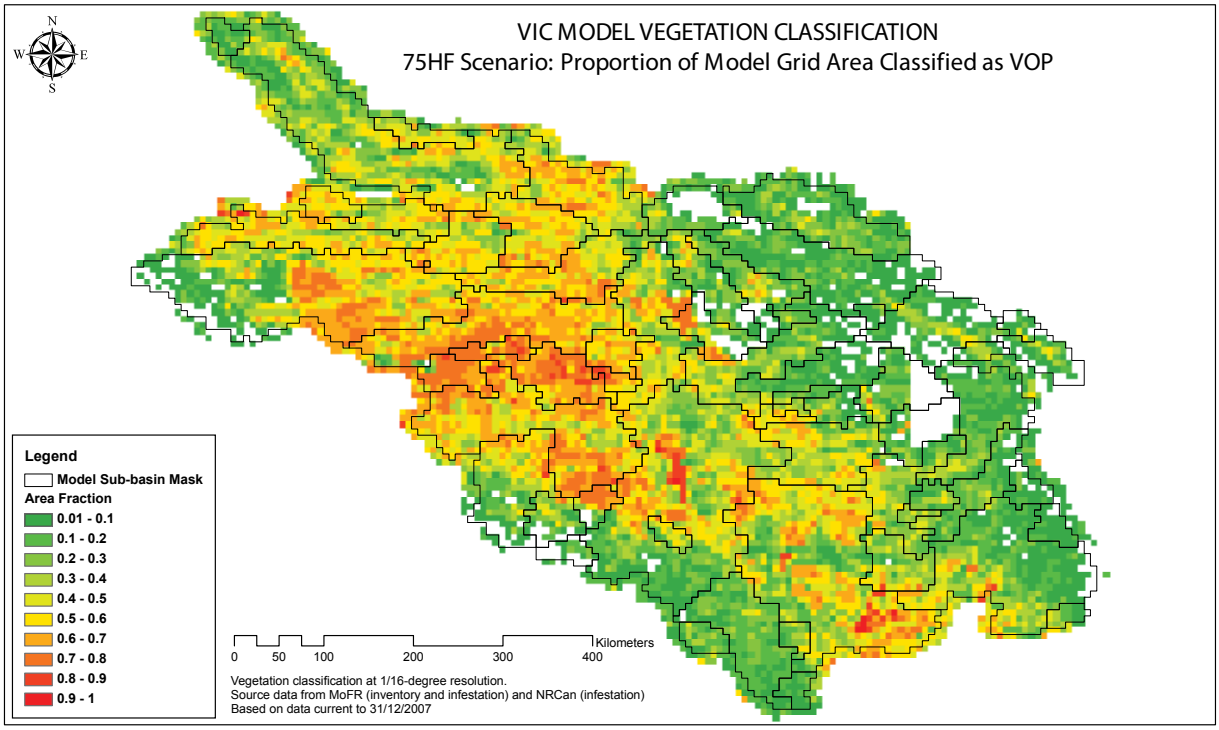

Figure 26. Same as Figure 23, but for scenario *95_75HF*

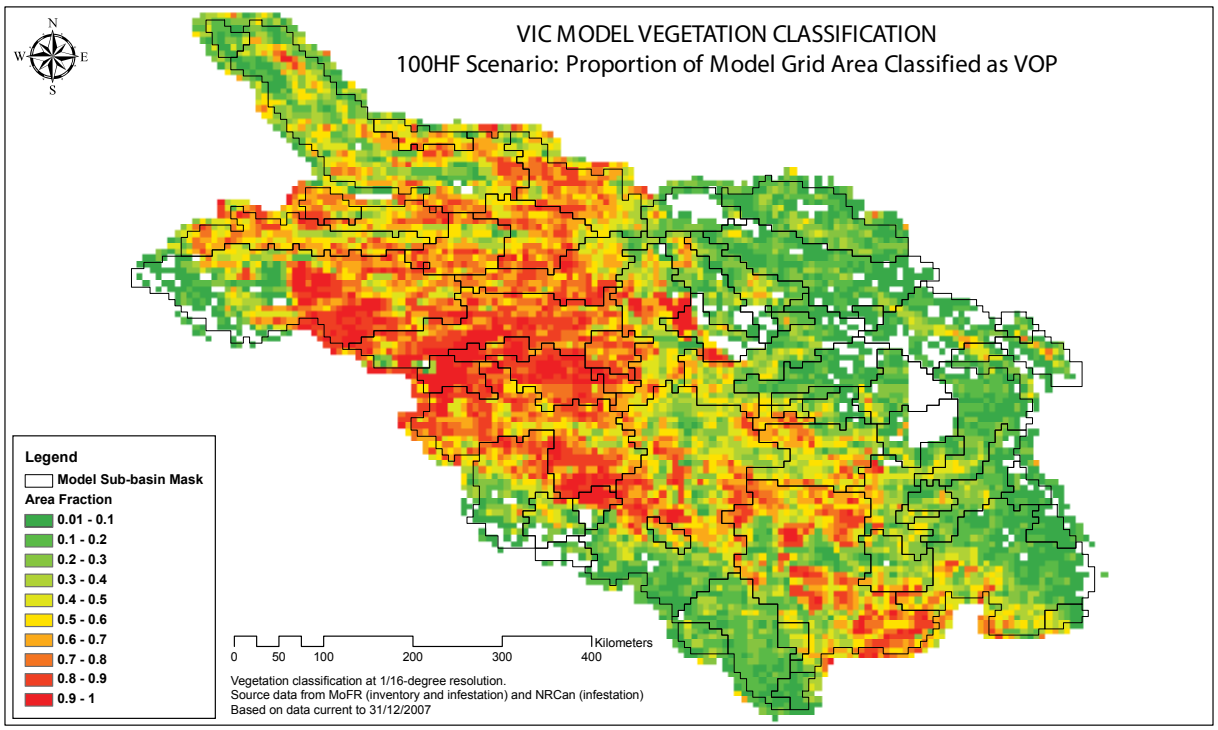

Figure 27. Same as Figure 23, but for scenario *95_100HF*

3. Results and discussion

3.1 Fraser River Basin baseline hydro-climatology

The simulated baseline hydro-climatology for the Fraser River Basin is shown in Figure 28. Its hydro-climatology fields are based on the average grid-cell fluxes (precipitation, evapotranspiration, and runoff) or states (snow water) simulated using the 1995 forest cover (Scenario 95_BASE) run using the 1916–2006 driving data. The fields represent contoured values rather than raw grid cell output. The hydro-climatology does not reconstruct actual hydro-climatology because the static 1995 forest cover does not represent actual forest cover change or disturbance between 1916 and 2006. The baseline hydro-climatology qualitatively assesses overall VIC model performance, details the spatial distribution of major water balance components, and provides context to the peak-flow regime changes presented below.

As the precipitation climatology (Figure 28a) is derived directly from the driving data (except for a $Padj$ factor for basins shown in Figure 18), it qualitatively resembles the 1961–1990 climatology shown in Figure 6. Precipitation is highest along the spine of the Coast and Rocky Mountains and also is high in the Columbia Mountains. Precipitation gradients within the basin are strong, ranging from over 3000 mm/year in the Coquihalla basin near the outlet to less than 500 mm/year throughout much of the Fraser Plateau. The spatial pattern of annual average precipitation translates into a similar pattern for annual average April 1st snow water equivalent (Figure 28b). Snow water accumulates with elevation, ranging from over 2000 mm in parts of the Coast, Rocky, and Columbia Mountains to less than 300 mm in much of the Fraser Plateau.

Evapotranspiration—collectively transpiration, canopy evaporation, bare soil evaporation, and snow sublimation—correlates highly with vegetation density, as shown by the June LAI values (Figure12). Its annual average varies from less than 200 mm in bare alpine regions to more than 600 mm in densely vegetated areas along the windward side of the Columbia, Rocky, and Cascade Mountains (Figure 28c). Some areas of near-permanent snow cover at very high elevation have simulated evapotranspiration values less than zero, which implies that annual condensation exceeds evaporation.

Average annual runoff, composed of baseflow and quick flow, is highest in areas of high precipitation (and snow water) and low evapotranspiration (Figure 28d). It has a strong gradient, ranging from over 2500 mm at high elevations to 200 mm or less throughout most of the Fraser Plateau. Strikingly, the headwaters of the Nechako, Chilcotin, upper Fraser, lower Fraser, and North and South Thompson, collectively a small area, generates a high runoff production of more than 1000 mm/year, which is roughly 80% of the total flow at Hope (not shown).

3.2 Peak-flow regime changes

Peak-flow regime changes are initially assessed using the frequency analysis technique, which compares the cumulative density function of peak-flow events quantile by quantile between the baseline Scenario 95_BASE and respective disturbance scenarios. Using the discharge simulated with the 1916–2006 driving data, the annual maximum peak-flow event for each year is applied to generate a sub-sample of 91 peak-flow events for each scenario. Assuming that annual maximum peak flow can be represented as the random variable Y, the pth quantile y_p is estimated as

$$F_Y(y_p) = p \tag{4}$$

where F_Y is the cumulative distribution function of Y. Given a sample of peak-flow events Yi of sample size n, the values can be ranked such that $Y_{(i)}$ is the ith largest value in the sample, where $Y(1) > Y(2) > \cdots > Y(n)$. An estimate of the cumulative probability for ranked event $Y_{(i)}$ is estimated from:

$$F_Y[Y_{(i)}] = 1 - \frac{i - 0.4}{n + 0.2} \tag{5}$$

where the right-hand side of (5) is the quantile-unbiased plotting position (Stedinger et al. 1993). By equating Equations 4 and 5, the ranked discharge event $Y_{(i)}$ becomes an empirical estimate of the p^{th} quantile y_p. As each scenario generates a peak-flow sub-sample of equal size, and as we are not extrapolating to events beyond the range of those simulated, the empirical quantile estimates can be compared directly without needing to fit hypothetical frequency distributions. The cumulative probability p of quantile y_p is commonly referred to in terms of its return period, T, estimated as:

(6) $$T = \frac{1}{1 - p}$$

Impacts from forest disturbance are then assessed by examining changes in y_p for a given T, or changes in T for a given y. Sensitive basins will experience large changes in quantile or frequency for a given harvest disturbance.

An example comparison of two sub-basins, Baker Creek at Quesnel (BAKER) and the Fraser River at Hope (FRSHP), is given in Figure 29. These two sub-basins were chosen for the extreme contrast in their hydro-climatologies, topographies, and physiographies. Baker Creek is a relatively small (1 552 km^2) basin of low relief with nearly 100% forest cover, much of it lodgepole pine, and lies on the relatively arid Interior Plateau. In contrast, the Fraser River at Hope drains the entire 217 000 km^2 study area. The confidence bounds shown in the figure, which represent a non-parametric 95% confidence region derived from bootstrap re-sampling of the baseline scenario order statistics, indicate the statistical significance of any quantile change due to forest disturbance. The uncertainty bounds for the highest (lowest) order statistic are estimated assuming that the error is distributed symmetrically such that the upper (lower) bound is equivalent in departure from $Y_{(i)}$ as the re-sampled lower (upper) bound. The uncertainty represented is attributable solely to sampling uncertainty that affects the estimate of the cumulative probability from Equation 5.

Sensitivity of the peak-flow regime (i.e., change in quantile values) to forest disturbance varies widely between the two basins (Figure 29). Baker Creek is highly sensitive, whereas the entire Fraser River watershed (Fraser River at Hope) shows very low sensitivity. Also, the impact on the peak-flow regime (assessed visually as a shift in the disturbance peak-flow frequency curve from that of the baseline) increases with disturbance severity.

For instance, forest disturbance at Baker Creek shifts the peak-flow frequency curve upward so a given frequency has a bigger magnitude, and events of a given magnitude occur more frequently. A 1-in-20-year peak-flow event (T=20 years), or Q_{20}, increases from approximately 39 m^3/s at baseline (95_BASE) to 49 m^3/s for Scenario 95_25HF. Conversely, for a magnitude of 39 m^3/s, the frequency increases from 20 years at baseline to approximately seven years for Scenario 95_25HF. Results for Baker Creek indicate that beetle-kill alone has less of an impact on peak-flow quantiles than the combined effect of beetle-kill and salvage harvesting does (compare Scenario 95_100K to Scenario 95_25HF). In addition, the historical 2007 forest cover (07_CURR) influences Baker Creek peak-flow quantiles more than the hypothetical 100% beetle-kill scenario (95_100K). Although the 95_100K scenario is slightly bigger (beetle-kill plus harvest) than 07_CURR (72% versus 68%, respectively, of basin area), the 07_CURR scenario contains nearly twice the harvest area of the 95_100K scenario (21% versus 12% by area). When disturbance has a significant impact on the peak-flow regime (i.e., most scenarios for Baker Creek), the entire frequency curve rises (i.e., to higher magnitudes) and impacts are seen for the full range of frequencies explored (T = 1.01 to 152 years). This example also indicates that changes in frequency (i.e., T) can often be larger than changes in magnitude, particularly in snowmelt-dominated watersheds where the slope of the frequency curve is quite low. For the Baker Creek example previously used (Q_{20} for Scenario 95_25HF), a 25% increase in quantile magnitude corresponds to a 50% reduction in frequency, which generally agrees with similar modelling studies of land cover change conducted in snowmelt-dominated basins in British Columbia (Schnorbus and Alila 2004, 2005; FPB 2007a) and Washington State (Cuo et al. 2009).

A snowpack's water volume largely determines water yield from snow-dominated basins, but in the interior of western North America, the peak-flow frequency response of snowmelt-dominated basins is fundamentally governed by the snowmelt process (Loukas et al. 2000; Troendle et al. 2001). These freshet peaks are therefore dominated by spring and early summer meteorological conditions controlling snowmelt (Kattelmann 1991). The magnitude of peak annual discharge is limited by both the radiant and turbulent energy available for snowmelt, which is controlled by vegetation and terrain shading (Adams et al. 1998; Tarboton et al. 2000), and the synchronization of runoff from contributing areas of the basin, which is a function of the extent of the snow cover (Kattelmann 1991). Despite a reduction in longwave radiation, removing forest canopy in clearcut areas generally increases melt rates at the time of peak discharge (mid-May to mid-June), primarily as a function of increased solar radiation at the snow surface (Adams et al. 1998). Mortality and defoliation of overstorey vegetation due to beetle-kill has an intermediate effect on melt rates. Observed ablation rates in live, dead, and clearcut stands in the interior of British Columbia confirm that the melt rates in dead pine stands are generally higher than those of live stands, but lower than clearcuts (Teti 2009; Boon 2009). Individual energy

components observed by Boon (2009) showed that the snow surface below dead stands balances quite differently from both live stands and clearcuts. Nevertheless, net melt energy is still higher than in live stands, but lower than clearcuts. Given forest canopies' control over snow surface energetics and subsequent melt rates, large (low frequency) events will likely respond similarly and as sensitively as small (high frequency) events to changes to the canopy. Schnorbus and Alila (2004) demonstrated that, in the absence of significant rain-on-melting snow events within the peak-flow sample, increases in melt rates and runoff synchronization following forest removal result in increased event magnitudes across the entire event frequency range.

Although Figure 29 presents estimates of peak-flow quantiles in absolute values, the reader is cautioned against strictly interpreting the given peak-flow magnitudes as accurate projections based on the forest disturbance scenarios. Large prediction error and/or bias can exist with the predicted annual maximum peak-flow magnitudes (see for example Figure 19). Nevertheless, the seasonality and timing of the freshet peak are reasonably well simulated by the VIC model, which can still be exploited when examining peak-flow sensitivity. Relative comparison of simulations to the base scenario offers a more appropriate assessment of peak-flow sensitivity, as it is assumed to remove bias from the simulation of annual maximum flood magnitudes (Hamlet and Lettenmaier 2007). As such, we report relative changes in flood quantiles for the remainder of this discussion. The relative peak-flow quantile change is calculated as:

$$\Delta y_p = \frac{y_p^D - y_p^B}{y_p^B} \quad (7)$$

where superscripts B and D refer to baseline and disturbance, respectively. Equation 7 calculates the change in magnitude of a given quantile for a given disturbance scenario relative to the baseline (95_BASE) quantile magnitude. A tabular summary of Δy_p for all sub-basins for all scenarios is given in Appendix Tables A3 to A7 for quantiles corresponding to T= 2, 10 , 20 , 50 , and 100 years, respectively. For T= 20 years, the Δy_p for all sub-basins are categorized and mapped in Figures 30 through 35 for scenarios 07_CURR through 95_100HF, respectively. The statistical significance of any individual quantile change is assessed using the non-parametric percentile test described by Helsel and Hirsch (2002), which tests whether a percentile $y_p > y_0$ (it specifically tests if the one-sided confidence interval of y_p lies entirely above y_0). All significance tests are based on a confidence level of 5%.

Using the 1-in-20-year (or $y0.05$) event as an example (also referred to as Q_{20}), it is evident that sensitivity to forest disturbance is highly variable between sub-basins (as indicated using respective hydrometric gauge locations in Figures 30 through 35) for a given forest disturbance. We see again that Δy_p also generally increases with increasing forest disturbance at a given hydrometric location. Values of Δy_p range from no change ($\Delta y_p = \pm 0.05$) to maximum values 0.08, 0.08, 0.47, 0.91, 1.30, and 1.72 for scenarios 07_CURR, 95_100K, 95_25HF, 95_50HF, 95_75HF, and 95_100HF, respectively. It is noted that for several sub-basins (i.e., BAKER, NARCO, WEST, MAHOO, and ENDAK) the impact is larger for Scenario 07_CURR than for Scenario 95_100K (compare Figures 30 and 31; see also Figure 29a for BAKER). Although the 95_100K scenario comprises greater beetle-kill than 07_CURR, the 2007 forest cover has more harvest areas (class VOP) in these sub-basins than 95_100K, which represents harvest conditions circa 1995 (Table 3). Further, Δy_p is less than 0.1 for all sub-basins for scenarios 95_100K and 07_CURR, but increases considerably for Scenario 95_25HF, exceeding 0.1 for ten sub-basins and 0.2 for six sub-basins (Figure 32). These two points suggest that Δy_p is more sensitive to harvest disturbance (i.e., salvage harvesting) than to beetle-kill alone. Scenarios 07_CURR (Figure 30) and 95_100K (Figure 31) significantly increase Q_{20} for only a handful of sub-basins (three and six sub-basins, respectively); whereas the cumulative impact of beetle kill and increased salvage harvest causes substantially more widespread statistically significant impacts (i.e., 18 sub-basins for Scenario 95_25HF; Figure 32).

3.3 Effect of disturbance area

The spatial distribution of Δy_p suggests that the greatest sensitivity to beetle-related forest disturbance occurs in sub-basins on the Fraser Plateau; specifically, in the Nechako River basin (ENDAK, STELL, NAUTL, and NECHV), the West Road River basin (WEST, BAEZA, and NAZKO), the middle Fraser (BAKER and NARCO), the Stuart River (KAZCH and STUAR), and parts of the Quesnel (MOFFA) and North Thompson (MAHOO). These sub-basins contain a forest cover composed predominantly of pine (Figure 11) and, as such, these same sub-basins sustain the highest disturbance levels in terms of relative area affected (see Figure 22). It is self-evident that sub-basins with high pine content are potentially more sensitive than sub-basins with low (or no) pine content. To that end, this section focuses on how well sub-basin sensitivity to disturbance (measured as Δy_p) can be correlated to a simple, and seemingly obvious, index of (potential) disturbance area. The index selected is the change in disturbance area from baseline relative to total sub-basin area given as:

$$\Delta X_i = (X_i^D - X_i^B)/BA_i \quad (8)$$

where X is disturbance area, BA is the total basin area upstream of the outlet of sub-basin i, and superscripts D and B are as previously defined. The ΔX variable can stand in for relative changes in either beetle-kill (referred to as ΔPx) or harvest area (ΔVOP), with separate indices used to explore each disturbance. The beetle-kill disturbance area, Px, is calculated by aggregating the area of all beetle-kill classes. Values of ΔPx and ΔVOP are tabulated for each sub-basin in Appendix Table A8.

The sensitivity of individual sub-basins versus ΔPx is shown graphically in Figure 36a for T=20 years quantile ($y_{0.05}$) and Scenario 95_100K. Based on the local polynomial regression trend line, sub-basin sensitivity is generally inconsequential until $\Delta Px \geq 40\%$, and then increases as ΔPx increases. Nevertheless, the data show high scatter about the trend line, $\Delta y_{0.05}$ does not exceed 8%, and in many cases $\Delta y_{0.05}$ is negative. The relationship between relative harvest area changes (ΔVOP) and $\Delta y_{0.05}$, which is shown in Figure 36c, shows a clearer relationship. The data for this figure are based on aggregated results from scenarios 95_25HF through 95_100HF. For the cumulative effect of beetle-kill and salvage harvesting, there is a qualitatively clearer trend of increasing $\Delta y_{0.05}$ with increasing ΔVOP (again based on local polynomial regression); note however that the variability of $\Delta y_{0.05}$ also increases with ΔVOP and ranges from 0 to ≈ 1.0 for ΔVOP as high as 50%. Once ΔVOP is greater than 50%, however, the value of $\Delta y_{0.05}$ is 0.6 or higher. Comparison of Figures 36a and b indicates that for a given disturbance area the cumulative effect of beetle-kill plus salvage harvest has a substantially larger impact (i.e., larger Δy_p) than beetle-kill alone.

Scenarios were constructed such that beetle-related disturbance (beetle-kill and salvage harvest) is proportional to baseline pine content: sub-basins with high pine content have far more severe disturbance than sub-basins with little or no pine. As peak-flow impacts tend to increase with increasing disturbance area (much more so for salvage harvest than beetle-kill), and potential disturbance area is proportional to pre-disturbance pine content, it would seem that the extent of pine-dominated forest cover is a simple and straightforward tool for *a priori* characterization of watershed sensitivity. This approach has led to mapping the extent of forest consisting of more than 40% lodgepole pine in conjunction with all third-order and higher watershed boundaries in the southern and northern interior forest regions (see http://www.for.gov.bc.ca/hfp/mountain_pine_beetle/stewardship/hydrology/ for details). But the extent of lodgepole pine (and, therefore, potential disturbance area) does not explain why some sub-basins with high in pine forest cover throughout the Fraser basin, such as in the Chilcotin and lower Thompson, show low sensitivity to beetle-related disturbance. It is hypothesized that in such cases freshet discharge at the gauged point of interest is predominantly derived from high snowmelt in sub-alpine and alpine areas (cf. Figure 28) which are devoid of pine forest cover, rendering these basins more robust to beetle-related disturbance (i.e., NECHC, TASEK, CHILK, BIGCR, and THOMS).

This issue of how the runoff source affects disturbance sensitivity was analyzed by weighting the relative change in disturbance area variable (ΔX from Equation 8), previously examined by some measure describing the predominant runoff source area. Preliminary data exploration led to using the following weight, w, with the relative change in disturbance area:

$$w \cdot \Delta X_i = \Delta X_i \cdot (R_{Pi}/R_{Ti}) \quad (9)$$

where R_{Pi} and R_{Ti} are the average (1916–2006) annual runoff from the lodgepole pine-forested (subscript P) and total (subscript T) area, respectively, upstream of the outlet of sub-basin i estimated for the baseline (1995 forest cover) scenario. The weight, w, is therefore the ratio of runoff originating from a lodgepole pine forested area of a sub-basin to total runoff originating from the

sub-basin. The distribution of w is shown in Figure 37. Generally, sub-basins along the east side of the Fraser River watershed that collect runoff from the windward side of the Columbia and Coast Mountains (cf. Figure 28) have low values of w (typically < 10%). Conversely, sub-basins located on the west side of the Fraser River watershed tend to have higher w values, although watersheds that drain the high snowfields along the Coast Mountains (such as the headwaters of the Nechako and Chilcotin Rivers; Figure 28) have w values < 20%. The highest runoff ratios are found for watersheds located on the Fraser Plateau with no substantial sub-alpine/alpine snow and runoff component (Figure 28), such as the West Road River and its tributaries, Baker Creek and Narcosli Creek. Values of w for each sub-basin are tabulated in Appendix Table A8. Weighting the relative change in beetle-kill area (ΔPx) using Equation 9 does not appear to account for any additional variation when compared to the relative change in Q_{20} (Figure 36b). However, using w to weight the relative change in salvage harvest area (ΔVOP) does produce a stronger relationship to describe the expected change in Q_{20} (compare Figures 36c and d). This result affirms that basin sensitivity to potential salvage harvesting, although certainly a function of lodgepole pine forest extent, must also be considered with respect to the proportion of runoff generated from the pine-forested area within the basin. In short, one can expect that watersheds with a large proportion of pine and a high proportion of runoff from that pine-forested area will be highly sensitive to beetle-related disturbance. Conversely, watersheds with a small proportional pine extent (or no pine) and/or proportionately low runoff generating from that pine forested-area (due predominantly to a topological connection to sub-alpine or alpine regions) will have low sensitivity to beetle-related disturbance.

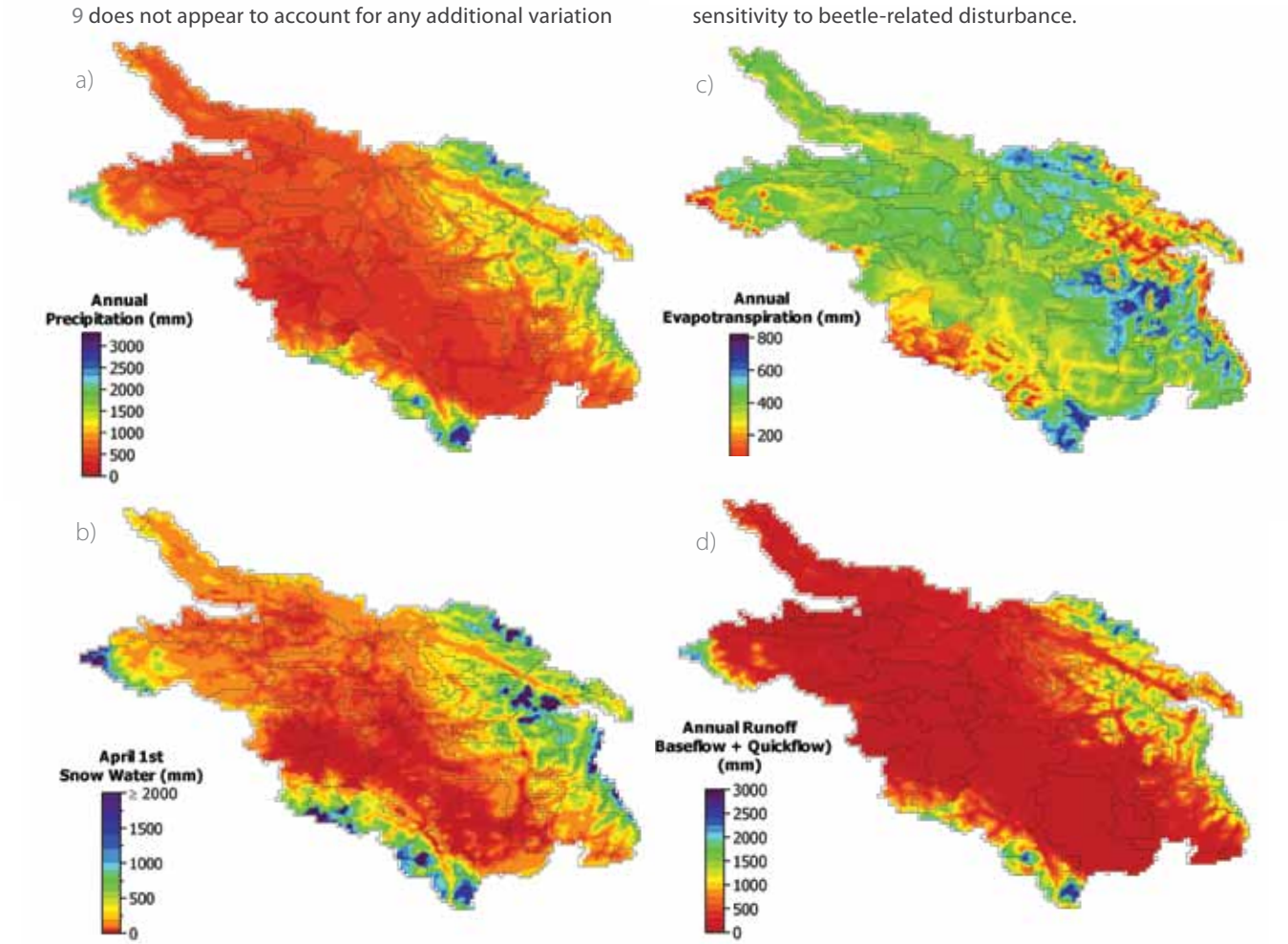

Figure 28. Fraser River base scenario (95_BASE) hydro-climatology as average of fluxes and states simulated with 1916–2006 driving data: a) annual precipitation, b) April 1 snow water equivalent, c) annual evapotranspiration, and d) annual runoff (baseflow plus quickflow).

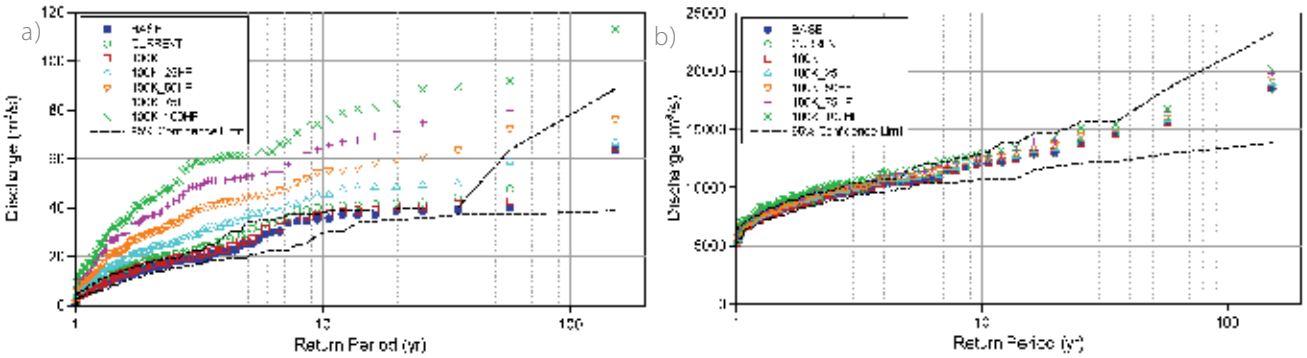

Figure 29. Peak-flow frequency curves by scenario for a) Baker Creek at Quesnel (BAKER) and b) Fraser River at Hope (FRSHP). The 95% confidence region for the baseline scenario is shown by the dashed lines.

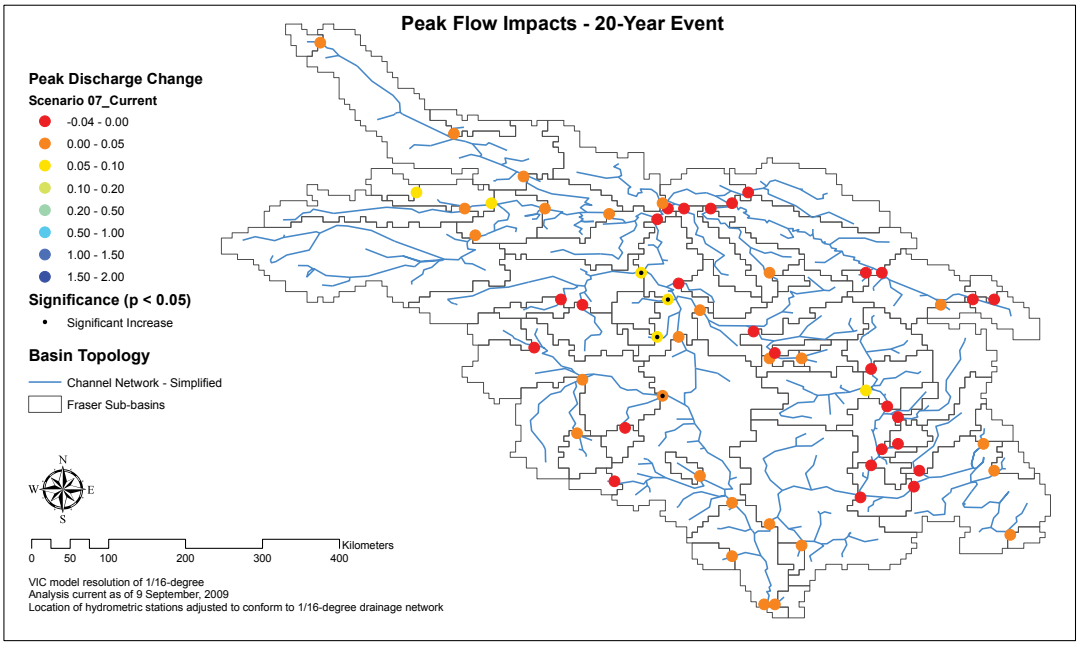

Figure 30. Relative change (from baseline; 95_BASE) in the 1-in-20-year peak-flow (Q_{20}) event for Scenario 07_CURR for individual hydrometric locations; black dots indicate locations of statistically significant ($p < 0.05$) increase (based strictly on quantile estimator uncertainty).

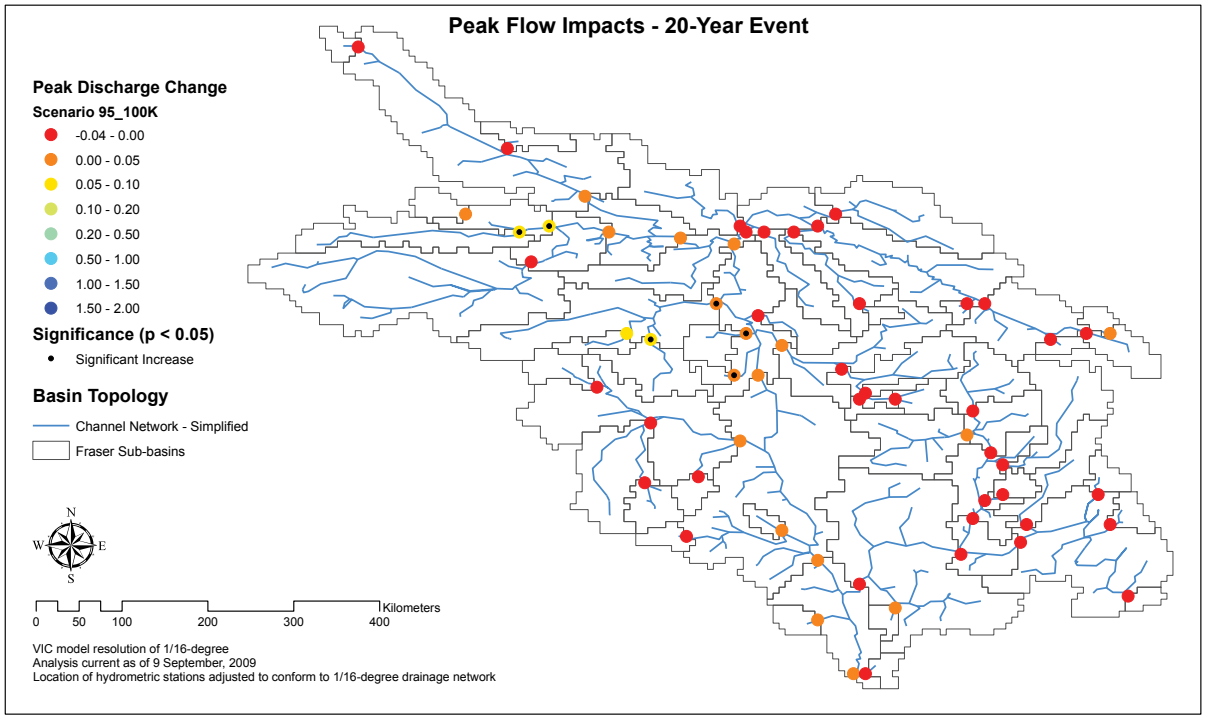

Figure 31. Relative change (from baseline; 95_BASE) in 1-in-20-year peak-flow (Q_{20}) event for Scenario 95_100K for individual hydrometric locations

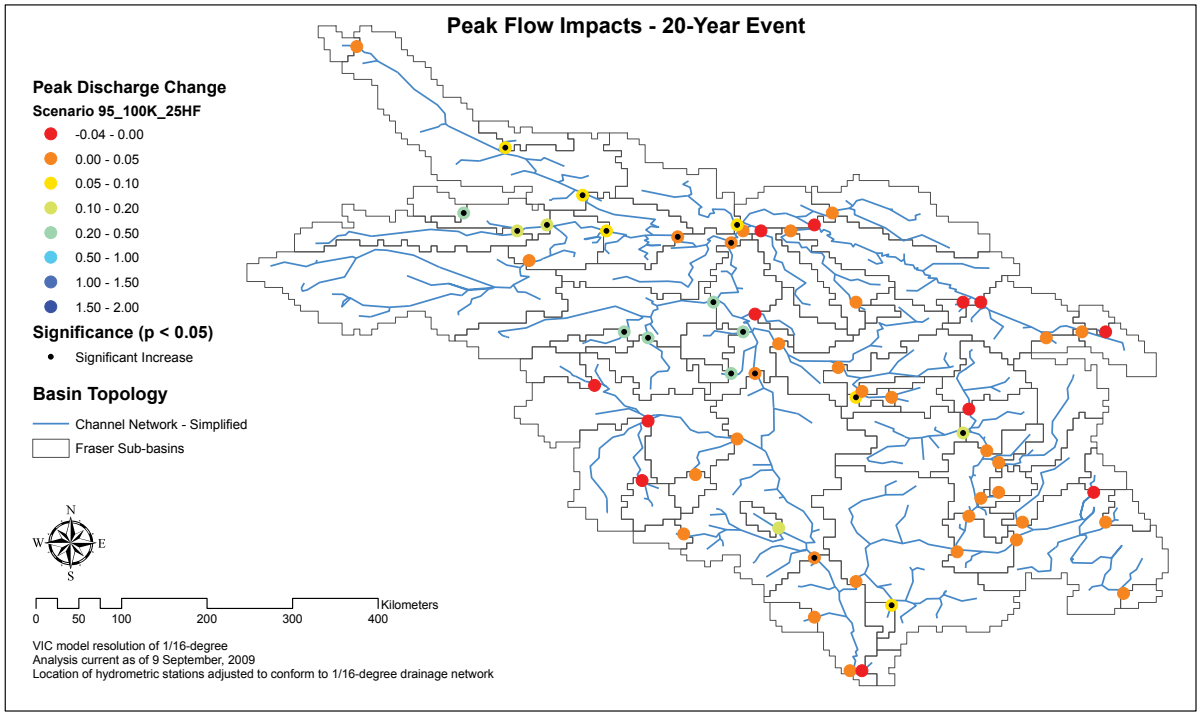

Figure 32. Relative change (from baseline; 95_BASE) in 1-in-20-year peak-flow (Q_{20}) event for Scenario 95_25HF for individual hydrometric locations

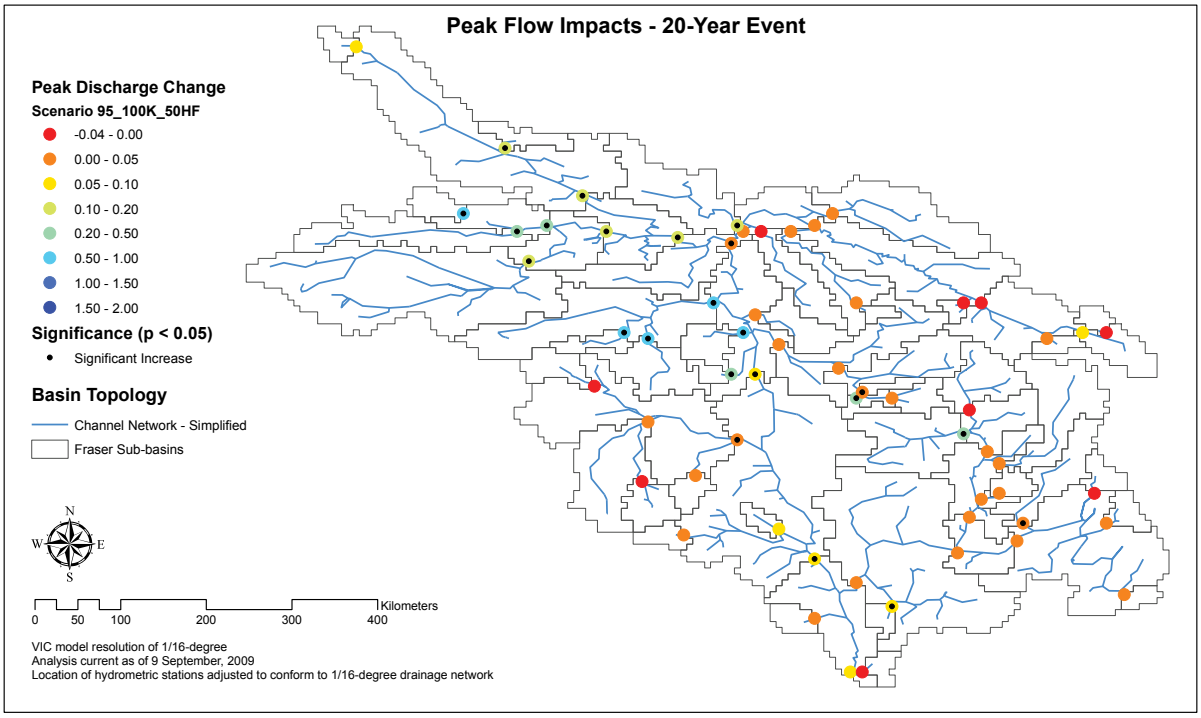

Figure 33. Relative change (from baseline; 95_BASE) in 1-in-20-year peak-flow (Q_{20}) event for Scenario 95_50HF for individual hydrometric location

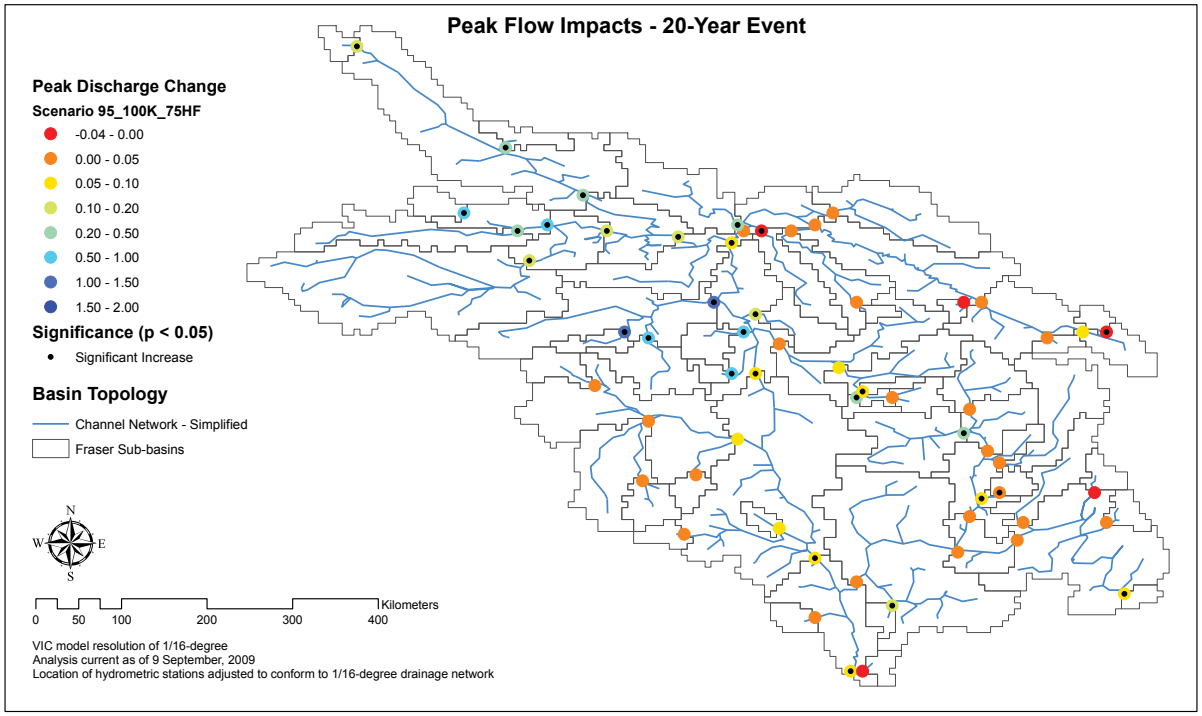

Figure 34. Relative change (from baseline; 95_BASE) in 1-in-20-year peak-flow Q_{20}) event for Scenario 95_75HF for individual hydrometric locations

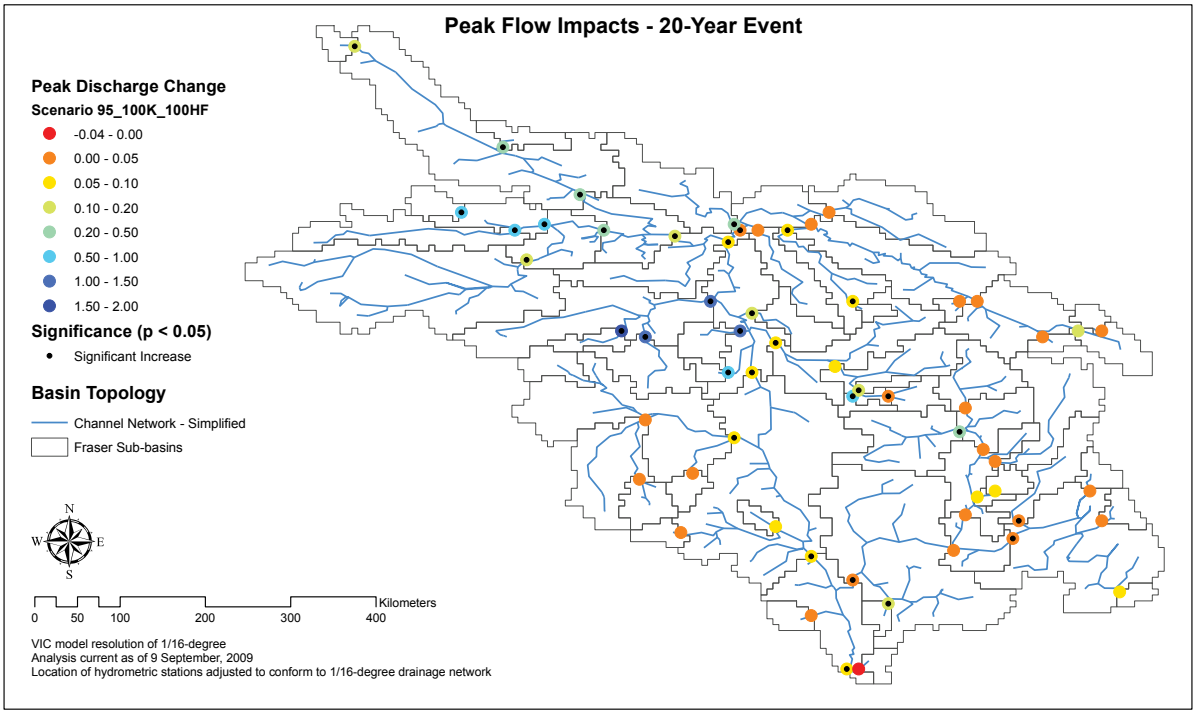

Figure 35. Relative change (from baseline; 95_BASE) in 1-in-20-year peak-flow (Q_{20}) event for Scenario 95_100HF for individual hydrometric locations

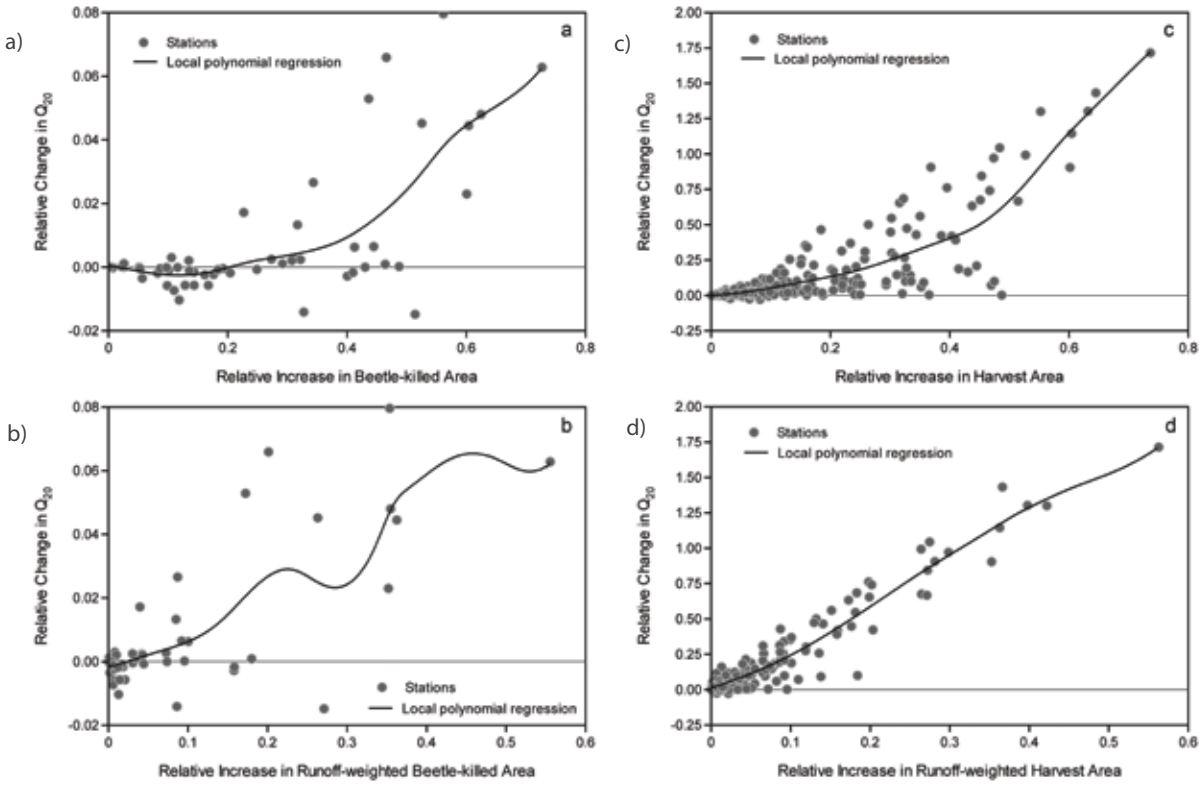

Figure 36. Relative change in T=20-year quantile (Q_{20}) as a function of the following relative changes in disturbance area: a) beetle-killed pine (Px) for Scenario 95_100K, b) runoff-weighted beetle-killed pine for Scenario 95_100K, c) harvest area (VOP) for scenarios $95\_25HF, 95\_50HF, 95\_75HF, 95\_100HF$, and d) runoff-weighted harvest area for scenarios $95\_25HF, 95\_50HF, 95\_75HF, 95\_100HF$. Trend lines are based on local polynomial regression.

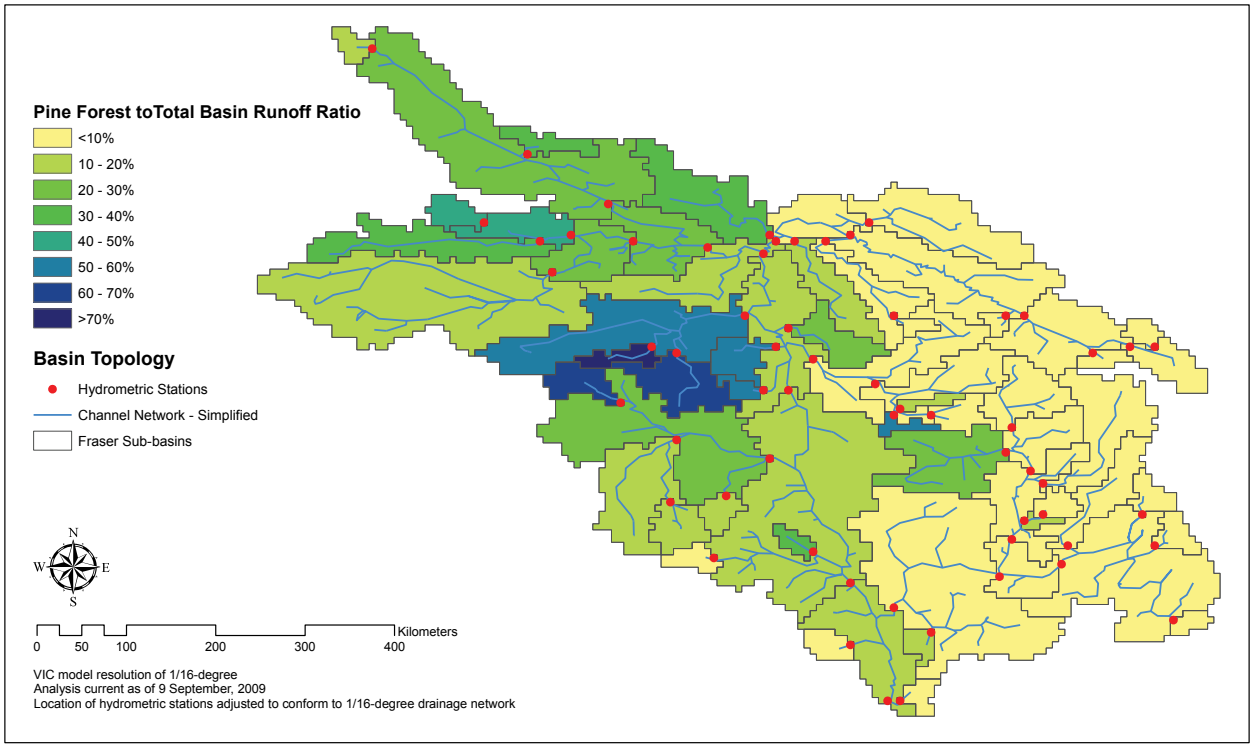

Figure 37. Spatial distribution by sub-basin of the proportion of average (1916–2006) annual runoff derived from lodgepole pine-forested area to annual runoff derived from the total sub-basin area (variable w in Equation 9) for the baseline scenario. The colors for each sub-basin represent the w value for the entire basin upstream of the hydrometric gauge; for nested basins the change in color represents changes in w with increasing drainage area.

4. Conclusions

Numerical hydrologic simulation was used to assess the sensitivity of the peak-flow regime within the Fraser River Basin to beetle kill and associated salvage harvesting operations. Sensitivity of the peak-flow regime to forest disturbance was assessed in 60 sub-basins representing a range of scales (400–217 000 km^2) and climatic and physiographic conditions. Forest cover representing two time periods (1995 and 2007) along with five hypothetical disturbance scenarios (based on 1995 forest cover) were used to assess peak-flow impacts. These scenarios lie along a broad disturbance spectrum, ranging from relatively low disturbance at the beginning of the current infestation (1995), to current forest cover (2007, current infestation and harvest operations), to hypothesized maximum infestation plus various harvesting levels from 0% to 100% of beetle-killed pine. Each scenario was forced with observed climate data collected from 1916–2006.

Peak-flow impacts were measured by comparing empirical peak-flow quantiles (estimated as the plotting position of the ranked sample value) for each scenario to the baseline value (generated using the 1995 forest cover). Results show that forest disturbance tends to increase the magnitude of peak-flow quantiles, with the relative change in quantile magnitude increasing with disturbance severity. The impact is generally lowest for current conditions (i.e., 2007) or the hypothetical 100% beetle-kill (Scenario 95_100K); the ranking of these scenarios varies with sub-basin depending upon variations in beetle-kill and harvest area between the two scenarios. Following from Scenario 95_100K, peak-flow impacts clearly increase with increasing harvest area. When peak-flow quantiles are increased following disturbance, all quantiles (from frequencies of 1.01 to 152 years) increase, indicating that large events are just as sensitive to forest disturbance as small events.

As exemplified by the 1-in-20 year quantile, sensitivity by sub-basin to forest disturbance varies spatially within the Fraser River Basin. As expected, the relative change in peak-flow quantile correlates positively with the relative increase in disturbance area (normalized by sub-basin area) between the baseline and disturbance conditions. Forest harvesting (in conjunction with beetle-kill) tends to manifest a stronger signal than beetle-kill alone, suggesting that the peak-flow regime is more sensitive to forest harvesting (represented as clearcuts) than to the conversion of live forest to dead forest. Not unexpectedly, sub-basins with large percentages (by area) of mature pine cover may, depending upon actual harvest rates, be most affected by beetle infestation and subsequent harvest operations. Thus, it follows that sub-basins without substantial susceptible pine cover are less sensitive to mountain pine beetle-related disturbance.

Despite the positive trend between relative disturbance area and relative change in quantile magnitude, a sub-basin's particular hydro-climatology can have a strong, and perhaps confounding, influence on peak-flow sensitivity to forest disturbance. Generally, for a given extent of beetle-kill and salvage harvesting, basins with high proportional runoff from the pine-forested areas tend to be more sensitive than basins with low proportional runoff. The degree of proportional runoff from the pine-forested extent is largely affected by the absence or presence of a topological connection to the high runoff areas in the sub-alpine and alpine regions of the Coast, Columbia, or Rocky Mountains. Although not yet examined in detail, this connectivity is likely a function not only of network topology, but also of basin scale. In other words, as drainage areas become larger, the likelihood of incorporating runoff from these wet sub-alpine and alpine regions increases.

The effects of beetle-related disturbance vary by location along the Fraser River drainage network. Streamflow in the Fraser River main stem from Prince George to Hope and within such major tributaries as the Thompson River at Kamloops, the Quesnel River at Quesnel, and the Chilcotin River shows little sensitivity to beetle-related disturbance. In these large drainages streamflow is predominantly composed of snowmelt runoff from the high snowfields of the Coast, Columbia, and Rocky Mountains and the peak-flow regime is largely robust to forest-cover effects taking place on the relatively arid Interior Plateau. The greatest sensitivity to infestation-induced forest disturbance is exhibited by modestly sized sub-basins located on the Interior Plateau (i.e., Baker Creek, West Road River, Salmon River, Mahood River, and parts of the Nechako and Stuart drainages). These areas are characterized by pine-dominated forest cover (i.e., potentially high-disturbance areas) and low topographic relief (i.e., no significant regions of sub-alpine or alpine runoff). In these highly sensitive areas, peak-flow changes are substantial and can have significant local impacts on channel morphology, water quality, aquatic ecosystems, and flood risk.

This project can be considered a work in progress. Further effort is required to better understand the mechanisms that control sub-basin sensitivity to beetle-related forest

disturbance, and specifically how sub-basin hydro-climate and physiography relate to basin sensitivity. In particular, simple indices need to be made for quickly and effectively predicting peak-flow sensitivity to beetle-related forest disturbance at various scales and regions of the Fraser River Basin. We also recommend examining more forest disturbance scenarios and additional hydrometric locations.

Lastly, the preparation and set-up of a hydrological model such as VIC typically involves collecting and processing many data sets from various sources to create the model input and parameter files. These VIC model files may prove valuable in similar hydrologic or other beetle-related studies. The various model data and parameter files are summarized with basic metadata in Appendix Table A1. Interested readers can contact the primary author for additional details.

5. Acknowledgements

Thanks go to Allan Chapman for his guidance, support, and vision. The authors also thank Peter Tschaplinski, Robin Pike, Todd Redding, and Martin Carver for their assistance, helpful suggestions, and review comments. We are grateful to the staff of the Climate Impacts Group (University of Washington), and in particular Alan Hamlet and Marketa McGuire Elsner, for their expertise and encouragement in getting the VIC model off the ground. Bob Nicholson of the Integrated Land Management Bureau (ILMB) assisted us greatly by preparing the selected fields of the VRI Rank 1 polygon coverage for the Fraser River watershed. This project is in no small part indebted to the efforts of Paul Nienaber for his work in keeping all the VIC and MOCOM codes and scripts working well, working efficiently, and working correctly.

This project was funded by the Government of Canada through the Mountain Pine Beetle Program, administered by Natural Resources Canada, Canadian Forest Service. Publication does not necessarily signify that the contents of this report reflect the views or policies of Natural Resources Canada, Canadian Forest Service.

6. Literature cited

Abuelgasim, A.A.; Fernandes, R.A.; Leblanc, S.G. 2006. Evaluation of national and global LAI products derived from optical remote sensing instruments over Canada. IEEE Transactions on Geoscience and Remote Sensing 44(7):1872–1884.

Adams, R.S.; Spittlehouse, D.L.; Winkler, R.D. 1998. The snowmelt energy balance of a clearcut, forest and juvenile stand. *In* 23rd Conference Agricultural and Forest Meteorology, American Meteorological Society, Albuquerque, NM 2–6 November 1998.

Bartlett, P.A.; Mackay, M.D.; Verseghy, D.L. 2006. Modified snow algorithms in the Canadian Land Surface Scheme: Model runs and sensitivity analysis at three boreal forest stands. Atmosphere-Ocean 43(3):207–222.

Beschta, R.L.; Pyles, M.R.; Skaugest, A.E.; Surfleet, C.G. 2000. Peakflow response to forest practices in the western Cascades of Oregon, USA. Journal of Hydrology 233:102–120.

Boon, S. 2009. Snow ablation energy balance in a dead forest stand. Hydrological Processes 23: 2600–2610.

Bras, R.L. 1990. Hydrology: An introduction to hydrologic science. Addison-Wesley Publishing Company, Reading, MA. 643 p.

(BCILMB) British Columbia Integrated Land Management Bureau. 1995. Baseline thematic mapping: Present land use mapping, Release 1.0, February 1995.

(BCMoF) British Columbia Ministry of Forests. 1981. Growth and yield. Chapter 8 *in* Forest and range inventory manual. Inventory Branch, BC Ministry of Forests, Victoria, BC.

BCMoF. 2004. Quesnel timber supply area. Rationale for annual allowable cut (AAC) determination, effective 1 October 2004. 63 p.

(BCMoFR) Ministry of Forests and Range. 2005. Merritt timber supply area. Rationale for annual allowable cut (AAC) determination, effective 1 July 2005. 58 p.

BCMoFR. 2009 Beetle facts: Infestation information. http://www.for.gov.bc.ca/hfp/mountain_pine_beetle/facts.htm#infestation. Accessed Dec 1, 2009.

Burton, T.A. 1997. Effect of basin-scale timber harvest on water yield and peak streamflows. Journal of the American Water Resources Association 33(6):1187–1196.

Campbell, G.S.; Norman, J.M. 1998. An introduction to environmental biophysics. 2nd ed. Springer-Verlag, New York, NY. 286 p.

(CHRS) Canadian Heritage Rivers System. 2009. Website: http://www.chrs.ca/Rivers/Fraser/Fraser_e.htm. Accessed 16 March 2009.

Carver, M.; Weiler, M.; Scheffler, C.; Rosin, K. 2010. Development and application of a peak-flow hazard model for the Fraser Basin (British Columbia). Mountain pine beetle working paper 2009-13. Natural Resources Canada, Canadian Forest Service, Pacific Forestry Centre. Victoria, BC. 34 p.

Carver, M.; Weiler, M.; Stahl, K.; Scheffler, C.; Schneider, J.; Naranjo, J.A.B. 2010. Development of a low flow hazard model for the Fraser Basin, British Columbia. Mountain pine beetle working paper 2009-14. Natural Resources Canada, Canadian Forest Service, Pacific Forestry Centre. Victoria, BC. 24 p.

Cheng, J.D. 1989. Streamflow changes after clear-cut logging of a pine beetle-infested watershed in southern British Columbia, Canada. Water Resources Research 47(6):1063–1067.

Coates, K.D.; DeLong, C.; Burton, P.J.; Sachs, D.L. 2006. Abundance of secondary structure in lodgepole pine stands affected by the mountain pine beetle. Report for the Chief Forester, August 2006. 17 p.

Cosby, B.J.; Hornberger, G.M.; Clapp, R.B.; Ginn, T.R. 1984. A statistical exploration of the relationships of soil moisture characteristics to the physical properties of soils. Water Resources Research 20(6):682–690.

Cuo, L.; Lettenmaier, D.P.; Alberti, M.; Richey, J.E. 2009. Effects of a century of land cover and climate change on the hydrology of the Puget Sound basin. Hydrological Processes 23(6):907–933. doi: 10.1002/hyp.7228.

Daly, C.; Neilson, R.P.; Phillips, D.L. 1994. A statistical-topographic model for mapping climatological precipitation over mountainous terrain. Journal of Applied Meteorology 33:140–158.

Demarchi, D.A. 1996. An introduction to the ecoregions of British Columbia. Wildlife Branch, BC Ministry of Environment, Lands and Parks, Victoria, BC. http://www.env.gov.bc.ca/ecology/ecoregions/title_author.html. Accessed 22 February 2009.

Dickinson, R.E.; Henderson-Sellars, A.; Rosenzweig, C.; Sellars, P.J. 1991. Evapotranspiration models with canopy resistance for use in climate models, a review. Agricultural and Forest Meteorology 54:373–388.

Ducoudré, N.I.; Laval, K.; Perrier, A. 1993. SECHIBA, a new set of parameterizations of the hydrologic exchanges at the land-atmosphere interface within the LMD atmosphere general circulation model. Journal of Climate 6:248–273.

Duursam, R.A.; Marshall, J.D.; Robinson, A.P. 2003. Leaf area index inferred from solar beam transmission in mixed conifer forests on complex terrain. Agricultural and Forest Meteorology 118:221–236.

Eng, M.; Fall, F.A.; Hughes, J.; Shore, T.; Riel, B.; Hall, P.; Walton, A. 2005. Provincial-level projection of the current mountain pine beetle outbreak: An overview of the model (BCMPBv2) and results of year 2 of the project. BC Ministry of Forests and Range and Canadian Forest Service. http://www.for.gov.bc.ca/hre/bcmpb/Year2.htm.

Fernandes, R.; Butson, C.; Leblanc, S.; Latifovic, R. 2003. Landsat-5 TM and Landsat-7 ETM+ based accuracy assessment of leaf area index products for Canada derived from SPOT-4 VEGETATION data. Canadian Journal of Remote Sensing 29(2):241–258.

(FPB) Forest Practices Board. 2007a. The effect of mountain pine beetle attack and salvage harvesting on streamflows. Special Investigation Report 16. Victoria, BC. 27 p.

FPB. 2007b. Lodgepole pine stand structure 25 years after mountain pine beetle attack. Special Investigation Report 32. Victoria, BC. 16 p.

(GSDT) Global Soil Data Task. 2000. Global Soil Data Products CD-ROM (IGBP-DIS). CD-ROM. International Geosphere-Biosphere Programme, Data and Information System, Potsdam, Germany. Available from Oak Ridge National Laboratory Distributed Active Archive Center, Oak Ridge, TN. http://www.daac.ornl.gov"http://www.daac.ornl.gov.

Gray, D.M.; Prowse, T.D. 1993. Snow and floating ice. Chapter 7 *in* D.R. Maidment, ed. Handbook of Hydrology. McGraw-Hill, New York, NY. 1424 p.

Hamlet, A.F.; Lettenmaier, D.P. 1995. Production of temporally consistent gridded precipitation and temperature fields for the continental United States. Journal of Hydrometeorology 6:330–336.

Hamlet, A.F.; Lettenmaier, D.P. 2007. Effects of 20th century warming and climatic variability on flood risk in the western U.S. Water Resources Research, W06247. doi: 10.1029/2006WR005099.

Hélie, J.F.; Peters, D.L.; Tattrie, K.R.; Gibson, J.J. 2005. Review and synthesis of potential hydrologic impacts of mountain pine beetle and related harvesting activities in British Columbia. Canadian Forest Service, Pacific Forestry Centre, Victoria, BC. Mountain Pine Beetle Initiative Working Paper 2005-23. 27 p.

Helsel, D.R.; Hirsch, R.M. 2002. Statistical methods in water resources. Book 4, Chapter A3 *in* Techniques of Water Resources Investigations. U.S. Geological Survey. 522 p.

Jackson, R.B.; Canadell, J.; Ehleringer, J.R.; Mooney, H.A.; Sala, O.E.; Schulze, E.D. 1996. A global analysis of root distributions for terrestrial biomes. Oecologia 108(3):389–411.

Kalnay, E.; Kanamitsu, M.; Kistler, R.; Collins, W.; Deaven, D.; Gandin, L.; Iredell, M.; Saha, S.; White, G.; Woollen, J.; Zhu, Y.; Chelliah, M.; Ebisuzaki, W.; Higgins, W.; Janowiak, J.; Mo, K.C.; Ropelewski, C.; Wanj, J.; Leetmaa, A.; Reynolds, R.; Jenne, R.; Joseph, D. 1996. The NCEP/NCAR 40-year reanalysis project. Bulletin of the American Meteorological Society 77:437–471.

Kattelmann, R. 1991. Peak flows from snowmelt runoff in the Sierra Nevada, USA. Pages 203–212 *in* Snow, hydrology and forest in high alpine areas. International Association of Hydrological Sciences Publication 205. 250 p.

Liang, X.; Lettenmaier, D.P.; Wood, E.F. 1994. A simple hydrologically based model of land surface water and energy fluxes for general circulation models. Journal of Geophysical Research 99(D7):14 415–14 428.

Lohmann, D.; Nolte-Holube, R.; Raschke, E. 1996. A large-scale horizontal routing model to be coupled to land surface parameterization schemes. Tellus 48A:708–721.

Lohmann, D.; Raschke, E.; Nijssen, B.; Lettenmaier, D.P. 1998a. Regional scale hydrology: I. Formulation of the VIC-2L model coupled to a routing model. Hydrological Sciences Journal 43(1):131–141.

Lohmann, D.; Raschke, B.; Nijssen, B.; Lettenmaier, D.P. 1998b. Regional scale hydrology: II. Application of the VIC-2L model to the Weser River, Germany. Hydrological Sciences Journal 43(1):143–151.

Loukas, A.; Vasiliades L.; Dalezios, N.R. 2000. Flood producing mechanisms identification in southern British Columbia, Canada. Journal of Hydrology 227:218–235.

MacDonald, L.E.; Stednick, J.D. 2003. Forest and water: A state-of-the-art review for Colorado. Colorado State University, CWRRI Completion Report No. 196. 65 p.

Maurer, E.P.; Wood, A.W.; Adam, J.C.; Lettenmaier, D.P.; Nijssen, B. 2002. A long-term hydrologically based dataset of land surface fluxes and states for the conterminous United States. Journal of Climate 15:3237–3251.

Megahan, W.F.; King J.G.; Seyedbagheri, K.A. 1995. Hydrologic and erosional responses of a granitic watershed to helicopter logging and broadcast burning. Forest Science 41(4):777–795.

Meidinger, D.; Pojar, J., eds. 1991. Ecosystems of British Columbia. Research Branch, BC Ministry of Forests, Victoria, BC. 330 p.

Mekis, É.; Hogg, W.D. 1999. Rehabilitation and analysis of Canadian daily precipitation time series. Atmosphere-Ocean 37:53–85.

Pierce, L.L.; Running, S.W. 1988. Rapid estimation of coniferous forest leaf area index using a portable integrating radiometer. Ecology 69(6):1762–1767.

Potts, D.F. 1984. Hydrologic impacts of a large-scale mountain pine beetle (*Dendroctonus ponderosae* Hopkins) epidemic. Water Resources Bulletin 20(3):373–377.

Redding, T.; Winkler, R.; Teti, P.; Spittlehouse, D.; Boon, S.; Rex, J.; Dubé, S.; Moore, R.D.; Wei, A.; Carver, M.; Schnorbus, M.; Reese-Hansen, L.; Chatwin, S. 2008. Mountain pine beetle and watershed hydrology. BC Journal of Ecosystems and Management 9(3):33–50. http://www.forrex.org/publications/jem/ISS49/vol9_no3_MPBconference.pdf.

Roberts, J. 2000. The influence of physical and physiological characteristics of vegetation on their hydrologic response. Hydrological Processes 14:2885–2901.

Ryan, M.G.; Binkley, D.; Fownes, J.H. 1997. Age-related decline in forest productivity: Pattern and process. Advances in Ecological Research 27:213–262.

Scherer, R. 2001. Effects of changes in forest cover on streamflow: A literature review. Pages 44–55 *in* D.A.A. Toews and S. Chatwin, eds. Watershed assessment in the southern interior of British Columbia. Research Branch, British Columbia Ministry of Forests, Victoria, BC. Working Paper 2001-57. 247 p.

Schmid J.M.; Mata S.A.; Martinez, M.H.; Troendle, C.A. 1991. Net precipitation within small group infestations of the mountain pine beetle. US Department of Agriculture, Rocky Mountain Forest and Range Experiment Station, Research Note RM-508. 4 p.

Schnorbus, M.A.; Alila, Y. 2004. Forest harvesting impacts on the peak flow regime in the Columbia Mountains of southeastern British Columbia: An investigation using long-term numerical modelling. Water Resources Research 40, W05205. doi: 10.1029/2003WR002918.

Schnorbus, M.A.; Alila, Y. 2005. Simulated streamflow response to large-scale forest harvesting in Upper Penticton Creek, British Columbia. Pages 223–245 *in* Water – Our limiting resource: Towards sustainable management in the Okanagan, 2005 Conference Proceeding, 23–25 February 2005. Canadian Water Resources Association, BC Branch.

Shepard, D.S. 1984. Computer mapping: The SYMAP interpolation algorithm. Pages 133–145 *in* G.L. Gaille and C.J. Willmott, eds. Spatial statistics and models. D. Reidel Publishing Company, Dordrecht, The Netherlands. 500 p.

Shore, T.L.; Riel, B.G.; Safranyik, L.; Fall, A. 2006. Decision support systems. Pages 193–230 *in* L. Safranyik and B. Wilson, eds. The mountain pine beetle: A synthesis of biology, management, and impacts on lodgepole pine. Natural Resources Canada, Canadian Forest Service, Pacific Forestry Centre, Victoria, BC, Canada.

Shore, T.L.; Safranyik, L. 1992. Susceptibility and risk rating system for the mountain pine beetle in lodgepole pine stands. Forestry Canada, Pacific and Yukon Region, Information Report BC-X-336. 12 p.

Shuttleworth, W.J. 1993. Evaporation. Chapter 4 *in* D.R. Maidment, ed. Handbook of Hydrology. McGraw-Hill, New York, NY. 1424 p.

Stahl, K.; Moore, R.D.; Floyer J.A.; Asplin, M.G.; McKendry I.G. 2006. Comparison of approaches for spatial interpolation of daily air temperature in a large region with complex topography and highly variable station density. Agricultural and Forest Meteorology 139: 224–236.

Stedinger, J.R.; Vogel, R.M.; Foufoula-Georgiou, E. 1993. Frequency analysis of extreme events. Chapter 18 *in* D.R. Maidment, ed. Handbook of Hydrology. McGraw-Hill, New York, NY. 1424 p.

Storck, P.; Lettenmaier, D.P. 1999. Predicting the effect of forest canopy on ground snow accumulation and ablation in maritime climates. Pages 1–12 *in* C. Troendle, ed. Proceedings of the 67th Western Snow Conference. Colorado State University, Fort Collins, CO.

Tarboton, D.G.; Blöschl, G.; Cooley, K.; Kirnbauer, R.; Luce, C. 2000. Spatial snow cover processes at Kühtai and Reynolds Creek. Pages 158–186 *in* R. Grayson and G. Blöschl, eds. Spatial Patterns in Catchment Hydrology: Observations and Modelling,. Cambridge University Press, New York, NY. 432 p.

Taylor, S.W.; Carrol., A.L. 2004. Disturbance, forest age, and mountain pine beetle outbreak dynamics in BC: A historical perspective. Pages 41–51 *in* T.L. Shore, J.E. Brooks, and J.E. Stone, eds. Mountain Pine Beetle Symposium: Challenges and Solutions, October 30–31, 2003. Natural Resources Canada, Canadian Forest Service, Pacific Forestry Centre, Victoria, BC. Information Report BC-X-399. 287 p.

Teti, P. 2009. Effects of overstory mortality on snow accumulation and ablation. Natural Resources Canada, Canadian Forest Service, Pacific Forestry Centre, Victoria, BC. Mountain Pine Beetle Working Paper 2008-13. 34 p.

Troendle, C.A.; King, R.M. 1985. The effect of timber harvest on the Fool Creek watershed, 30 years later. Water Resources Research 21(12):1915–1922.

Troendle, C.A.; King, R.M. 1987. The effect of partial and clearcutting on streamflow at Deadhorse Creek, Colorado. Journal of Hydrology 90:145–157.

Troendle, C.A.; Wilcox, M.S.;Bevenger, G.S.; Porth, L.S. 2001. The Coon Creek water yield augmentation project: Implementation of timber harvesting technology to increase streamflow. Forest Ecology and Management 143:179–187.

Uunila, L.; Guy, B.; Pike, R. 2006. Hydrologic effects of mountain pine beetle in the interior pine forests of British Columbia: Key questions and current knowledge. Streamline Watershed Management Bulletin 9(2):1–6.

Vincent, L.A.; Gullett, D.W. 1999. Canadian historical and homogeneous temperature datasets for climate change analyses. International Journal of Climatology 19:1375–1388.

Walton, A.; Hughes, J.; Eng, M.; Fall, A.; Shore, T.; Riel, B.; Hall, P. 2007. Provincial-level projection of the current mountain pine beetle outbreak: Update of the infestation projection based on the 2006 Provincial aerial overview of forest health and revisions to the "Model" (BCMPB.v4). BC Ministry of Forests and Range. http://www.for.gov.bc.ca/hre/bcmpb/Year4.htm. Accessed 14 March, 2008.

Westfall, J. 2005. 2005 Summary of forest health conditions in British Columbia. Forest Practices Branch, British Columbia Ministry of Forests and Range. Pest Management Report No. 15. 45 p.

Wigmosta, M.S.; Vail, L.W.; Lettenmaier, D.P. 1994. A distributed hydrology-soil-vegetation model for complex terrain. Water Resources Research 30(6):1665–1679.

Wilson, B. 2004. An overview of the mountain pine beetle initiative. Pages 3–9 *in* T.L. Shore, J.E. Brooks, and J.E. Stone, eds. Mountain Pine Beetle Symposium: Challenges and solutions. Canadian Forest Service, Pacific Forestry Centre, Victoria, BC. Information Report BC-X-399. 298 p.

Winkler, R.D.; Spittlehouse D.L.; Golding, D.L. 2005. Measured differences in snow accumulation and melt among clearcut, juvenile, and mature forests in southern British Columbia. Hydrological Processes 19(1):51–62.

Winkler, R.; Rex, J.; Teti, P.; Maloney, D.; Redding, T. 2008. Mountain pine beetle, forest practices, and watershed management. BC Ministry of Forests and Range. Extension Note No. 88. 11 p. http://www.for.gov.bc.ca/hfd/pubs/Docs/En/En88.pdf.

Wood, C.S.; Unger, L. 1996. Mountain pine beetle: A history of outbreaks in pine forests in British Columbia, 1910 to 1995. Natural Resources Canada, Canadian Forest Service, Pacific Forestry Centre, Victoria, BC. 61 p.

Yapo, P.O.; Gupta, H.V.; Sorooshian, S. 1998. Multi-objective global optimization for hydrologic models. Journal of Hydrology 204:83–97.

Ziemer, R.R.; Lisle, T.E. 1998. Hydrology. Pages 43–68 *in* R.J. Naiman and R.E. Bilby, eds. River Ecology and Management: Lessons from the Pacific Coastal Ecoregion. Springer-Verlag, New York, NY. 705 p.

9 Appendix

Table A1. Datasets produced for describing the boundary conditions of the VIC Fraser River application
Water Survey of Canada (WSC) hydrometric stations and corresponding VIC-model sub-basins, with entries ordered by WSC ID (generally upstream to downstream)

Data Set	Data Type	Spatial Extent§	Spatial Resolution	Time Period
Daily Precipitation	Gridded surface time series	British Columbia	0.0625°	1/1/1915 to 31/12/2006
Daily maximum temperature	Gridded surface time series	British Columbia	0.0625°	1/1/1915 to 31/12/2006
Daily minimum temperature	Gridded surface time series	British Columbia	0.0625°	1/1/1915 to 31/12/2006
Daily 10-m wind speed	Gridded surface time series	British Columbia	0.0625°	1/1/1915 to 31/12/2006
Soil Parameter File	Text or ESRI shapefile	British Columbia	0.0625°	N/A
1995 Vegetation Classification	Gridded surface	Fraser River	3-arc seconds	N/A
2007 Vegetation Classification	Gridded surface	Fraser River	3-arc seconds	N/A
Vegetation Library	Text file	Fraser River	N/A	N/A
Flow direction	Gridded surface	Fraser River	0.0625°	N/A
Flow distance	Gridded surface	Fraser River	0.0625°	N/A
Flow fraction	Gridded surface	Fraser River	0.0625°	N/A
Drainage Features	Gridded surface	Fraser River	0.0625°	N/A
Routing Wave Velocity	Gridded surface	Fraser River	0.0625°	N/A
Routing Channel Diffusivity	Gridded surface	Fraser River	0.0625°	N/A

§ Refer to Figure 3 of this report.

Table A2. Sub-basin metadata for the VIC Fraser River application

Water Survey of Canada (WSC) hydrometric stations and corresponding VIC-model sub-basins, with entries ordered by WSC ID (generally upstream to downstream)

WSC ID	WSC Station Name	Basin Name	Latitude§	Longitude§	Area (km^2)‡
08JA017	NECHAKO RIVER BELOW CHESLATTA FALLS	NECHC	53.71875	-124.84375	15,717
08JB002	STELLAKO RIVER AT GLENANNAN	STELL	54.03125	-124.96875	3,996
08JB003	NAUTLEY RIVER NEAR FORT FRASER	NAUTL	54.09375	-124.65625	6,514
08JB012	ENDAKO RIVER AT OUTLET OF BURNS LAKE	ENDAK	54.21875	-125.53125	767
08JC001	NECHAKO RIVER AT VANDERHOOF	NECHV	54.03125	-124.03125	25,360
08JC002	NECHAKO RIVER AT ISLE PIERRE	NECHI	53.96875	-123.28125	42,916
08JD006	DRIFTWOOD RIVER ABOVE KASTBERG CREEK	DRIFT	55.96875	-126.65625	442
08JE001	STUART RIVER NEAR FORT ST. JAMES	STUAR	54.40625	-124.28125	13,683
08JE005	KAZCHEK CREEK NEAR THE MOUTH	KAZCH	54.90625	-125.09375	916
08KA001	DORE RIVER NEAR MCBRIDE	DORE	53.28125	-120.28125	407
08KA004	FRASER RIVER AT HANSARD	FRSHA	54.09375	-121.84375	18,016
08KA005	FRASER RIVER AT MCBRIDE	FRSMC	53.28125	-120.09375	6,813
08KA007	FRASER RIVER AT RED PASS	FRSRP	52.96875	-119.03125	1,772
08KA008	MOOSE RIVER NEAR RED PASS	MOOSE	52.96875	-118.78125	485
08KA011	MCLENNAN RIVER NEAR THE MOUTH	MCLEN	52.90625	-119.40625	460
08KB001	FRASER RIVER AT SHELLEY	FRSSH	54.03125	-122.59375	32,197
08KB003	MCGREGOR RIVER AT LOWER CANYON	MCGRE	54.21875	-121.65625	4,735
08KC001	SALMON RIVER NEAR PRINCE GEORGE	SALMO	54.09375	-122.65625	4,379
08KD001	BOWRON RIVER NEAR WELLS	BOWRW	53.28125	-121.40625	436
08KD006	WILLOW RIVER ABOVE HAY CREEK	WILLO	54.03125	-122.40625	2,855
08KD007	BOWRON RIVER BELOW BOX CANYON	BOWRB	54.03125	-122.09375	3,377
08KE009	COTTONWOOD RIVER NEAR CINEMA	COTTO	53.15625	-122.46875	2,158
08KE016	BAKER CREEK AT QUESNEL	BAKER	52.96875	-122.59375	1,552
08KE018	FRASER RIVER AT SOUTH FORT GEORGE	FRSFG	53.90625	-122.71875	79,798
08KE036	NARCOSLI CREEK BELOW RAMSEY CREEK	NARCO	52.53125	-122.71875	560
08KF001	NAZKO RIVER ABOVE MICHELLE CREEK	NAZKO	52.90625	-123.59375	3,270
08KG001	WEST ROAD RIVER NEAR CINEMA	WEST	53.28125	-122.90625	12,311
08KG003	BAEZAEKO RIVER AT LOT 10262	BAEZA	52.96875	-123.84375	995
08KH001	QUESNEL RIVER AT LIKELY	QUESL	52.59375	-121.59375	5,864
08KH006	QUESNEL RIVER NEAR QUESNEL	QUESQ	52.84375	-122.21875	11,535
08KH010	HORSEFLY RIVER ABOVE MCKINLEY CREEK	HORSE	52.28125	-121.03125	1,246
08KH019	MOFFAT CREEK NEAR HORSEFLY	MOFFA	52.28125	-121.40625	535
08KH025	LITTLE HORSEFLY RIVER ABOVE GRUHS LAKE	LHRSE	52.34375	-121.34375	503
08LA001	CLEARWATER RIVER NEAR CLEARWATER STATION	CLEAS	51.71875	-120.03125	10,730
08LA007	CLEARWATER RIVER AT OUTLET OF CLEARWATER LAKE	CLEAO	52.15625	-120.21875	3,041
08LA008	MAHOOD RIVER AT OUTLET OF MAHOOD LAKE	MAHOO	51.90625	-120.28125	5,094
08LB020	BARRIERE RIVER AT THE MOUTH	BARRM	51.21875	-120.09375	1,181
08LB047	NORTH THOMPSON RIVER AT BIRCH ISLAND	NTHMB	51.59375	-119.90625	4,552
08LB064	NORTH THOMPSON RIVER AT MCLURE	NTHMM	51.03125	-120.21875	20,360
08LB069	BARRIERE RIVER BELOW SPRAGUE CREEK	BARRS	51.28125	-119.90625	847
08LC049	CHERRY CREEK NEAR CHERRYVILLE	CHERR	50.21875	-118.59375	469
08LD001	ADAMS RIVER NEAR SQUILAX	ADAMS	50.96875	-119.65625	2,987

Table A2. …cont. Sub-basin metadata for the VIC Fraser River application

WSC ID	WSC Station Name	Basin Name	Latitude§	Longitude§	Area (km^2)‡
08LE024	EAGLE RIVER NEAR MALAKWA	EAGLE	50.96875	-118.78125	884
08LE027	SEYMOUR RIVER NEAR SEYMOUR ARM	SEYMO	51.28125	-118.90625	829
08LE031	SOUTH THOMPSON RIVER AT CHASE	STHOM	50.78125	-119.71875	15,656
08LF023	THOMPSON RIVER NEAR KAMLOOPS	THOMK	50.65625	-120.34375	38,565
08LF051	THOMPSON RIVER NEAR SPENCES BRIDGE	THOMS	50.34375	-121.40625	55,934
08LG008	SPIUS CREEK NEAR CANFORD	SPIUS	50.09375	-121.03125	748
08MA001	CHILKO RIVER NEAR REDSTONE	CHILK	52.03125	-123.59375	6,604
08MA003	TASEKO RIVER AT OUTLET OF TASEKO LAKES	TASEK	51.40625	-123.65625	1,788
08MB005	CHILCOTIN RIVER BELOW BIG CREEK	CHILB	51.84375	-122.65625	19,300
08MB006	BIG CREEK ABOVE GROUNDHOG CREEK	BIGCR	51.46875	-123.09375	1,000
08MB010	CHILCOTIN RIVER ABOVE CLUSKO RIVER	CHILC	52.40625	-124.15625	1,438
08MC018	FRASER RIVER NEAR MARGUERITE	FRSMG	52.53125	-122.46875	114,024
08ME025	YALAKOM RIVER ABOVE ORE CREEK	YALAK	50.90625	-122.21875	671
08ME028	BRIDGE RIVER ABOVE DOWNTOWN LAKE	BRIDG	50.84375	-123.21875	722
08MF005	FRASER RIVER AT HOPE	FRSHP	49.40625	-121.46875	216,627
08MF040	FRASER RIVER ABOVE TEXAS CREEK	FRSTX	50.59375	-121.84375	153,907
08MF065	NAHATLATCH RIVER BELOW TACHEWANA CREEK	NAHAT	49.96875	-121.84375	792
08MF068	COQUIHALLA RIVER ABOVE ALEXANDER CREEK	COQUI	49.40625	-121.34375	575

§ Coordinates of VIC model grid cell centre in which hydrometric station is located

‡ Area based on 1/16° model resolution

Table A3. Relative change in T = 2-year peak discharge quantile

Relative change in Q_2 ($y_{0.5}$) quantile magnitude from baseline (95_BASE) by scenario

BASIN	Baseline						
	Q_2 (m³/s)	*07_CURR*	*95_100K*	*95_25HF*	*95_50HF*	*95_75HF*	*95_100HF*
ADAMS	201	-0.01	0.00	0.01	0.01	0.02	0.03
BAEZA	7	-0.01	0.03	0.39	0.72	1.05	1.36
BAKER	15	0.23	0.10	0.49	0.94	1.40	1.85
BARRM	59	-0.01	0.00	0.03	0.07	1.10	0.14
BARRS	52	-0.01	0.00	0.02	0.06	0.09	0.12
BIGCR	24	0.00	0.00	0.00	0.00	0.01	0.00
BOWRB	271	-0.08	0.00	0.02	0.03	0.05	0.07
BOWRW	41	0.00	0.00	0.02	0.04	0.05	0.08
BRIDG	225	0.00	0.00	0.00	0.00	0.00	0.00
CHERR	11	0.03	0.00	0.03	0.05	0.08	0.11
CHILB	333	0.00	0.00	0.05	0.06	0.07	0.08
CHILC	23	-0.01	0.01	-0.02	-0.01	0.01	0.07
CHILK	299	0.01	0.00	0.02	0.03	0.04	0.05
CLEAO	543	0.00	0.00	0.00	0.00	0.00	0.00
CLEAS	941	0.00	0.00	0.00	0.02	0.03	0.03
COQUI	137	0.00	0.00	0.00	0.01	0.01	0.01
COTTO	71	0.05	0.00	0.12	0.24	0.41	0.57
DORE	66	0.00	0.00	0.00	0.00	0.00	0.00
DRIFT	40	0.01	-0.01	0.02	0.06	0.10	0.14
EAGLE	218	0.00	0.00	0.00	0.00	0.00	0.00
ENDAK	6	0.10	0.09	0.38	0.67	0.97	1.26
FRSFG	3925	0.00	0.00	0.03	0.05	0.07	0.08
FRSHA	2084	-0.01	0.00	0.01	0.02	0.02	0.03
FRSHP	8917	0.00	0.00	0.02	0.04	0.08	0.10
FRSMC	1130	0.00	0.00	0.00	0.00	0.01	0.01
FRSMG	4713	0.00	0.00	0.02	0.05	0.07	0.10
FRSRP	257	0.00	0.00	0.00	0.02	0.03	0.05
FRSSH	3173	-0.01	0.00	0.01	0.02	0.03	0.04
FRSTX	5496	0.00	0.00	0.01	0.04	0.08	0.10
HORSE	144	0.01	0.01	0.02	0.03	0.04	0.04
KAZCH	27	0.02	0.01	0.13	0.24	0.35	0.47
LHRSE	17	0.01	0.00	0.07	0.12	0.20	0.26
MAHOO	163	0.02	-0.02	0.11	0.21	0.33	0.46
MCGRE	1009	-0.01	0.00	0.00	0.00	0.01	0.01
MCLEN	54	0.00	0.00	0.00	0.01	0.02	0.03
MOFFA	26	0.05	0.01	0.18	0.42	0.63	0.92
MOOSE	60	0.01	0.00	0.04	0.05	0.05	0.05
NAHAT	219	0.00	-0.01	-0.01	-0.01	-0.01	-0.01
NARCO	5	0.09	0.04	0.27	0.49	0.74	0.97
NAUTL	48	0.04	0.06	0.20	0.38	0.56	0.75
NAZKO	14	-0.02	0.08	0.43	0.86	1.25	1.64
NECHC	647	0.01	0.01	0.05	0.10	0.13	0.18

Table A3. …cont. Relative change in T = 2-year peak discharge quantile

BASIN	Baseline Q_2 (m³/s)	*07_CURR*	*95_100K*	*95_25HF*	*95_50HF*	*95_75HF*	*95_100HF*
NECHI	961	0.01	0.01	0.05	0.10	0.16	0.21
NECHV	699	0.02	0.01	0.08	0.14	0.18	0.26
NTHMB	627	0.00	0.00	0.00	0.01	0.02	0.03
NTHMM	1738	0.01	0.00	0.01	0.03	0.04	0.05
QUESL	375	0.01	0.00	0.01	0.02	0.03	0.03
QUESQ	714	-0.01	0.00	0.01	0.03	0.05	0.06
SALMO	144	0.03	0.01	0.15	0.26	0.45	0.62
SEYMO	212	0.00	0.00	0.00	0.00	0.00	0.00
SPIUS	137	-0.01	0.00	0.05	0.10	0.17	0.23
STELL	37	0.02	0.04	0.19	0.30	0.44	0.60
STHOM	948	0.00	0.00	0.01	0.02	0.03	0.04
STUAR	261	0.02	0.02	0.09	0.17	0.26	0.32
TASEK	163	0.00	0.00	0.00	0.00	0.01	0.02
THOMK	2559	0.00	0.00	0.01	0.02	0.02	0.03
THOMS	2625	-0.01	0.00	0.01	0.03	0.04	0.05
WEST	78	0.09	0.08	0.43	0.79	1.13	1.50
WILLO	155	0.01	0.00	0.04	0.09	0.13	0.18
YALAK	18	0.01	0.00	0.00	0.00	0.01	0.02

Shaded text indicates change from baseline statistically significant at $p < 0.05$

Table A4. Relative change in T = 10-year peak discharge quantile

Relative change in Q_{10} ($y_{0.1}$) quantile magnitude from baseline (95_BASE) by scenario

BASIN	Baseline						
	Q_{10} (m³/s)	*07_CURR*	*95_100K*	*95_25HF*	*95_50HF*	*95_75HF*	*95_100HF*
ADAMS	256	-0.01	0.00	0.00	0.01	0.02	0.03
BAEZA	9	-0.01	0.07	0.47	0.91	1.35	1.76
BAKER	35	0.13	0.05	0.28	0.55	0.83	1.12
BARRM	92	-0.01	0.00	0.02	0.06	0.10	0.13
BARRS	87	-0.01	0.00	0.02	0.05	0.06	0.08
BIGCR	34	0.00	0.00	0.01	0.01	0.01	0.01
BOWRB	402	-0.08	0.00	0.01	0.03	0.04	0.06
BOWRW	65	-0.01	-0.01	0.00	0.02	0.04	0.07
BRIDG	310	0.00	0.00	0.00	0.00	0.01	0.01
CHERR	19	0.03	0.00	0.03	0.05	0.08	0.10
CHILB	528	0.00	0.00	0.01	0.03	0.04	0.06
CHILC	67	0.00	0.01	-0.09	-0.11	-0.09	-0.14
CHILK	486	0.00	0.00	0.00	0.01	0.02	0.03
CLEAO	624	0.00	0.00	0.00	0.00	0.00	0.00
CLEAS	1150	0.00	0.00	0.01	0.03	0.05	0.07
COQUI	197	-0.01	0.00	0.00	0.00	0.00	0.01
COTTO	130	0.01	0.00	0.08	0.15	0.24	0.33
DORE	120	0.00	0.00	0.00	0.00	0.00	0.00
DRIFT	56	-0.01	-0.02	0.00	0.03	0.07	0.11
EAGLE	269	0.00	0.00	0.00	0.00	0.00	0.00
ENDAK	10	0.09	0.08	0.28	0.49	0.74	0.97
FRSFG	5971	0.00	0.00	0.03	0.05	0.08	0.10
FRSHA	3455	0.00	0.00	0.01	0.01	0.02	0.02
FRSHP	12090	0.00	0.00	0.01	0.03	0.05	0.07
FRSMC	1796	0.00	0.00	0.01	0.02	0.03	0.03
FRSMG	7257	0.00	0.00	0.03	0.06	0.09	0.11
FRSRP	418	0.00	0.00	0.00	0.01	0.02	0.03
FRSSH	4889	-0.01	0.00	0.01	0.02	0.02	0.03
FRSTX	8107	0.00	0.00	0.04	0.07	0.09	0.11
HORSE	221	0.00	0.00	0.02	0.03	0.03	0.04
KAZCH	36	0.00	0.00	0.08	0.17	0.29	0.41
LHRSE	26	-0.01	0.01	0.04	0.11	0.16	0.21
MAHOO	256	0.03	0.00	0.12	0.25	0.38	0.52
MCGRE	1452	-0.01	0.00	0.00	0.00	0.00	0.01
MCLEN	80	0.00	0.00	0.00	0.02	0.03	0.03
MOFFA	53	0.00	-0.03	0.10	0.24	0.48	0.69
MOOSE	103	-0.01	0.00	-0.03	-0.03	-0.03	-0.02
NAHAT	278	0.00	0.00	0.00	0.00	0.00	0.00
NARCO	9	0.07	0.03	0.22	0.43	0.62	0.83
NAUTL	69	0.05	0.07	0.19	0.34	0.50	0.67
NAZKO	25	0.02	0.08	0.37	0.61	0.87	1.14
NECHC	853	0.00	0.00	0.03	0.07	0.12	0.17

Table A4. …cont. Relative change in T = 10-year peak discharge quantile

BASIN	Baseline Q_{10} (m^3/s)	*07_CURR*	*95_100K*	*95_25HF*	*95_50HF*	*95_75HF*	*95_100HF*
NECHI	1197	0.01	0.01	0.06	0.10	0.17	0.25
NECHV	909	0.01	0.01	0.04	0.10	0.17	0.24
NTHMB	763	0.01	0.00	0.01	0.01	0.01	0.02
NTHMM	2141	0.00	0.00	0.01	0.02	0.03	0.05
QUESL	514	0.01	0.00	0.01	0.02	0.03	0.05
QUESQ	1064	-0.01	0.00	0.02	0.04	0.07	0.09
SALMO	235	0.01	0.00	0.07	0.15	0.24	0.36
SEYMO	256	0.00	0.00	0.00	0.00	0.00	0.00
SPIUS	191	-0.01	-0.01	0.05	0.09	0.12	0.18
STELL	50	0.01	0.04	0.18	0.31	0.45	0.60
STHOM	1226	0.00	0.00	0.01	0.02	0.03	0.04
STUAR	345	0.02	0.01	0.08	0.15	0.22	0.29
TASEK	286	0.00	0.00	-0.01	0.00	0.01	0.02
THOMK	3100	0.00	0.00	0.01	0.02	0.03	0.04
THOMS	3222	0.00	0.00	0.01	0.02	0.04	0.05
WEST	129	0.06	0.06	0.35	0.65	0.99	1.31
WILLO	245	0.01	0.00	0.03	0.07	0.11	0.15
YALAK	32	-0.01	0.00	0.02	0.02	0.03	0.08

Shaded text indicates change from baseline statistically significant at $p < 0.05$

Table A5. Relative change in T = 20-year peak discharge quantile

Relative change in Q_{20} ($y_{0.05}$) quantile magnitude from baseline (95_BASE) by scenario

BASIN	Baseline Q_{20} (m³/s)	*07_CURR*	*95_100K*	*95_25HF*	*95_50HF*	*95_75HF*	*95_100HF*
ADAMS	269	-0.02	0.00	0.01	0.02	0.02	0.03
BAEZA	10	-0.02	0.06	0.47	0.91	1.30	1.72
BAKER	39	0.08	0.04	0.26	0.55	0.84	1.14
BARRM	107	-0.04	-0.01	0.01	0.04	0.06	0.08
BARRS	101	-0.04	-0.01	0.01	0.03	0.05	0.07
BIGCR	44	0.00	0.00	0.01	0.01	0.00	0.00
BOWRB	435	-0.03	0.00	0.01	0.03	0.05	0.05
BOWRW	70	0.00	0.00	0.03	0.04	0.04	0.05
BRIDG	324	0.00	0.00	0.02	0.02	0.02	0.02
CHERR	23	0.03	0.00	0.02	0.04	0.05	0.07
CHILB	592	0.00	0.00	0.02	0.04	0.06	0.07
CHILC	80	-0.01	-0.02	-0.01	0.00	0.00	-0.07
CHILK	561	0.00	0.00	0.00	0.00	0.01	0.01
CLEAO	720	0.00	0.00	0.00	0.00	0.00	0.00
CLEAS	1359	0.00	0.00	0.01	0.01	0.02	0.03
COQUI	220	0.00	0.00	0.00	0.00	0.00	0.00
COTTO	170	-0.02	-0.01	-0.03	0.03	0.12	0.19
DORE	134	-0.01	0.00	0.00	0.00	0.00	0.00
DRIFT	62	0.03	-0.01	0.02	0.06	0.11	0.16
EAGLE	298	0.00	0.00	0.00	0.00	0.00	0.00
ENDAK	12	0.06	0.05	0.26	0.50	0.76	0.99
FRSFG	6412	0.00	0.00	0.01	0.03	0.05	0.08
FRSHA	3793	-0.01	0.00	0.00	0.00	0.01	0.01
FRSHP	13059	0.00	0.00	0.03	0.05	0.07	0.10
FRSMC	2060	0.00	0.00	-0.01	0.00	0.00	0.01
FRSMG	7846	0.00	0.00	0.03	0.06	0.08	0.10
FRSRP	531	0.00	-0.01	0.04	0.07	0.09	0.11
FRSSH	5422	-0.01	0.00	0.00	0.01	0.02	0.03
FRSTX	8560	0.00	0.00	0.04	0.06	0.08	0.10
HORSE	246	0.01	0.00	0.01	0.01	0.01	0.02
KAZCH	39	0.00	0.00	0.08	0.18	0.30	0.42
LHRSE	30	-0.01	0.00	0.02	0.05	0.08	0.10
MAHOO	296	0.05	0.03	0.12	0.21	0.31	0.43
MCGRE	1687	-0.01	0.00	0.00	0.00	0.00	0.01
MCLEN	104	0.00	0.00	0.00	0.01	0.01	0.02
MOFFA	62	0.04	-0.01	0.10	0.26	0.42	0.67
MOOSE	149	-0.02	0.00	-0.01	-0.01	0.00	0.00
NAHAT	293	0.00	0.00	0.00	0.01	0.01	0.02
NARCO	10	0.08	0.02	0.22	0.454	0.68	0.90
NAUTL	76	0.06	0.07	0.19	0.37	0.56	0.74
NAZKO	28	0.00	0.08	0.35	0.65	0.97	1.30
NECHC	948	0.00	0.00	0.04	0.11	0.15	0.17
NECHI	1350	0.01	0.01	0.05	0.10	0.15	0.19

Table A5. …cont. Relative change in T = 20-year peak discharge quantile

BASIN	Baseline						
	Q_{20} (m³/s)	*07_CURR*	*95_100K*	*95_25HF*	*95_50HF*	*95_75HF*	*95_100HF*
NECHV	1025	0.01	0.01	0.06	0.11	0.14	0.21
NTHMB	910	0.00	0.00	0.00	0.01	0.01	0.02
NTHMM	2477	0.00	0.00	0.00	0.01	0.02	0.05
QUESL	590	0.00	-0.01	0.01	0.03	0.05	0.07
QUESQ	1226	0.00	0.00	0.02	0.03	0.05	0.06
SALMO	271	0.01	0.00	0.08	0.17	0.28	0.39
SEYMO	275	0.00	0.00	0.00	0.00	0.00	0.00
SPIUS	200	0.01	0.02	0.05	0.08	0.12	0.18
STELL	58	0.02	0.05	0.16	0.31	0.47	0.63
STHOM	1270	0.00	0.00	0.01	0.01	0.02	0.03
STUAR	370	0.01	0.01	0.08	0.14	0.20	0.27
TASEK	337	0.00	0.00	-0.01	0.00	0.00	0.01
THOMK	3508	0.00	0.00	0.01	0.01	0.02	0.02
THOMS	3509	0.00	0.00	0.01	0.02	0.03	0.04
WEST	138	0.07	0.05	0.34	0.68	1.04	1.43
WILLO	301	-0.01	-0.01	-0.02	-0.02	0.00	0.02
YALAK	50	0.04	0.00	0.11	0.10	0.09	0.10

Shaded text indicates change from baseline statistically significant at $p < 0.05$

Table A6: Relative change in T = 50-year peak discharge quantile

Relative change in Q_{50} ($y_{0.02}$) quantile magnitude from baseline (95_BASE) by scenario

BASIN	Baseline						
	Q_{50} (m³/s)	*07_CURR*	*95_100K*	*95_25HF*	*95_50HF*	*95_75HF*	*95_100HF*
ADAMS	297	-0.01	0.00	0.01	0.02	0.03	0.04
BAEZA	12	-0.04	0.05	0.45	0.85	1.26	1.67
BAKER	40	0.18	0.06	0.42	0.76	0.98	1.29
BARRM	111	-0.02	0.00	0.03	0.05	0.07	0.08
BARRS	106	-0.03	0.00	0.02	0.05	0.07	0.08
BIGCR	51	0.01	0.00	-0.03	-0.03	-0.03	-0.03
BOWRB	592	-0.07	0.00	0.01	0.03	0.04	0.04
BOWRW	89	0.00	-0.01	0.01	0.04	0.06	0.08
BRIDG	351	0.00	0.00	-0.02	-0.02	-0.01	-0.01
CHERR	25	0.01	0.00	0.02	0.04	0.06	0.07
CHILB	628	0.00	0.00	0.01	0.02	0.04	0.05
CHILC	118	-0.01	0.00	0.00	0.00	0.02	-0.01
CHILK	592	0.00	0.00	0.00	0.01	0.02	0.02
CLEAO	801	0.00	0.00	0.00	0.00	0.00	0.00
CLEAS	1551	0.00	0.00	0.01	0.03	0.04	0.06
COQUI	285	-0.01	0.00	0.00	0.00	0.00	0.00
COTTO	194	0.04	0.00	0.07	0.15	0.23	0.36
DORE	159	0.00	0.00	0.00	0.00	0.00	0.00
DRIFT	75	-0.01	-0.01	0.03	0.07	0.12	0.16
EAGLE	334	0.00	0.00	0.00	0.00	0.00	0.00
ENDAK	13	0.06	0.05	0.26	0.48	0.72	0.97
FRSFG	7776	0.00	0.00	0.02	0.03	0.05	0.06
FRSHA	4542	-0.01	0.00	0.00	0.00	0.01	0.01
FRSHP	15417	0.00	0.00	0.02	0.03	0.05	0.07
FRSMC	2345	0.00	0.00	0.00	0.00	0.01	0.01
FRSMG	9212	0.00	0.00	0.02	0.04	0.06	0.08
FRSRP	706	0.00	-0.01	0.00	0.01	0.02	0.02
FRSSH	6550	0.00	0.00	0.00	0.01	0.02	0.02
FRSTX	10146	0.00	0.00	0.02	0.04	0.06	0.08
HORSE	297	0.00	0.00	0.01	0.02	0.03	0.05
KAZCH	44	0.00	0.00	0.07	0.17	0.28	0.39
LHRSE	37	-0.01	0.00	0.05	0.13	0.21	0.28
MAHOO	412	0.06	0.00	0.11	0.22	0.33	0.45
MCGRE	2187	0.00	0.00	0.00	0.00	0.00	0.00
MCLEN	116	0.00	0.00	0.01	0.02	0.03	0.04
MOFFA	78	0.11	0.04	0.17	0.31	0.44	0.65
MOOSE	198	0.00	-0.01	-0.01	0.00	0.01	0.02
NAHAT	321	0.01	0.00	0.00	0.01	0.01	0.01
NARCO	12	0.07	0.01	0.28	0.55	0.81	1.04
NAUTL	85	0.06	0.05	0.24	0.43	0.60	0.78
NAZKO	34	0.01	0.05	0.27	0.62	0.99	1.32
NECHC	1040	0.00	0.00	0.02	0.07	0.09	0.13
NECHI	1430	0.01	0.01	0.06	0.09	0.12	0.17
NECHV	1121	0.00	0.00	0.05	0.07	0.11	0.17

Table A6. …cont. Relative change in T = 50-year peak discharge quantile

BASIN	Baseline Q_{50} (m³/s)	*07_CURR*	*95_100K*	*95_25HF*	*95_50HF*	*95_75HF*	*95_100HF*
NTHMB	1061	0.00	0.00	0.00	0.01	0.01	0.02
NTHMM	2984	0.00	0.00	0.01	0.02	0.03	0.04
QUESL	655	0.00	0.00	0.01	0.02	0.03	0.05
QUESQ	1305	0.00	0.00	0.02	0.04	0.06	0.09
SALMO	279	0.00	-0.02	0.08	0.19	0.31	0.41
SEYMO	282	0.00	0.00	0.00	0.00	0.00	0.00
SPIUS	225	-0.01	0.02	0.03	0.05	0.08	0.15
STELL	66	0.01	0.03	0.19	0.35	0.52	0.68
STHOM	1446	0.00	0.00	0.01	0.02	0.03	0.04
STUAR	413	0.01	0.00	0.06	0.13	0.19	0.26
TASEK	351	0.00	0.00	-0.01	-0.01	-0.01	0.00
THOMK	4217	0.00	0.00	0.01	0.02	0.03	0.04
THOMS	4281	0.00	0.00	0.01	0.03	0.04	0.06
WEST	168	0.06	0.07	0.25	0.62	0.99	1.39
WILLO	336	0.01	-0.01	0.03	0.06	0.09	0.12
YALAK	61	0.00	0.00	0.02	0.02	0.03	0.03

Shaded text indicates change from baseline statistically significant at $p < 0.05$

Table A7. Relative change in T = 100-year peak discharge quantile

Relative change in Q_{100} ($y_{0.01}$) quantile magnitude from baseline (95_BASE) by scenario

BASIN	Baseline						
	Q_{100} (m³/s)	*07_CURR*	*95_100K*	*95_25HF*	*95_50HF*	*95_75HF*	*95_100HF*
ADAMS	352	-0.01	0.00	0.01	0.02	0.03	0.05
BAEZA	23	-0.04	0.04	0.26	0.48	0.68	0.68
BAKER	56	0.06	0.02	0.14	0.33	0.59	0.89
BARRM	151	-0.02	-0.01	0.02	0.04	0.07	0.07
BARRS	142	-0.02	-0.01	0.01	0.03	0.06	0.06
BIGCR	63	0.00	0.00	0.00	0.00	0.00	0.00
BOWRB	812	-0.08	0.00	0.01	0.03	0.04	0.06
BOWRW	132	-0.01	0.00	0.01	0.03	0.05	0.07
BRIDG	432	0.00	0.00	0.00	0.00	0.00	0.00
CHERR	33	0.00	0.00	0.01	0.03	0.05	0.06
CHILB	719	0.00	0.00	0.01	0.03	0.04	0.06
CHILC	133	-0.05	0.01	-0.04	-0.04	-0.04	-0.04
CHILK	678	0.00	0.00	0.00	0.01	0.02	0.03
CLEAO	938	0.00	0.00	0.00	0.00	0.00	0.00
CLEAS	1660	0.00	0.00	0.01	0.02	0.03	0.04
COQUI	315	0.00	0.00	0.00	0.00	0.00	0.01
COTTO	268	0.05	0.01	0.11	0.21	0.32	0.39
DORE	181	0.00	0.00	0.00	0.00	0.00	0.00
DRIFT	83	0.00	-0.01	0.03	0.08	0.12	0.17
EAGLE	345	0.00	0.00	0.00	0.00	0.00	0.00
ENDAK	15	0.06	0.05	0.27	0.51	0.75	1.00
FRSFG	9299	0.00	0.00	0.02	0.04	0.06	0.08
FRSHA	5966	-0.01	0.00	0.01	0.01	0.02	0.02
FRSHP	17620	0.00	0.00	0.02	0.04	0.06	0.08
FRSMC	3008	0.00	0.00	0.01	0.02	0.02	0.03
FRSMG	11489	0.00	0.00	0.03	0.05	0.07	0.10
FRSRP	743	0.00	0.00	0.02	0.03	0.04	0.05
FRSSH	8238	-0.01	0.00	0.01	0.02	0.02	0.03
FRSTX	12129	0.00	0.00	0.03	0.05	0.08	0.10
HORSE	313	-0.01	-0.01	0.00	0.01	0.02	0.02
KAZCH	48	0.00	-0.01	0.08	0.17	0.26	0.36
LHRSE	46	0.00	0.00	0.06	0.15	0.23	0.31
MAHOO	444	0.05	-0.01	0.10	0.22	0.33	0.45
MCGRE	2282	-0.01	0.00	0.00	0.00	0.00	0.00
MCLEN	152	0.00	0.00	0.01	0.02	0.03	0.04
MOFFA	106	-0.05	-0.05	0.01	0.06	0.12	0.29
MOOSE	235	0.00	-0.01	0.02	0.03	0.05	0.06
NAHAT	361	0.00	0.00	0.00	0.01	0.01	0.02
NARCO	12	0.07	0.01	0.21	0.41	0.63	1.08
NAUTL	91	0.04	0.05	0.20	0.37	0.59	0.81
NAZKO	37	-0.02	0.05	0.30	0.62	0.94	1.22
NECHC	1081	0.00	0.00	0.02	0.05	0.09	0.14
NECHI	1454	0.01	0.01	0.04	0.10	0.16	0.22

Table A7. …cont. Relative change in T = 100-year peak discharge quantile

BASIN	Baseline						
	Q_{100} (m³/s)	*07_CURR*	*95_100K*	*95_25HF*	*95_50HF*	*95_75HF*	*95_100HF*
NECHV	1146	0.01	0.00	0.04	0.10	0.16	0.23
NTHMB	1160	0.00	0.00	0.01	0.01	0.01	0.02
NTHMM	3166	0.00	0.00	0.01	0.02	0.03	0.04
QUESL	854	0.01	0.00	0.01	0.02	0.04	0.05
QUESQ	1843	-0.01	0.00	0.02	0.04	0.06	0.08
SALMO	329	0.00	0.00	0.01	0.04	0.12	0.21
SEYMO	283	0.00	0.00	0.00	0.00	0.00	0.00
SPIUS	231	-0.01	0.02	0.06	0.09	0.13	0.20
STELL	73	0.02	0.04	0.17	0.31	0.46	0.60
STHOM	1615	0.00	0.00	0.01	0.02	0.03	0.04
STUAR	421	0.01	0.00	0.07	0.14	0.20	0.28
TASEK	416	0.00	0.00	0.00	0.00	0.01	0.01
THOMK	4592	0.00	0.00	0.01	0.02	0.03	0.04
THOMS	4604	0.00	0.00	0.01	0.02	0.03	0.05
WEST	222	0.03	0.04	0.25	0.50	0.76	1.01
WILLO	447	0.01	0.00	0.03	0.05	0.08	0.11
YALAK	67	-0.03	0.00	0.02	0.02	0.01	0.00

Shaded text indicates change from baseline statistically significant at $p < 0.05$

Table: A8. Disturbance area by scenario and sub-basin

Baseline Area Fractions, Relative Disturbance Area by Scenario and Pine Forest-extent Runoff Ratio[§]

BASIN	Relative area by cover type for 1995 baseline scenario				Relative change in disturbance area (as fraction) from baseline by scenario and cover type													
					07_CURRENT		*95_100K*		*95_100K_25HF*		*95_100K_50HF*		*95_100K_75HF*		*95_100K_100HF*		$w^{\dagger}$
	P	*Px*	*CC*	*VOP*	*CC*	*VOP*	*Px*	*VOP*	*Px*	*VOP*	*Px*	*VOP*	*Px*	*VOP*	*Px*	*VOP*	*Px*	
ADAMS	0.08	0.00	0.00	0.09	0.00	-0.01	0.03	0.00	0.08	0.02	0.06	0.04	0.04	0.06	0.02	0.08	0.00	0.05
BAEZA	0.73	0.01	0.00	0.15	0.00	-0.04	0.70	0.00	0.73	0.18	0.54	0.37	0.36	0.55	0.17	0.74	-0.01	0.76
BAKER	0.60	0.00	0.01	0.12	0.01	0.09	0.45	0.00	0.60	0.15	0.45	0.30	0.30	0.45	0.15	0.60	0.00	0.60
BARRM	0.17	0.00	0.00	0.10	0.00	0.02	0.08	0.00	0.17	0.04	0.13	0.08	0.08	0.13	0.04	0.17	0.00	0.12
BARRS	0.14	0.00	0.00	0.09	0.00	0.01	0.07	0.00	0.14	0.04	0.11	0.07	0.07	0.11	0.04	0.14	0.00	0.10
BIGCR	0.49	0.00	0.00	0.11	0.00	0.01	0.32	0.00	0.49	0.12	0.37	0.24	0.24	0.37	0.12	0.49	0.00	0.20
BOWRB	0.05	0.00	0.00	0.15	0.00	-0.08	0.04	0.00	0.05	0.01	0.04	0.03	0.03	0.04	0.01	0.05	0.00	0.04
BOWRW	0.10	0.01	0.00	0.10	0.00	0.00	0.09	0.00	0.10	0.03	0.07	0.05	0.05	0.08	0.02	0.10	-0.01	0.07
BRIDG	0.03	0.04	0.00	0.01	0.01	0.01	-0.04	0.00	0.03	0.02	0.01	0.03	-0.01	0.05	-0.02	0.06	-0.04	0.04
CHERR	0.12	0.00	0.00	0.09	0.00	0.02	0.02	0.00	0.12	0.03	0.09	0.06	0.06	0.09	0.03	0.12	0.00	0.07
CHILB	0.31	0.16	0.00	0.13	0.00	0.02	0.19	0.00	0.31	0.12	0.19	0.23	0.07	0.35	-0.04	0.47	-0.16	0.23
CHILC	0.67	0.07	0.00	0.12	0.00	0.02	0.58	0.00	0.67	0.19	0.49	0.37	0.30	0.56	0.11	0.74	-0.07	0.70
CHILK	0.19	0.13	0.00	0.06	0.00	0.04	0.01	0.00	0.19	0.08	0.11	0.16	0.03	0.24	-0.05	0.32	-0.13	0.16
CLEAO	0.01	0.00	0.00	0.12	0.00	0.00	0.00	0.00	0.01	0.00	0.01	0.00	0.00	0.01	0.00	0.01	0.00	0.00
CLEAS	0.18	0.00	0.00	0.10	0.00	0.02	0.13	0.00	0.18	0.04	0.13	0.09	0.09	0.13	0.04	0.18	0.00	0.05
COQUI	0.02	0.00	0.00	0.08	0.00	0.00	0.01	0.00	0.02	0.01	0.02	0.01	0.01	0.02	0.01	0.02	0.00	0.02
COTTO	0.33	0.00	0.00	0.04	0.00	0.03	0.17	0.00	0.33	0.08	0.25	0.16	0.16	0.25	0.08	0.33	0.00	0.26
DORE	0.00	0.00	0.00	0.09	0.00	-0.01	0.00	0.00	0.00	0.00	0.00	0.00	0.00	0.00	0.00	0.00	0.00	0.00
DRIFT	0.12	0.00	0.00	0.06	0.00	0.01	0.00	0.00	0.12	0.03	0.09	0.06	0.06	0.09	0.03	0.12	0.00	0.11
EAGLE	0.00	0.00	0.00	0.05	0.00	0.01	0.00	0.00	0.00	0.00	0.00	0.00	0.00	0.00	0.00	0.00	0.00	0.00
ENDAK	0.53	0.00	0.01	0.12	0.00	-0.01	0.43	0.00	0.53	0.13	0.39	0.26	0.26	0.40	0.13	0.53	0.00	0.50
FRSFG	0.29	0.00	0.00	0.10	0.00	0.01	0.22	0.00	0.29	0.07	0.22	0.15	0.15	0.22	0.07	0.29	0.00	0.12
FRSHA	0.05	0.00	0.00	0.07	0.00	-0.02	0.02	0.00	0.05	0.01	0.04	0.03	0.03	0.04	0.01	0.05	0.00	0.04
FRSHP	0.27	0.02	0.00	0.12	0.00	0.02	0.19	0.00	0.27	0.07	0.20	0.15	0.13	0.22	0.05	0.29	-0.02	0.11
FRSMC	0.09	0.00	0.00	0.03	0.00	0.00	0.02	0.00	0.09	0.02	0.07	0.04	0.04	0.07	0.02	0.09	0.00	0.05
FRSMG	0.32	0.00	0.00	0.11	0.00	0.02	0.25	0.00	0.32	0.08	0.24	0.16	0.16	0.24	0.08	0.33	0.00	0.13
FRSRP	0.10	0.00	0.00	0.01	0.00	0.00	0.01	0.00	0.10	0.02	0.07	0.05	0.05	0.07	0.02	0.10	0.00	0.06
FRSSH	0.10	0.00	0.00	0.10	0.00	-0.01	0.06	0.00	0.10	0.03	0.08	0.05	0.05	0.08	0.03	0.10	0.00	0.05
FRSTX	0.31	0.03	0.00	0.12	0.00	0.02	0.22	0.00	0.31	0.08	0.22	0.17	0.14	0.25	0.06	0.34	-0.03	0.14

Table A8. ... cont. Disturbance area by scenario and sub-basin

BASIN	Relative area by cover type for 1995 baseline scenario		Relative change in disturbance area (as fraction) from baseline by scenario and cover type															
					07_CURRENT		95_100K		95_100K_25HF		95_100K_50HF		95_100K_75HF		95_100K_100HF		$w^{\dagger}$
	P	Px	CC	VOP	CC	VOP	Px	VOP	Px	VOP	Px	VOP	Px	VOP	Px	VOP	Px	
HORSE		0.09									0.00	0.01	0.10	-0.01	0.01	0.06	0.00	
0.09		0.02									0.07	0.04	0.04	0.07	0.02	0.09	0.00	
0.04																		
KAZCH	0.40	0.00	0.01	0.10	-0.01	0.00	0.32	0.00	0.40	0.10	0.30	0.20	0.20	0.30	0.10	0.40	0.00	0.39
LHRSE	0.14	0.00	0.01	0.07	0.00	0.01	0.12	0.00	0.14	0.04	0.11	0.07	0.07	0.11	0.04	0.14	0.00	0.13
MAHOO	0.34	0.00	0.00	0.13	0.01	0.03	0.27	0.00	0.34	0.09	0.26	0.17	0.17	0.26	0.09	0.34	0.00	0.25
MCGRE	0.01	0.00	0.00	0.14	0.00	-0.01	0.00	0.00	0.01	0.00	0.01	0.00	0.00	0.01	0.00	0.01	0.00	0.01
MCLEN	0.18	0.00	0.00	0.04	0.00	0.00	0.02	0.00	0.18	0.05	0.14	0.09	0.09	0.14	0.04	0.19	0.00	0.09
MOFFA	0.51	0.00	0.01	0.12	-0.01	0.09	0.37	0.00	0.51	0.13	0.39	0.26	0.26	0.39	0.13	0.51	0.00	0.53
MOOSE	0.11	0.00	0.00	0.01	0.00	0.00	0.01	0.00	0.11	0.03	0.08	0.05	0.05	0.08	0.03	0.11	0.00	0.08
NAHAT	0.03	0.00	0.00	0.17	0.00	0.00	0.00	0.00	0.03	0.01	0.02	0.01	0.01	0.02	0.01	0.03	0.00	0.01
NARCO	0.60	0.00	0.01	0.20	-0.01	0.05	0.49	0.00	0.60	0.15	0.45	0.30	0.30	0.45	0.15	0.60	0.00	0.59
NAUTL	0.47	0.00	0.00	0.13	0.00	-0.01	0.39	0.00	0.47	0.12	0.35	0.23	0.23	0.35	0.12	0.47	0.00	0.43
NAZKO	0.56	0.07	0.00	0.21	0.00	-0.03	0.50	0.00	0.56	0.16	0.40	0.32	0.25	0.47	0.09	0.63	-0.07	0.63
NECHC	0.43	0.00	0.00	0.07	0.00	0.03	0.37	0.00	0.43	0.11	0.32	0.22	0.22	0.32	0.11	0.43	0.00	0.17
NECHI	0.41	0.00	0.00	0.09	0.00	0.02	0.33	0.00	0.41	0.10	0.31	0.21	0.20	0.31	0.10	0.42	0.00	0.24
NECHV	0.44	0.00	0.00	0.09	0.00	0.02	0.38	0.00	0.44	0.11	0.33	0.22	0.22	0.33	0.11	0.45	0.00	0.21
NTHMB	0.06	0.00	0.00	0.09	0.00	0.01	0.01	0.00	0.06	0.01	0.04	0.03	0.03	0.04	0.01	0.06	0.00	0.03
NTHMM	0.16	0.00	0.00	0.10	0.00	0.02	0.10	0.00	0.16	0.04	0.12	0.08	0.08	0.12	0.04	0.16	0.00	0.05
QUESL	0.11	0.00	0.00	0.08	0.00	0.02	0.08	0.00	0.11	0.03	0.08	0.05	0.05	0.08	0.03	0.11	0.00	0.05
QUESQ	0.13	0.01	0.00	0.10	0.00	0.02	0.10	0.00	0.13	0.04	0.10	0.07	0.06	0.11	0.03	0.14	-0.01	0.07
SALMO	0.41	0.00	0.01	0.18	-0.01	-0.01	0.32	0.00	0.41	0.10	0.31	0.20	0.20	0.31	0.10	0.41	0.00	0.39
SEYMO	0.00	0.00	0.00	0.06	0.00	0.01	0.00	0.00	0.00	0.00	0.00	0.00	0.00	0.00	0.00	0.00	0.00	0.00
SPIUS	0.23	0.00	0.00	0.10	0.00 -	0.01	0.05	0.00	0.23	0.06	0.17	0.11	0.11	0.17	0.06	0.23	0.00	0.17
STELL	0.44	0.00	0.01	0.15	0.00	-0.01	0.35	0.00	0.44	0.11	0.33	0.22	0.22	0.33	0.11	0.44	0.00	0.39
STHOM	0.10	0.00	0.00	0.11	0.00	0.01	0.03	0.00	0.10	0.02	0.07	0.05	0.05	0.07	0.02	0.10	0.00	0.04
STUAR	0.32	0.01	0.00	0.09	0.00	0.01	0.20	0.00	0.32	0.08	0.24	0.16	0.15	0.24	0.07	0.32	-0.01	0.27
TASEK	0.25	0.00	0.00	0.02	0.00	0.00	0.02	0.00	0.25	0.06	0.19	0.12	0.12	0.19	0.06	0.25	0.00	0.18
THOMK	0.14	0.00	0.00	0.11	0.00	0.02	0.07	0.00	0.14	0.03	0.10	0.07	0.07	0.10	0.03	0.14	0.00	0.04
THOMS	0.20	0.00	0.00	0.13	0.00	0.02	0.12	0.00	0.20	0.05	0.15	0.10	0.10	0.15	0.05	0.20	0.00	0.06
WEST	0.62	0.02	0.00	0.14	0.00	0.01	0.55	0.00	0.62	0.16	0.46	0.32	0.30	0.48	0.14	0.64	-0.02	0.57
WILLO	0.13	0.00	0.01	0.10	0.00	0.01	0.08	0.00	0.13	0.03	0.10	0.06	0.06	0.10	0.03	0.13	0.00	0.11
YALAK	0.46	0.01	0.00	0.04	0.00	0.02	0.02	0.00	0.46	0.12	0.35	0.24	0.23	0.36	0.11	0.47	-0.01	0.39

§ P = all mature pine classes (L5, L6, MN5, MN6, AK5 and AK6); Px = all beetle-kill pine classes (Lx5, Lx6, MNx5, MNx6, AKx5 and AKx6); CC = clearcut; VOP = vegetated opening.

† Lodgepole-pine forest runoff ratio (see Eqn. (9) of main text)

For more information about the Canadian Forest Service, visit our website at **cfs.nrcan.gc.ca** or contact any of the following Canadian Forest Service establishments

cfs.nrcan.gc.ca

Canadian Forest Service Contacts

1 Atlantic Forestry Centre
P.O. Box 4000
Fredericton, NB E3B 5P7
Tel.: (506) 452-3500 Fax: (506) 452-3525
cfs.nrcan.gc.ca/regions/afc

Atlantic Forestry Centre – District Office
Sir Wilfred Grenfell College Forestry Centre
University Drive
Corner Brook, NF A2H 6P9
Tel.: (709) 637-4900 Fax: (709) 637-4910

2 Laurentian Forestry Centre
1055 rue du P.E.P.S., P.O. Box 3800
Sainte-Foy, PQ G1V 4C7
Tel.: (418) 648-5788 Fax: (418) 648-5849
cfs.nrcan.gc.ca/regions/lfc

3 Great Lakes Forestry Centre
P.O. Box 490 1219 Queen St. East
Sault Ste. Marie, ON P6A 5M7
Tel.: (705) 949-9461 Fax: (705) 759-5700
cfs.nrcan.gc.ca/regions/glfc

4 Northern Forestry Centre
5320-122nd Street
Edmonton, AB T6H 3S5
Tel.: (403) 435-7210 Fax: (403) 435-7359
cfs.nrcan.gc.ca/regions/nofc

5 Pacific Forestry Centre
506 West Burnside Road
Victoria, BC V8Z 1M5
Tel.: (250) 363-0600 Fax: (250) 363-0775
cfs.nrcan.gc.ca/regions/pfc

6 Headquarters
580 Booth St., 8th Fl.
Ottawa, ON K1A 0E4
Tel.: (613) 947-7341 Fax: (613) 947-7396
cfs.nrcan.gc.ca/regions/nrc

Canadian Wood Fibre Centre
A virtual research centre of
the Canadian Forest Service,
Natural Resources Canada
cfs.nrcan.gc.ca/subsite/cwfc